JPRS L/10002

22 September 1981

USSR Report

PHYSICS AND MATHEMATICS

(FOUO 8/81)

FBIS FOREIGN BROADCAST INFORMATION SERVICE

NOTE

JPRS publications contain information primarily from foreign newspapers, periodicals and books, but also from news agency transmissions and broadcasts. Materials from foreign-language sources are translated; those from English-language sources are transcribed or reprinted, with the original phrasing and other characteristics retained.

Headlines, editorial reports, and material enclosed in brackets [] are supplied by JPRS. Processing indicators such as [Text] or [Excerpt] in the first line of each item, or following the last line of a brief, indicate how the original information was processed. Where no processing indicator is given, the information was summarized or extracted.

Unfamiliar names rendered phonetically or transliterated are enclosed in parentheses. Words or names preceded by a question mark and enclosed in parentheses were not clear in the original but have been supplied as appropriate in context. Other unattributed parenthetical notes within the body of an item originate with the source. Times within items are as given by source.

The contents of this publication in no way represent the policies, views or attitudes of the U.S. Government.

APPROVED FOR RELEASE: 2007/02/09: CIA-RDP82-00850R000400050052-5

JPRS L/10002

22 September 1981

USSR REPORT

PHYSICS AND MATHEMATICS

(FOUO 8/81)

CONTENTS

CRYSTALS AND SEMICONDUCTORS

UDC 548.5+537.311.33

LITHIUM IODATE: CRYSTAL GROWING, PROPERTIES AND APPLICATIONS

Novosibirsk IODAT LITIYA: VYRASHCHIVANIYE KRISTALLOV, IKH SVOYSTVA I PRIMENENIYE in Russian 1980 (signed to press 23 Oct 80) pp 2-5

[Annotation, preface and table of contents from book "Lithium Niobate: Crystal Growing, Properties and Applications" by Klavdiya Il'inichna Avdiyenko, Sergey Vasil'yevich Bogdanov (general editor), Stanislav Mikhaylovich Arkhipov, Boris Ivanovich Kidyarov, Viktor Vasil'yevich Lebedev, Yuriy Yevgenevich Nevskiy, Vladimir Ivanovich Trunov, Dmitriy Vasil'yevich Sheloput and Rozaliya Mikhaylovna Shklonskaya, Institute of Physics of Semiconductors, Siberian Department of the USSR Academy of Sciences, Izdatel'stvo "Nauka", 1200 copies, 125+ pages]

[Text] Data are given on the physicochemical properties of lithium iodate, and the technique for growing crystals in the hexagonal modification. Results are given from studies of the actual structure and defects of crystals, the influence of various factors on their optical, piezoelectric and other physical properties, generation of the second harmonic of laser emission and parametric conversion of infrared images to the visible range. An examination is made of the application of lithium iodate crystals in devices of nonlinear optics, acousto-optics and acousto-electronics.

For scientists and engineers engaged in growing and using crystals in applied physics, and also for undergraduate and graduate students. Figures 61, tables 28, references 190.

Preface

Among the large number of piezoelectric and nonlinear optics crystals of halogenate compounds with physical properties under intense study in recent years, the most widely used in applied physics have been crystals of hexagonal modification of lithium iodate (α-$LiIO_3$).

The properties of lithium iodate crystals were first described in 1969 by (Nat) and (Hauszyul'). Practical interest in these crystals stems from the fact that their effective nonlinear optical coefficients are comparable to those of lithium niobate, and at the same time, lithium iodate presents no problems involving optically induced inhomogeneities, which are a severe restriction in the use of lithium niobate. Therefore, lithium iodate crystals are used as effective laser radiation frequency doublers in intracavity generation of the second harmonic. In particular, the

second harmonic of the yttrium-aluminum garnet laser used to pump the first industrial light generator was stimulated in a lithium iodate crystal. This material was chosen because of its resistance to optical radiation. In subsequent years a great deal of research was done on detailed investigation of different physical properties of lithium iodate crystals, and their extensive possibilities were noted for practical application in laser physics, acousto-electronics and acousto-optics as a piezoelectric and nonlinear optical material.

The use of such materials, that have a high conversion efficiency and a wide relative transmission passband, considerably improves the working characteristics and appreciably expands the frequency range of various optical, acousto-electronic and acousto-optical devices, for example for delaying and processing radio signals, modulators, laser emission deflectors.

This book attempts a systematic exposition of the set of problems relating to crystal growing, investigation of physical properties and the use of lithium iodate crystals in devices of nonlinear optics, acousto-optics and acoustoelectronics. In the description of physicochemical properties, and primarily optical and piezoelectric properties, attention is turned to their connection with production techniques, purity of the initial materials, specially introduced dopants and structural perfection. In addition to analysis of Soviet and non-Soviet research dealing with lithium iodate, the main part of the book presents materials of original research done by the authors from 1970 through 1978.

We hope that this publication will stimulate the investigation of other interesting properties of lithium iodate crystals, and will promote more extensive use and development of new technical devices in applied physics and their introduction in the national economy.

The book was written by researchers at the Institute of Physics of Semiconductors of the Siberian Department of the USSR Academy of Sciences K. I. Avdiyenko, (chapters I and IV), S. V. Bogdanov (chapter III), B. I. Kidyarov (preface, conclusion, chapter II), V. V. Lebedev (chapter V), Yu. Ye. Nevskiy (chapter VI), V. I. Trunov (chapter V), D. V. Sheloput (preface, chapter VI), and researchers at Novosibirsk Rare Metals Plant S. M. Arkhipov and R. M. Shklovskaya (chapter I). The authors thank their colleagues in the work for useful advice and technical assistance in preparation of the manuscript. Critical comments should be addressed to: 630090, Novosibirsk, 90, pr. Nauki, 13, Institut fiziki poluprovodnikov SO AN SSSR, kand. fiz.-mat. nauk K. I. Avdiyenko.

Contents

6610
CSG: 1862/186

LASERS AND MASERS

ELECTRON BEAM-CONTROLLED COPPER VAPOR LASER

Leningrad PIS'MA V ZHURNAL TEKHNICHESKOY FIZIKI in Russian Vol 7, No 7, 12 Apr 81 (signed to press 18 Mar 81) pp 427-430

[Article by I. M. Isakov, A. G. Leonov and A. N. Starostin, Moscow Physicotechnical Institute]

[Text] The independent variation of field strength and electron concentration required for optimum conditions of gas laser operation is impossible in a self-maintained discharge. The use of an electron beam-controlled discharge is more convenient in this sense. In this case, the field strength will now be determined by the electron concentration set up by the time the discharge is activated by the electron beam (or more precisely by the ratio between the resistance of the discharge gap and the internal resistance of the excitation oscillator) rather than by the conditions of breakdown. Such experiments have been extensively done for example in the initiation of excimer lasers. We have been the first to use a method of this kind for excitation of a laser based on dense copper vapor.

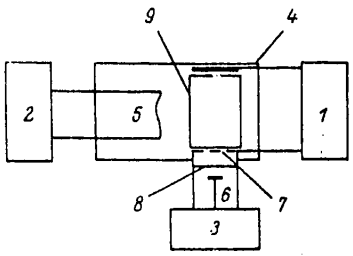

Fig. 1. Diagram of the installation: 1--electric discharge generator; 2--exploding wire generator; 3--voltage pulse generator; 4--laser chamber; 5--exploding conductor; 6--vacuum diode; 7--grid electrode; 8--separative film; 9--output window

Copper vapor with density of $(1-3)\cdot10^{18}$ cm^{-3} was produced in our experiments by the method of electrical explosion of conductors [Ref. 3]. A diagram of the installation is shown in Fig. 1. The electron source in our experiments was a vacuum diode with cold cathode fed by a 12-stage Marx generator with output capacitance of 0.83 nF. The generator was based on K15-10 ceramic capacitors, and was placed together with the divider and dischargers in a cylindrical jacket filled with nitrogen under a pressure of 4-8 atmospheres.

A beam of electrons with energy of 100-300 keV and current density of 10-20 A/cm^2 was coupled into the chamber through a window measuring 4 x 21 cm covered with Mylar

film 25 μm thick. The absence of any part subject to heating in the installation enables the use of ordinary sealing of the separative film. Beam current duration was 100 ns. The current density and pulse shape were measured by using an electron collector with signal recorded by the I2-7 nanosecond meter. The beam energy beyond the output window was measured by the method of foils. Beam homogeneity and divergence were monitored from the glow of a UFD-89 luminescent x-ray screen. The discharge was excited by a Blumlein generator based on striplines with total capacity of 13.5 nF made from foil-covered glass Textolite 1 mm thick. Interelectrode distance was 10 cm.

Excitation by electron beam, electric discharge and a combined method were studied separately in our work. In all cases the delay between explosion of the conductor and the excitation pulse was 600 μs.

In the first version, the cavity used in the research was formed by flat dielectric mirrors with reflectivities R ~ 99% and 67% on a wavelength of 5105 Å. Lasing energy was 11 μJ for copper vapor density of $3 \cdot 10^{18}$ cm^{-3}. The reason for such low lasing energy was due to the fact that the laser in all probability was working in near-threshold conditions. This is clearly evident from the dependence of lasing energy on vapor density and reflectivity of the output mirror (Fig. 2a). A situation of this kind is due to the small energy contribution of the beam to the active medium. According to estimates [see for example Ref. 2], the amount of this contribution is ~400 $\mu J/cm^3$ at a vapor density of $3 \cdot 10^{18}$ cm^{-3}.

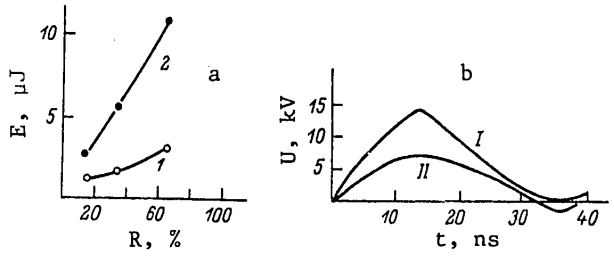

Fig. 2. Lasing energy as a function of output mirror reflectivity: 1--$N = 10^{18}$ cm^{-3}; 2--$N = 3 \cdot 10^{18}$ cm^{-3}; b--oscillograms of voltage across the discharge without beam action (I), and with the beam (II)

Upon excitation by an electric discharge the maximum lasing energy was considerably higher and amounted to E = 5 mJ at a charging voltage of 25 kV. The output mirror was a quartz plate without any coating. Increasing the reflectivity in this case only reduced the lasing energy. Laser pulse duration was 20 ns.

Upon a transition to combined excitation the energy of the laser pulse increased to 10 mJ despite the fact that the beam energy absorbed by the copper vapor was much less than the energy contribution from the discharge (~2 J). Lasing duration also increased to 30 ns. Let us note that the discharge pulse was delayed relative to the beam current by $\tau = 60$-80 ns.

An investigation of the current-voltage characteristics of the discharge showed that the pulse shape of the discharge current and of the voltage across the discharge gap changes with a transition to the combined method (Fig. 2b). Just as was assumed, there was a considerable reduction in the amplitude of the voltage across the discharge since the medium already had considerable conductivity by the time of arrival of the exciting pulse. According to estimates [Ref. 2] the electron concentration at beam parameters of $U_b = 200$ keV and $j_b = 20$ A/cm^2 may reach $3 \cdot 10^{13}$ cm^{-3} at $N = 10^{18}$ cm^{-3}. It has been pointed out previously [Ref. 3] that in the case of short-pulse excitation of copper vapor lasers using a Blumlein line, the high voltage across the discharge gap at the instant of the main energy contribution reduces lasing efficiency. On the other hand, a reduction in the voltage across the discharge makes for more optimum conditions of inversion formation. Let us note that although laser efficiency was doubled over the case of pure discharge excitation, the actual gain is even greater since lasing efficiency with respect to the energy investment in copper vapor was tripled due to a reduction in efficiency of energy transfer to the discharge by a factor of 1½. Based on measurement results we can conclude that the proposed excitation arrangement may be quite useful for large volumes of copper vapor or high-density vapor. The vapor density in our experiments was limited by the energy storage of the explosive capacitor bank.

In conclusion, the authors express their sincere gratitude to I. Brchka and A. N. Steklov for assisting with the experiments.

REFERENCES

1. I. M. Isakov, A. G. Leonov, ZHURNAL TEKHNICHESKOY FIZIKI, Vol 50, 1980, p 126.

2. V. A. Danilychev, O. M. Kerimov, I. B. Kovsh, TRUDY FIAN, Vol 83, p 147.

3. I. M. Isakov, A. G. Leonov, "Tezisy dokladov na Vtorom Vsesoyuznom seminare po fizike gazovykh lazerov" [Abstracts of Papers to the Second All-Union Seminar on Physics of Gas Lasers], Uzhgorod, 1978, p 65.

6610
CSO: 1862/196

UDC 621.378.001

PHYSICAL PROCESSES IN GENERATORS OF COHERENT OPTICAL RADIATION

Moscow FIZIKA PROTSESSOV V GENERATORAKH KOGERENTNOGO OPTICHESKOGO IZLUCHENIYA in Russian 1981 (signed to press 12 Aug 80) pp 2-5, 434-439

[Annotation, preface and table of contents from book "Physics of Processes in Generators of Coherent Optical Radiation: Lasers, Resonators, Dynamics of Processes", by Candidate of Physical and Mathematical Sciences Lev Vasil'yevich Tarasov, docent, Moscow Institute of Electronic Machine Building, Izdatel'stvo "Radio i svyaz'", 4000 copies, 440 pages]

[Text] The book deals with the physics of processes in lasers. Three groups of problems are considered: methods of producing inverted active media, formation of the radiation field in the resonator, and the dynamics of processes in lasers. The choice of material reflects the current level of development of laser technology. A systematic examination is made of methods used in the theory of lasers, various approaches and approximations.

The book is intended for scientists and engineers working in the field of laser technology, and also for instructors and students in institutions of higher education. Figures 224, Tables 14, References 295.

Preface

Generators of coherent optical radiation include two groups of devices. The main group is lasers. The second group includes generators of optical harmonics, parametric light generators and so on. This book is devoted to the physics of processes in lasers.*

The writing of a book that reflects the current level of laser technology from a physical standpoint is topical in view of the fact that lasers are being more and more extensively used both in research and in different areas of the national economy. There is a continuous rise in the number of engineers and researchers engaged in the field of laser technology and related areas.

It has been the author's intention for this book to handle two jobs: first, to systematize and expand the reader's notions of the physics of processes in lasers,

*Generators of optical harmonics and parametric light generators will be the subject of another book by this author.

to acquaint the reader with the latest advances and directions; secondly, to provide the reader with information that might be of help in improving the facility for future use of the special literature. The author has tried to reflect the current level of development of laser technology, and at the same time to provide a systematized examination of methods used in the theory of lasers, to discuss different approaches and approximations. In doing so, the author has attempted to produce a book that would be not only of definite interest to scientists and engineers, but might also serve as a scientific and procedural basis for developing special academic courses and textbooks.

The book examines three groups of problems: methods of producing inverted active media, formation of the radiation field in the optical cavity, and the dynamics of processes.

In examining methods of producing inversion in active media, the first chapter discusses the principles and peculiarities of operation of lasers of different types: solid-state, dye, photodissociation, gas-discharge, electron-beam controlled, gasdyramic, chemical and plasma lasers.

The second chapter analyzes the role of the resonator in formation of the radiation field of the laser, gives the fundamentals of the theory of open resonators. The author uses the geometric optics approximation, the Fox-Li iteration method, the gaussian beam model, the ABCD law. Consideration is taken of the apertures of mirrors, the presence of a lens or diaphragm within the cavity, misalignment of components in the resonator. Cavities of different geometries--both stable and unstable--are examined. In the case of active resonators the author discusses effects of the heat lens, frequency pulling and "hole burning." Consideration is given to problems of longitudinal mode selection and also to the physics of waveguide resonators and film lasers with distributed feedback.

The third chapter begins with a survey of different modes of stimulated emission of the laser, including modes of active and passive Q-switching of the cavity, longitudinal and transverse mode locking, load modulation. Balance equations (Statz-de Mars equations and their modifications) are introduced, analyzed and put to extensive use. These euqations are used as a basis for examining different aspects of the dynamics of single-mode lasers: transient processes that lead to damped emission power pulsations; undamped power pulsations that show up in the presence of weak modulation of losses, generation of giant pulses with instantaneous Q-switching. The electro-optic and acousto-optic methods of active Q-switching are compared. A detailed analysis is made of processes in lasers with phototropic filters. Longitudinal mode locking is discussed with the use of both spectral and temporal approaches. A temporal description based on fluctuational concepts is used in considering self-mode locking in a laser with phototropic filter. The temporal approach is also used to describe acousto-optic mode locking in a laser with uniformly broadened amplification line. Methods of studying ultrashort light pulses are discussed separately. The appendices examine Hermite polynomials, Jones matrices, singular points of a two-dimenional dynamic system and other questions.

This book is a logical continuation of the author's previous work "Fizicheskiye osnovy kvantovoy elektroniki" [Physical Principles of Quantum Electronics] (Moscow, Sovetskoye radio, 1976), giving the general physical picture of the interaction of optical radiation with matter.

The author is sincerely grateful to V. G. Dmitriyev, V. R. Kushnir, V. K. Novokreshchenov, Ye. A. Shalayev, V. N. Morozov, V. A. D'yakov, V. V. Nikitin, Yu. N. Pchel'nikov, A. M. Amel'yants, A. A. Solov'yev and V. F. Trukhin, who read the manuscript of the book and offered constructive comments and wishes. The author thanks A. N. Tarasova for assistance in preparing the manuscript for printing.

Contents page

6610
CSO: 1862/216

UDC 539.1

OPTICAL RESONATORS AND THE PROBLEM OF LASER EMISSION DIVERGENCE

Moscow OPTICHESKIYE REZONATORY I PROBLEMA RASKHODIMOSTI LAZERNOGO IZLUCHENIYA in Russian 1979 (signed to press 29 Oct 79) pp 135-154, 172-188, 220-301

[Excerpts from book "Optical Resonators and the Problem of Laser Emission Divergence" by Yuriy Alekseyevich Anan'yev, Izdatel'stvo "Nauka", 4,000 copies, 328 pages]

[Excerpts] Section 2.6. Angular Radiation Selection Procedures

In this section an analysis will be made of the efforts to decrease the divergence of laser radiation with planar or stable resonators (or resonators similar to them; see below) which have been made at different times and with varying degrees of success. The majority of these methods are now only of historic interest; however, some of them are used even today.

Efforts To Solve the Divergence Problem on the Basis of Resonators With Small Diffraction Losses. In a number of papers a study has been made of the possibility of creating resonators from mirrors with aspherical surface, the shape of which is selected in such a way that the diffraction losses in the lowest mode are just as small as for stable resonators, but they increase with the transverse index faster than for stable resonators. This theoretically facilitates the achievement of unimodal oscillation. Some systems of this type are presented in Figure 2.22.

The resonators depicted in Figure 2.22, a, b, were made from dihedral reflectors, the angle between the flat faces of which is $\pi - \alpha$ in the former case, and $\pi/2 - \alpha$ in the latter case ($\alpha \ll 1$). The effect of the first type of reflector on a narrow light beam to a certain extent is similar to the effect of a concave mirror; some "fine focusing" of the beam is realized. The reflector of the second type only adds "inversion" of the beam cross section to this effect; therefore resonators of these two types are equivalent to each other in the absence of aberrations. It is possible to see that the transverse dimensions of the light beams corresponding to individual transverse modes increase in them with the transverse index faster than in stable resonators, which ensures greater selectivity for reflectors of finite dimensions. The properties of these resonators are described in more detail in [120, 121].

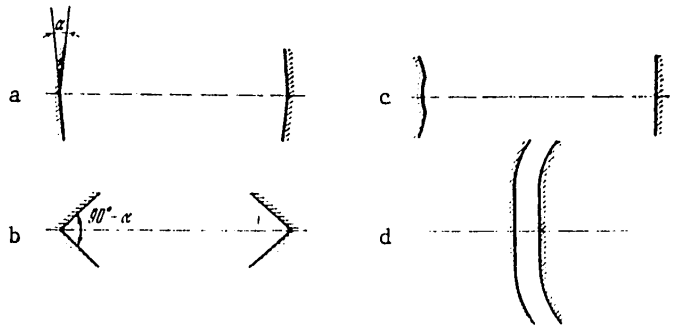

Figure 2.22. Some types of resonators with aspherical mirrors: a, b--resonators with dihedral reflectors [120, 121]; c--resonator with central "indentation" [122]; d--resonator proposed in [123].

Figure 2.22, c, depicts a resonator in which the eigenvalue spectrum is still more radically rarefied. The dimensions of the central section of the left-hand reflector--the "indentation"--can be taken so that they will be equal to the dimensions of the basic mode spot formed by this section and the right-hand mirror of a stable resonator. Then the losses of this mode will be small; broader beams corresponding to other modes will go beyond the limits of the central section and scatter quickly in the peripheral part of the resonator. This must lead to significant increase in the losses.

At first glance it may seem that an analogous effect is achieved by simple irising of the stable resonator. However, in the latter case as we have seen in Sections 2.1, 2.2, the high-order mode field begins to be confined inside the resonator by edge diffraction (the edge of the diaphragm has the same effect on the light beam as the edge of a mirror); in the resonator depicted in Figure 2.22, c, the diffraction on the edge of the "indentation" turns out to be significantly attenuated as a result of the presence of halation. Vaynshteyn [3] indicated the possibility of using a similar procedure; the effort at practical implementation in the optical range (in the example of a helium-neon laser) is described in [122].

Sometimes proposals for a different plan are encountered in the literature. Thus, in [123] the properties of the resonator depicted in Figure 2.22, d, were analyzed. With a strictly defined form of the components of its reflectors, the equation for finding the natural oscillations has only one solution. However, in [123] a study was made only of the equation of an empty resonator made up of infinite mirrors; consideration of the edge effects and the introduction of an active medium should change the situation sharply--nothing may remain of "unimodality." In addition to everything else it is unclear how such reflectors would be made with the precision required in the optical range.

In contrast to the last-mentioned version, the possibility of using the resonators depicted in Figure 2.22, a-c, is unquestioned. However, they are all characterized by the same deficiency as the ordinary stable resonator itself: under

conditions of unimodal oscillation it is possible to make effective use of only a very small volume of the optically uniform medium (it is sufficient to point out that in the mentioned experimental work [122] the depth of the "indentation" was ~λ/10). Therefore the devices with aspherical reflectors are not able to compete with the stable resonators which are simple to make and align.

It must be noted that for cross section dimensions of the active medium not exceeding several millimeters, unimodal oscillation can be achieved using both stable and planar resonators. In particular, it is appropriate to note the successful method of empirical selection of the optimal parameters of the resonator near the "stability" boundary used for the first time in [124] and also used successfully in a number of subsequent experiments. The method is based on the application of a combination of plane and concave spherical mirrors, the distance between which L varies near a value equal to the radius of curvature of the concave mirror R. For L = R (or in the case of the presence of an active element of length ℓ with an index of refraction n_0, for $L_{equiv} = L - \ell(1 - 1/n_0) = R$) a so-called semiconcentric resonator is realized which is equivalent to the planar resonator and thus is at the "stability" limit (Section 1.2). For shorter lengths, the resonator is stable; it is important that for L ≲ R small variations in the distance between the mirrors lead, as it is easy to see, to significant simultaneous variation of the diffraction losses and spot dimensions of the fundamental and other transverse modes. This makes it easy to select the optimal combination of them from the point of view of the output characteristics of the laser. Obviously, when this choice is made empirically, the "Lenticularness" of the sample is automatically taken into account if it exists, and so on.

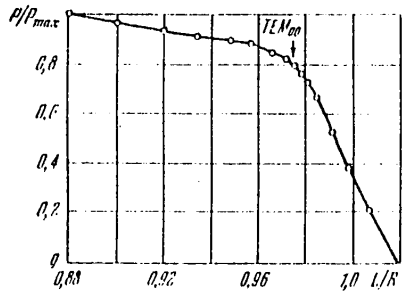

Figure 2.23. Results of experiments in oscillation selection in a resonator close to a semiconcentric resonator [128].

Figure 2.23 shows a standard graph for use of the indicated method borrowed from [28], where this method is discussed in great detail. The graph was obtained in experiments with a helium-neon laser; the ratio L/R is plotted along the x-axis, the line L/R = 1 is the "stability" limit. On approaching it from the left, the diffraction losses increase, the total oscillation power P decreases slowly, then the number of transverse modes present in the oscillations are reduced. At the point noted by the arrow, only the lowest mode TEM_{00} remains. The resonator length corresponding to this point can also be considered optimal: further movement toward the stability limit and transition to the region of instability

located to the right causes only a sharp decrease in power and then cessation of oscillation.

All of this is good, however, only in the case of lasers with small cross sections of the active medium for which the problem of radiation divergence in general is not acute. As for the lasers of primary interest to us which have a large exit aperture, for them the application of stable resonators leads, as has already been noted more than once, to oscillation on higher-order modes with a broad radiation pattern. Nevertheless, efforts have been renewed many times to solve the problem of divergence even in this case. In Chapter 5 there is a brief discussion of the conversion of light beams corresponding to the high-order modes to narrowly directional light beams by the methods of holographic correction. A search was also conducted for simpler methods; from the work in this direction there are some interesting papers (for example, [125]), but their practical significance is low. Therefore hereafter we shall limit ourselves to the investigation of the methods of angular selection (decreasing the angular divergence of the radiation) in planar resonators which has received significant development in its time.

Lasers With Planar Resonators and Angular Selectors. For constriction of the radiation pattern of a laser with planar resonator it is necessary in the general case also to decrease the number of modes in which oscillation is realized and, what is usually even more important, the deformations of these modes. The number of modes is determined primarily by the ratio between the diffraction and nonselective losses. Therefore for angular selection in the hypothetical case of an ideally uniform medium where the mode deformations are small, it is necessary to try to increase the differences of the diffraction losses.

In the presence of aberrations of any type, the most important problem turns out to be decreasing the mode deformations; in accordance with perturbation theory (Section 2.5), for this purpose it is necessary to increase the differences of the eigenvalues of the operator $\hat{P}$, including the phase corrections.

Making this remark of a general nature, let us proceed with investigation of the specific methods of angular selection.

In order to obtain the desired effect usually additional elements called angle selectors are introduced into the resonator. They are essentially filters, the transmission of which depends sharply on the direction of propagation of the radiation. Historically, the first type of angle selector was a system of two confocal lenses and a diaphragm with a small opening placed at their common focal point [126, 127]. A concentric resonator with a diaphragm in the central plane [128, 129] (Figure 2.24, b) is entirely identical to a planar resonator with such a selector (Figure 2.24, a). The operating principle of such a selector is obvious. Instead of a diaphragm a passive shutter can be used: part that clears first then acts as an iris aperture [130].

The effect of the selector based on the Fabry and Perot etalon [131, 132] is based on the fact that the transmission of the etalon depends not only on the

wavelength, but also the direction of propagation of the radiation. Inasmuch as for inclined incidence of the beam, this relation becomes sharper, the etalon is installed at an angle to the resonator axis (Figure 2.24, c). For realization of angular selection in both directions it is necessary to use two etalons.

Probably the method of selection based on using the dependence of the reflection coefficient at the interface of two media on the angle of incidence had the greatest popularity. Near the critical angle of total internal reflection, the indicated relation is especially sharp; therefore these angles of incidence are used. In order to eliminate the selective effect it is possible to make the light undergo multiple reflections (Figure 2.24, d). In the 1960's a large number of versions of selectors of this type [133-140] grouped under the general heading of total internal reflection selectors were proposed.

Let us consider the mechanism of the effect of the selectors on the angular divergence. From very general arguments it is clear that the presence of a filter, the transmission of which depends on the direction of propagation of the radiation is primarily felt in the magnitude of the losses of individual transverse modes. The phase corrections are determined for fixed configuration of the resonator in practice only by the number of angles of distribution of the amplitude with respect to cross section (that is, the transverse mode index), and in the presence of a selector, they must vary insignificantly (see Section 2.2 for the similarity of phase corrections in open and closed resonators). The results of strict calculations [141] confirm this obvious conclusion.

Let us present the data for the idealized case of a Gaussian selector, the shape of the passband of which is intermediate between the shapes of the bands of real selectors presented in Figure 2.24, and it is described by the formula $g^2(\phi) = \exp[-(\phi/\Delta\phi)^2]$ (Figure 2.25; see [141]); ϕ is the angle between the direction of propagation of the radiation and the resonator axis; $\Delta\phi$ is the passband width, g^2 is the transmission with respect to intensity. If we consider that the transverse modes with the index m correspond to values of $\phi \approx \pm(m + 1)\theta_{diff}/2$ (see Sections 2.2, 1.1; $\theta_{diff} = \lambda/2a$), the magnitude of the losses introduced by the selector follow directly $\Delta(2\delta_m'') = (m + 1)^2(\theta_{diff}/2\Delta\phi)^2$ (this same result was obtained in [141] by a stricter procedure).

Let us now trace how the magnitude of the angular divergence of the radiation must vary with the passband width of the selector.

In the absence of aberrations the role of the selector reduces to variation of the conditions of competition of the modes (Section 2.4) by increasing the loss differences. The losses introduced by the Gaussian selector turn out to be greater than the diffraction losses in an ideal empty resonator on satisfaction of the condition $2\Delta\phi/\theta_{diff} < (a^2/\lambda L)^{3/4}$. Inasmuch as for lasers with large cross section $a^2/\lambda L = N >> 1$, the angular divergence in the given idealized case can decrease sharply even for comparatively greater width of the selector passband. Estimation shows that to achieve the unimodal conditions with an ideal active medium it is sufficient to use a selector with $\Delta\phi$ several times greater than $\theta_{diff}/2$.

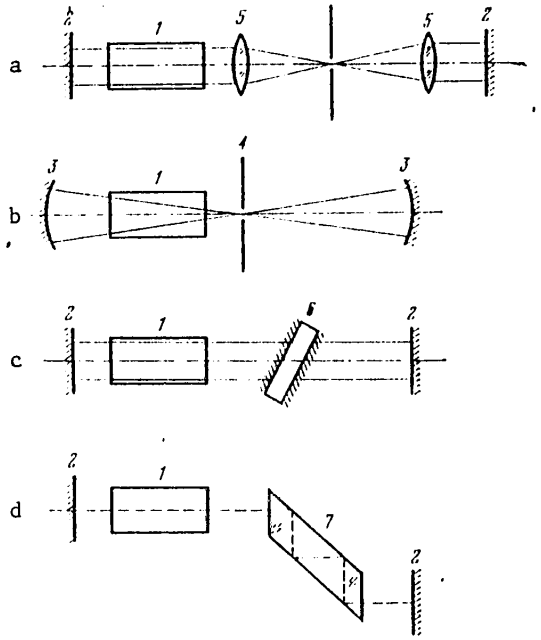

Figure 2.24. Diagrams of lasers with angle selectors: 1--active sample; 2--plane mirror; 3--spherical mirror; 4--diaphragm with hole; 5--lens; 6--Fabry and Perot etalon; 7--plane-parallel plate.

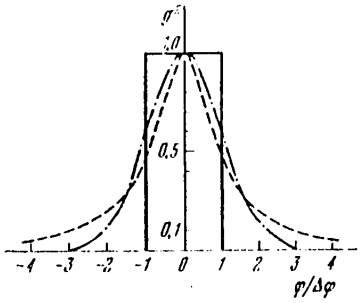

Figure 2.25. Shape of the passband of different angle selectors; Gaussian selector (dash-dot line), the selector based on the Fabry and Perot etalon (dotted line) and the ideal selector (solid line).

This possibility is based on the fact that the losses introduced by the given type of selector are even noticeable for $\phi << \Delta\phi$ (see Figure 2.25). Among real selectors, only the selector based on the Fabry and Perot etalon (see Figure 2.24, c) has this (quadratic) form of the function $g(\phi)$. The selectors with an opening (Figure 2.24, a, b) and the total internal reflection selectors (Figure

2.24, d) have a passband with shape approaching a rectangle ("ideal" selectors according to the terminology of [141, 142]). In this case, just as should be expected, the presence of a selector is felt noticeably in the value of the losses only for the modes, the indices of which are close to the value of $2\Delta\phi/\theta_{diff}$ [141]; therefore the selectors of the given type can decrease the amount of angular divergence only to a value approximately equal to $\Delta\phi$.

In the presence of noticeable aberrations the basic function of the selector must be to decrease the deformations of the oscillation with the highest Q. Let us remember that the mode deformations themselves can be interpreted as the result of the presence of induced oscillations in the modes of an ideal resonator (see the preceding section). Beginning with this fact, it is easy to see that in order to decrease the mode deformations the losses introduced by the selector must turn out to be larger in magnitude not only than the diffraction losses, but also the phase corrections in the empty resonator. Hence, it follows that for noticeable aberrations (that is, in practice always) only selectors with sufficiently narrow passband, independently of its shape, can turn out to be useful.

When using angular selectors, just as in the case of angular selection by increasing the length of the resonator which will be considered a little later, not only the angular radiation characteristics are of interest, but also the energy characteristics of the radiation. The possibility of decreasing the width of the radiation pattern without significant gain in radiation power is connected with the magnitude and the nature of the aberrations. This relation is exhibited most clearly when investigating the shape of the scattering index of a coherent light beam.

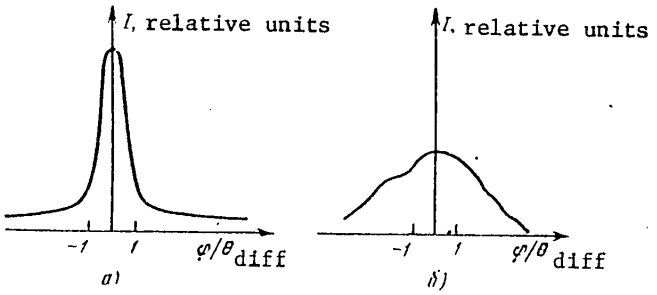

Figure 2.26. Radiation patterns after single passage of the light through the active medium: a--light dispersion on microinhomogeneities; b--low-order wave aberrations as a result of the presence of macroinhomogeneities.

Figure 2.26 contains a schematic representation of two radiation patterns of a light beam after single transmission through an active sample (at the entrance to the sample the wave front is planar). These patterns directly characterize the angular divergence of the beam at the exit from the laser system using the given sample as the final amplifier (of course, if a well-collimated beam is fed to its input).

The first of them (Figure 2.26, a) pertains to the case of weak light dispersion on microinhomogeneities. The greater part of the energy of the light passing through the sample (on the order of $1 - \rho_{dis}$, the presence of secondary diffraction peaks is neglected) is concentrated in the central core having diffraction width. The remainder of the radiation is distributed in a comparatively wide range of angles.

Figure 2.26, b, corresponds to the presence of low-order wave aberrations (refraction on macroinhomogeneities). Primarily the most central core of the pattern expands, the axial luminous intensity decreases significantly. From the Rayleigh number it follows that the core width begins to exceed the diffraction limit noticeably when the aberrations exceed $\lambda/4$.

It is obvious that the effort to realize angular selection will lead to essentially different results in the cases of Figures 2.26, a, and 2.26, b. The light dispersion on the microinhomogeneities does not prevent achievement of the diffraction limit; the power of the generated radiation in this case, if the pumping intensity is sufficiently high, decreases insignificantly (the effective losses increase by approximately ρ_{dis} [26]). In the case of Figure 2.26, b, an effort to constrict the angular divergence to less than the width of the central core of the scattered light indicatrix is coupled with unavoidable significant energy losses.

The experimental data correspond quite well to the above-discussed arguments. First of all, it must be noted that when using all types of angle selectors a decrease in angular divergence and an increase in the axial luminous intensity were actually observed. Nevertheless, the angle selectors have not found broad application. The reason for this lies both with the high requirements on the precision of their manufacture and alignment and a number of specific deficiencies characteristic of each type of selector.

The basic deficiency of systems with a diaphragm (see Figure 2.24, a, b) is undesirable concentration of the radiation in a small section of the cross section. In lasers of comparatively low power this leads to rupture of the diaphragm or electric breakdown near its surface (see, for example, [129]). Angular selection using the Fabry and Perot etalons is greatly complicated as a result of the presence of a large number of transmission peaks; therefore no one has followed the example of the authors of [131, 132] who were able to realize it in low-power ruby lasers. Only total internal reflection selectors have found some application in powerful pulsed lasers, but even they in the final analysis disappeared from the scene as a result of the extraordinary requirements on the precision of manufacture and alignment and also the degree of finish of the working surfaces.

Angular Selection of Laser Radiation With Planar Resonators by Decreasing the Number of Fresnel Zones. If we do away with angle selectors, it remains only to increase the selective properties of the planar resonator itself by decreasing the number of Fresnel zones N. This can be achieved by reducing the cross section or by increasing the length of the resonator.

A significant decrease in the active cross section by irising the resonator, of course, must lead to a corresponding drop in the output power, and therefore cannot be considered among the efficient selection procedures. Some movement in this direction is still possible. The fact is that a light beam always broadens somewhat on passage through a planar resonator (as a result, diffraction losses appear). If we use an exit mirror with cross section only somewhat less than the cross section of the active element, the latter will still be completely filled by the irised beam. It only remains to use the radiation exiting from the laser through a narrow circular zone around the mirror as the useful signal along with the radiation passing through the semitransparent exit mirror. Thus, it is possible to decrease N somewhat, almost without relinquishing output power. This procedure was described for the first time in [143]; the name of diffraction yield of radiation was attached to it. The same method was used with slight modifications in [144]; the given direction reached a logical conclusion in the laser described by Kalinin et al., the reflection coefficient of the exit mirror of which decreased smoothly from the center to the periphery [145]. In all of the enumerated cases, just as should be expected, an increase in the degree of directionality and a decrease in the sensitivity to the misalignment of the mirrors were observed (as a result of a decrease in the total or effective size of the exit mirror), but with intense pumping the angular divergence significantly exceeded the diffraction limit.

Let us note that lasers with mirror transmission that is variable with respect to cross section are a clear example of systems having extraordinary dependence of the mode structure on the excitation conditions. In the case of uniform distribution of pumping slightly exceeding the lasing threshold, the field configuration of the individual types of oscillations will be close to the configuration predicted by the theory of the corresponding empty resonators [146]. If the amount the threshold is exceeded is large, then as a result of the competition of the transverse modes the distribution of the gain with respect to cross section approaches the loss distribution, and the structure of the individual modes will become similar to the structure in lasers with ordinary mirrors.

A much more radical decrease in N without reduction of the working volume can be achieved by a simple increase in the distance between mirrors. This method of angular selection is the most natural and, in addition, very effective: here, in contrast to the case of the application of angular selectors, not only the losses increase, but also the phase corrections, which leads to a rapid decrease in the mode deformation. In addition, it is simpler by far to vary the length of the resonator than to introduce a selector and change the passband width; therefore the given method of constricting the radiation pattern has been studied most systematically.

The most important result of numerous studies was solid establishment of the fact that on variation of L within very broad limits the angular divergence of the radiation varies with a high degree of accuracy proportionally to $L^{-1/2}$--indeed the theoretical estimates based on any models pertaining to mode deformations and to multimode oscillations (Sections 2.4, 2.5) lead to the same relation! This relation has been exemplified by lasers of the most varied types: a ruby laser (the resonator length was varied by approximately 15 times) [147],

a neodymium glass laser (~15 times), a fluorite laser with samarium (~10^3 times) [26], and an alkyliodide molecule photodissociation laser (~30 times) [148]. The following is characteristic. If the medium has a comparatively high amount of optical nonuniformity, increasing the length of the resonator above some limit is accompanied by quite rapid decrease in power to complete cessation of oscillation, although it may still be far to diffraction divergence. As a result, the axial luminous intensity, initially increasing with resonator length, goes through a peak, the position and height of which depend on the degree of optical nonuniformity of the medium. This fact was noted for the first time by Sventsitskaya and Khazov in [147] (in this paper, the method of representing data on the angular distribution of radiation in the form of the dependence of the proportion of the beam energy included inside the axial cone on the angle at the apex of this cone, see Figure 4.4, 4.7, which has acquired deserved popularity was introduced). It is of interest that when the sharp lasing power drop begins, the angular divergence begins to decrease with an increase in L even faster than $L^{-1/2}$ [148]. This is explained by the fact that as a result of a sharp increase in the threshold, the lasing begins to be localized in individual sections of the cross section with the largest gradient of the index of refraction [147, 148]--the "effective" value of Δn decreases.

As the optical uniformity of the medium increases, it is possible to come closer and closer to diffraction divergence without noticeable loss of power (it is true in this case the requirements on the necessary precision of alignment of the resonator increase). Finally, when the medium is so uniform that $\Delta L < \lambda/4$, the diffraction limit can be reached. For this purpose the distance between the mirrors must be usually so large that N exceeds 1 somewhat. Herein lies the basic deficiency of the given selection method: for lasers in the visible range even with diameters of the active elements only 5-8 mm, the required resonator length is several meters. If we consider that for maintenance of the same N the length must increase proportionately to the square of the linear dimensions of the working cross section, it becomes clear that in the case of powerful lasers it is entirely unreasonable to solve the problem by a simple increase in distance between the mirrors. It is also necessary to consider that for short lasing pulses long length of the resonator is in general unacceptable inasmuch as the pulse development time increases together with the length.

The way out of the indicated difficulty consists in using resonators that have short actual length, but equivalent to the planar resonator with small N. This method of angular selection is of definite interest not only from the practical point of view, but also from the procedural point of view; therefore let us discuss it in somewhat more detail.

Plane Resonators of Long Effective Length. In Figure 2.27 several versions of devices of this type are presented. The first of them was used to decrease the angular divergence in 1963 [149], but correct notions of its properties were still not developed at that time. Using the methods discussed in Section 1.2, the corresponding analysis will be performed without special difficulty. However, we shall not consider the beam matrices of these resonators as a whole, but we shall use a more obvious procedure which will also be useful hereafter to consider unstable resonators.

A common characteristic of all resonators equivalent to the planar resonator (including the ones depicted in the figure) is the fact that in the geometric approximation all of the beams normal to the surface of one of the terminal mirrors, on passing through the resonator, are incident normally on the surface of the second terminal mirror and follow back along the same path. Accordingly, such resonators can be broken down entirely into sections, each of which is bounded by a pair of parallel planes or concentric spheres. The boundaries of the edge sections are the terminal mirrors themselves; the intermediate thin lenses can be considered, as usual, phase correctors, passing through which leads only to the corresponding change in curvature of the wave front (see Figure 2.27).

The result of passage of the light through these sections in the wave approximation can be calculated by using the apparatus of beam matrices or directly from the Huygens-Fresnel principle. Here it is expedient to give the distributions of the complex amplitude directly on the surfaces bounding the sections and in dimensionless coordinates r/a, where $2a$ is the difference between the edge beams in the geometric approximation (thus changing the scale on transition to the sections with another beam cross section). Then it is possible to arrive at the following simple laws.

On passage through a type I section (plane boundaries) $2a$ wide and L long, the complex distribution of the amplitude is transformed just as on passage through a section of the same type $2a_0$ wide and $L_{eff} = La_0^2/a^2$ long (this is understandable--the number of Fresnel zones N is the same in them). The passage through the type II section with light beam width in the geometric approximation at the entrance and exit surfaces $2a_1$ and $2a_2$ is equivalent to passing through a type I section of width $2a_0$ and length $L_{eff} = La_0^2/a_1a_2$; as a result of variation of the cross section, only an additional amplitude factor a_1/a_2 is acquired (see also (1.23)); the general phase multiplier $\exp(ikL)$ plays no special role in our investigation.

By this procedure, the passage through all of the type I and II sections reduces to passage through the corresponding distances of type I sections of the same width $2a_0$. Inasmuch as passage through several such sections, in turn, is equivalent to passage through a section of total length, the L_{eff} defined in this way for all type I and II sections can be simply added.

It is easy to demonstrate that passage through the type III sections with entrance and exit widths of $2a_1$ and $2a_2$ is equivalent to returning a distance $L_{eff} = La_0^2/a_1a_2$ in a type I section; inversion of the beam and variation of the amplitude in the ratio a_1/a_2 also occur. Therefore the effective lengths of the type III sections are subtracted from the total sum (the growth of the angular divergence of the radiation caused by this on introduction of the type III section into the system was observed experimentally, and it was explained in [115]). If we also consider the extraordinary energy concentration at the constriction points, it becomes obvious that the presence of such sections inside the resonator, as a rule, is undesirable.*

* In powerful amplifiers, on the contrary, such sections then called "optical relays" sometimes are specially introduced, for a decrease in L_{eff} helps to prevent self-focusing [330].

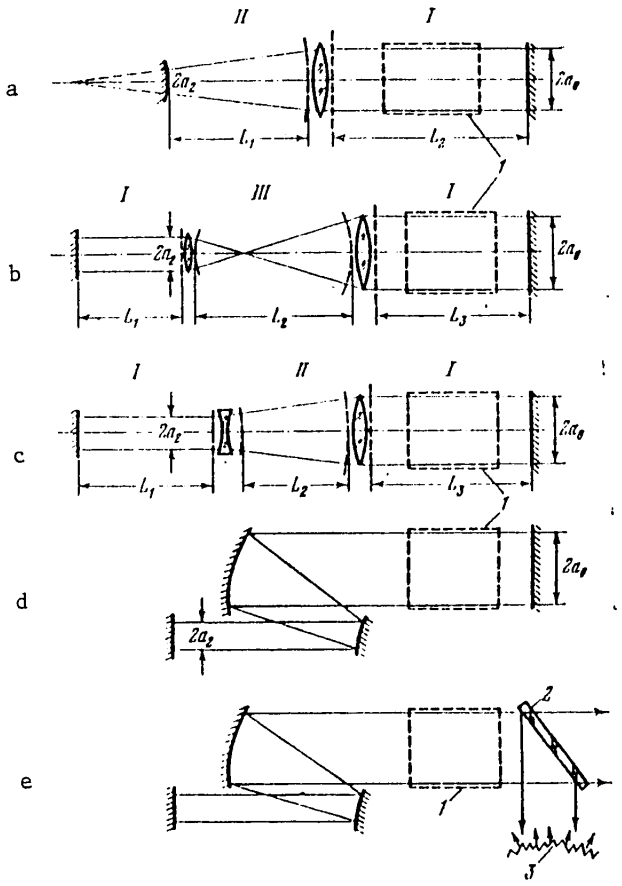

Figure 2.27. Resonators with long effective length: a--resonator described in [149]; b-d--planar resonators with telescope located inside them; e--resonator with telescope and nonresonant feedback; 1--active element; 2--partially reflecting plate; 3--diffuser.

Thus, all of the systems depicted in Figure 2.27 are equivalent to planar resonators with easily calculated effective length (let us note that if such a resonator is used as the Fabry-Perot interferometer, the angular distance between rings in it will be determined by this effective length). For the case of Figure 2.27, a, L_{eff} is equal to $L_2a_0/a_2 + L_1$; for Figure 2.27, b, $L_3 - L_2a_0/a_2 + L_1a_0^2/a_2^2$; for Figure 2.27, c, $L_3 + L_2a_0/a_2 + L_1a_0^2/a_2^2$. The width of the equivalent resonator $2a_0$ is selected in all cases equal to the beam width on the extreme right section where the active medium must be placed. It is obvious that the presence of sections with small beam cross section leads to a sharp increase in the effective length; the effective value of the parameter N decreases correspondingly (in the case most advantageous from this point of view in Figure

2.27, c, it is $N_{eff} = [(\lambda L_3/a_0^2) + (\lambda L_2/a_0 a_2) + (\lambda L_1/a_2^2)]^{-1}$). If such a section occupies the greater part of the length of the system, the effective length of the resonator turns out to be significantly greater than the actual length, approximately in the ratio of a_0^2/a_2^2. This leads to a gain in the amount of the angular divergence by a_0/a_2 times (let us note that in the case of Figure 2.27, b, c, the ratio a_0/a_2 is equal to the multiplicity of the telescope formed by the lenses). In the final analysis this gain is achieved as a result of concentration of the entire light flux in small sections, but nevertheless the increase in the radiation density here is not so large as in the case of selectors with a diaphragm (Figure 2.24, a, b). In addition, for attenuation of this undesirable effect it is possible to use the fact that the radiation flux incident on a totally reflecting mirror of a planar resonator is less than the flux incident on the semitransparent exit mirror with reflection coefficient R' by $(R')^{-1/2}$ times (Section 1.4). Thus, in order to decrease the radiation flux in the sections with a small cross section it is sufficient to realize the energy yield from the opposite (right) end of the resonator. The reflection coefficient of the exit mirror R' must be selected as small as possible [148]. This choice becomes possible when using active media with sufficiently large amplification coefficient.

We have given so much attention to the methods of angular selection in lasers with planar resonator primarily because there are situations where it is not possible to get along without a planar resonator. Thus, pulsed lasers exist in which the excitation occurs nonsimultaneously in the different parts of the resonator cross section. In such cases the use of unstable resonators which are now a commonly recognized means of achieving small divergence is impossible--lasers with unstable resonators operate satisfactorily only under condition of simultaneous and not too nonuniform excitation of the entire operating volume. Planar resonators with small N can turn out to be more advantageous than unstable resonators also in the case of the presence of noticeable light dispersion with indicatrix of the type depicted in Figure 2.25, a--as we have seen, it does not prevent achievement of minimum divergence in planar resonators with large L (or L_{eff}), but can have a sharply negative effect on the parameters of lasers with unstable resonators (Section 4.1). For these reasons, both the system depicted in Figure 2.27, c, and the angular selection system entirely equivalent to it with a mirror telescope (Figure 2.27, d) proposed by one of the authors of [148]--Danilov--at the end of the 1960's are sometimes used at the present time. The version of such systems with nonresonant feedback [118] (Figure 2.27, e) which can be used for enormous amplification in the active medium is also of noticeable interest. The nonresonant coupling makes the laser in practice nonmisalignable and sharply increases the stability of its operation under the conditions of optical nonuniformities which are variable in time.

Multistage Lasers. There is another truly universal method of obtaining narrowly directional emission which, although it is not a resonator method, on the basis of its traditionalness it deserves mention in this chapter. This method consists in using a master oscillator and a number of subsequent amplification stages. The master oscillator can be low-power and have low efficiency, the achievement of unimodality under such conditions presents no difficulty. The emission of the laser is directed toward a telescopic system which increases the

light beam diameter and then, to amplification stages with gradually increasing cross section. Matching telescopes are again placed between the amplifying stages. Gradual expansion of the beam cross section theoretically also keeps the density of the amplified radiation at a level that is not too high and reduces angular divergence.

The use of almost all of the active material when operating in a purely amplifying mode has obvious advantages from the point of view of divergence of the radiation--indeed here there is no multiple transmission of light with respect to the same nonuniformity leading to accumulation of aberrations as in the planar resonator (Section 2.5). In spite of this fact, only powerful monopulse lasers, primarily solid-state lasers, are now being made multistage.

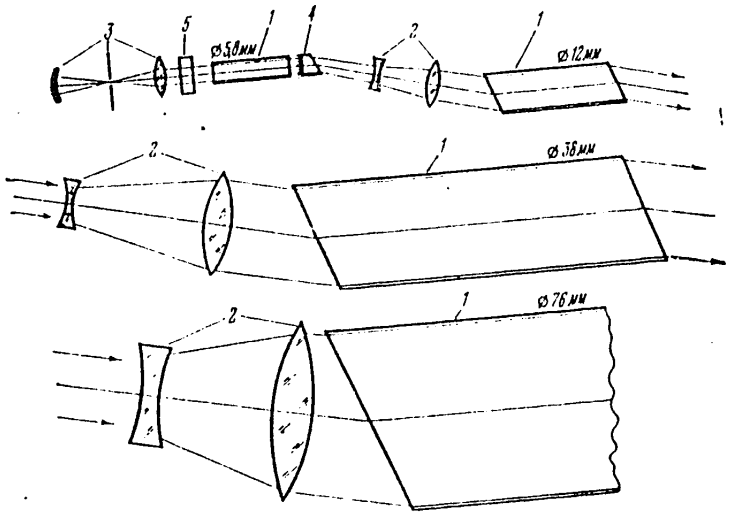

Figure 2.28. Example of a multistage system [129]: 1--active element; 2--telescopic system; 3--angular selector of the master oscillator with diamond diaphragm; 4--semitransparent mirror of the master oscillator based on a prism with Brewster angle; 5--shutter.

One of the first systems of this type assembled by the simplest "classical" system is depicted in Figure 2.28. Modern lasers for experiments in the field of laser thermonuclear fusion appear immeasurably more complex--they consist of a minimum of six parallel channels (for comprehensive illumination of the target), and they contain a truly enormous number of active rods, elements for splitting and reduction of the light beams, "decouplers" between the stages for separation of superluminescence, and so on. However, the main thing is that quite different factors determine the radiation divergence: as a result of extraordinarily high radiation density in the amplifying channel nonlinear processes develop leading to expansion of the radiation pattern and, in the final analysis, to self-focusing of the radiation inside the active material which is disastrous for such devices. Therefore the control of these processes acquires a decisive

role: In order that they not develop, the above-mentioned "optical relays" and other spatial filters are installed between the stages, which determines the angular divergence of the output radiation. Thus, the breakdown of the system into a set of stages here essentially pursues highly specific goals.

This situation is quite characteristic--the application of multistage devices turns out to be justified only in certain special cases and also when it is desirable to achieve record output parameters with universality of the device. Actually, in this way it is possible to obtain radiation density in the entire exit aperture close to the rupture threshold of the optical materials. The master oscillator is a small part of the system, and for mode changing it can simply be replaced by another one.

In the most frequently encountered cases where although not record, but very close to record parameters are required in combination with simplicity, modest size and weight characteristics, and so on, the lasers which are made with a single-oscillator system and one version or another of an unstable resonator take first position. We shall now proceed with a discussion of these lasers.

Chapter 3. Elements of the Theory of Unstable Resonators

Section 3.1. Some Initial Information

Brief Historical Survey. In 1965 the article by Sigmen [4] was published which established the beginning of the entire field of quantum electronics. This article discussed the possibility of the practical application of unstable resonators with large diffraction losses.

At that time the idea that resonators with large diffraction losses must have high selective properties began to win general recognition. This was promoted to a high degree by the explanation of the nature of multimode lasing presented by Tang and Statets (Section 2.4), from which it followed that in order to decrease the number of simultaneously excited transverse modes it is necessary to increase the differences of the diffraction losses (and not their ratios as was first assumed). The loss differences can be large obviously only when the losses themselves are large.

It was known that the transition from stable resonators to planar resonators is accompanied not only by an increase in volume of the lowest modes, but also an increase in the diffraction loss differences; both promote the achievement of lasing on a small number of the lowest transverse modes. The results of a few theoretical works (for example, [104]) also indicated that on passing through the stability limit and proceeding deep into the instability region the losses of the lowest mode continued to increase; this made it possible to hope that the losses of the other modes grow still more rapidly, and the selective properties of the resonator improve.

However, the transition to the instability region must, it would appear, also be accompanied by highly undesirable phenomena, above all, an increase in the threshold and corresponding reduction of the lasing power. In addition, numerical calculations have demonstrated that as a result of the growth of the field amplitude on the edge of the resonator and amplification of the edge diffraction the field distribution in the resonators with weakly convex mirrors is much more "cut up" than in the planar ones. What happens with field distribution with an increase in the curvature of the convex mirrors was unclear; by analogy with the planar misaligned resonator it seemed that it should become entirely unfavorable.

The results of the individual experiments in which variation of the parameters of the resonators near the stability limit was realized were not at all hopeful. Thus, in [150] when going into the instability region, a sharp decrease in the lasing power and an increase in the angular divergence of the radiation were observed. In [124] which was already referenced in Section 2.6, the transition to unstable resonators was accompanied only by a sharp decrease in the lasing power; the graph borrowed from [124, 28] and presented in Figure 2.23 could not point to the idea of the expediency of the application of unstable resonators with large diffraction losses.

Against this background Sigmen's article stood out sharply. The precariousness of the basic objections to the application of unstable resonators with large losses was demonstrated in it. The primary point of the paper was investigation of them in the geometric approximation. It led to results already known to us according to Section 1.2--a set of two spherical waves propagated in opposite directions converting into each other on reflection from the end mirrors can be found in an unstable resonator. The geometric investigation was strengthened by a very important argument that with large losses the influence of the edge diffraction can turn out to be weak, and the strict solution will differ little from the geometric solution. The fact is that although the peripheral part of the light beam is sharply disturbed by diffraction, as a result of significant expansion of the beam cross section on passing through the resonator, it then passes by the mirrors and the field distribution in them has little distortion. Running somewhat ahead, we see that the situation in reality turned out to be not so simple; the conditions under which edge diffraction does not play a special role and lasing is realized in a single transverse mode well described by the geometric approximation were finally discovered only in 1971 [151]. We shall discuss this in more detail in Section 3.3.

Sigmen also pointed out that in the case of unstable resonators with large diffraction losses it is expedient to realize diffraction output of the radiation, that is, use that part of the beam which bypasses the exit mirror as the useful signal (see also Section 2.6). Here it is possible to replace the semitransparent exit mirror by a totally reflecting one, thus leaving the total losses and the lasing threshold on the same level as in planar resonators. The adoption of these measures should help to avoid a sharp drop in the radiation power which previously appeared to be unavoidable.

Of course, all of these arguments needed comprehensive checking. It was even unclear whether the unstable resonators with large diffraction losses are actually selective; Sigmen himself stated the fear that the losses for the lowest and subsequent modes in such systems turn out to be approximately identical. Finally, the problem of sensitivity of the field distribution to the effect of intraresonator aberrations which is decisive for the problem of angular divergence of the radiation (see Chapter 2) is in general not discussed in this or all subsequent papers by Sigmen. It was investigated in 1968-1970 [152, 153]; it was only after this that the advantages of the unstable resonators with large diffraction losses in narrowly directional lasers were clearly recognized.

Section 3.3. Edge Effects and the Natural Oscillation Spectrum

Equivalence of Unstable Resonators and the Interrelation of the Solutions for the Various Types of Them. In the diffraction approximation the field distribution of unstable resonators, just as resonators of other types, is described by the eigenfunctions of a system of two integral equations relating the fields on the mirrors using the Huygens-Fresnel principle. For resonators with one-sided radiation output, when one of the mirrors is quite large and is totally reflecting (see Figure 3.3, a-d), it is possible to use the integral expression (1.24) or (1.24a) permitting a single equation to be compiled containing only the field distribution function on the other mirror.

If we go from field distribution on the exit mirror to the distribution on the equiphasal surface of the diverging wave of the geometric approximation (see above, Section 3.2), the desired equation acquires an especially obvious form [157]. Actually, substituting in (1.24a) $U(X, Y) = \chi(X, Y)\exp[i\pi N_{equiv}(X^2 + Y^2)]$ (by which the indicated transition is realized) and considering that $AD + BC = (M + 1/M)/2$, we obtain the following integral equation:

$$\gamma_m\chi_m(X, Y) \quad N\frac{\exp(2ikL_0)}{i}\int\int\exp\left\{i\pi NM\left[\left(X' - \frac{X}{M}\right)^2 + \left(Y' - \frac{Y}{M}\right)^2\right]\right\}\chi_m(X', Y')\,dX'\,dY'. \tag{12}$$

Let us write out the analogous equation for the two-dimensional case which will basically be considered; here we shall consider that the exit mirror has a peak reflection coefficient $\rho(x)$ which is variable with respect to cross section; the phase factor $\exp(2ikL_0)$ will be omitted:

$$\gamma_m\chi_m(X) \quad \sqrt{N/i}\int_{-\infty}^{\infty}\rho_1(X')\exp\left[i\pi NM\left(X' - \frac{X}{M}\right)^2\right]\chi_m(X')\,dX'. \tag{13}$$

Here, just as in (12), γ_m is the eigenvalue, $X \equiv x/a$ is the dimensionless coordinate; 2a is the characteristic size of the mirror; the parameter N_{equiv} used on making the transition to the new reference surface is, as before, related to N and M by the expression $N_{equiv} = (N/2)(M - 1/M)$; finally, $\rho_1(X) \equiv \rho(aX)$; for the case of a finite totally reflecting mirror

$$\rho_1(X) \quad \begin{cases} 1, & |X| \leqslant 1, \\ 0, & |X| > 1. \end{cases}$$

The equation for the symmetric resonator has the same form (Figure 3.3, e)* under the condition that the reflection coefficient of both of its mirrors is described by the same function $\rho_1(X)$.

* In this case the value of γ_m, just as M (see Section 3.1), pertains to passage through the resonator not at the bottom, but to one side.

Thus, all unstable resonators with one-sided radiation output equal to N and M (or M and N_{equiv}) and the same law of variation of the reflection coefficient of the exit mirror are equivalent to each other (for the special case of totally reflecting mirrors this result was obtained already in Section 1.2). Moreover, the eigenfunctions and the values for the resonators in which any two parameters out of three (N, M, N_{equiv}) are negative can be expressed in terms of the eigenfunctions and values of the resonator with the same with respect to absolute magnitude but positive parameters (it is true that for this when $M < 0$ it is necessary that the condition $\rho(-x) = \rho(x)$ be satisfied--indeed on changing the sign of M, the influence of only symmetrically distributed aberration sources can remain invariant; see Section 3.2). Let us demonstrate this in the example of resonators with $N > 0$, $M < 0$, $N_{equiv} < 0$ (these include, in particular, the confocal resonator depicted in Figure 3.3, c). On making the transition from (13) to the complex conjugate equation, replacing X' under the integral sign by -X' and using $\rho_1(-X') = \rho_1(X')$ and $M = -|M|$ we obtain

$$\frac{\gamma^*}{i}\chi^*(X) = \sqrt{\frac{N}{i}}\int_{-\infty}^{\infty}\rho_1(X')\exp\left|i\pi N|M|\left(X' - \frac{X}{|M|}\right)^2\right|\chi^*(-X')\,dX'$$

(the * indicates, just as everywhere, complex conjugation).

It is known that the eigenfunctions of such resonators are symmetric (χ_s) or antisymmetric (χ_a). Substituting the expression $\chi^*_{s,a}(-X') = \pm\chi^*_{s,a}(X')$ in the latter we obtained equations distinguished only by the factor for γ and for the rest coinciding entirely with the equation of the resonator having the parameters N, $|M|$. In the final analysis we have

$$\gamma_{s,a}(N, -|M|) = \mp i\gamma^*_{s,a}(N, |M|),$$
$$\chi_{s,a}(N, -|M|, X) = \chi^*_{s,a}(N, |M|, X).$$

For resonators with $N < 0$, $M > 0$, $N_{equiv} < 0$ (as an example we can use the symmetric resonator made of two sharply concave mirrors)

$$\gamma(-|N|, M) = \gamma^*(|N|, M), \quad \chi(-|N|, M, X) = \chi^*(|N|, M, X).$$

Finally, for $N < 0$, $M < 0$, $N_{equiv} > 0$ (for example, the confocal resonator made of concave mirrors in which a mirror with large R is used as the exit mirror)

$$\gamma_{s,a}(-|N|, -|M|) = \pm i\gamma_{s,a}(|N|, |M|),$$
$$\chi(-|N|, -|M|, X) = \chi(|N|, |M|, X).$$

From the presented formulas it is obvious that for all types of unstable resonators with identical N, M and N_{equiv} with respect to absolute magnitude, the eigenvalues are distinguished by phase factors, but they coincide with respect to modulus; thus, all of them have identical diffraction losses. The eigenfunctions recorded on the equiphasal surface of the diverging wave of the geometric approximation turn out to be complex-conjugate for resonators with $N_{equiv} < 0$

with respect to the eigenfunctions of resonators with $N_{equiv} > 0$. Inasmuch as the transition from the indicated reference surface to the surface of the mirrors is realized by multiplication by $\exp(i\pi N_{equiv} X^2)$, the distributions on the mirror surface are also complex-conjugate.

All of this permits us hereafter to limit ourselves to the investigation of any one type of resonator. We shall illustrate everything in the example of a resonator made up of two identical convex mirrors (Figure 3.3, e; $N > 0$, $M > 0$, $N_{equiv} > 0$), limiting ourselves, as a rule, to the investigation of the two-dimensional case and departing from this rule only when the transition to three dimensional leads to a qualitative change in the oscillation spectrum.

Unstable Resonators With Completely "Smoothed" Edge. Initially, following [151, 154], let us consider the properties of such unstable resonators for which the edge diffraction effects are insignificant. From the general arguments it is clear that this occurs in the case where the reflection coefficient of the mirrors, and with it also the field amplitude, smoothly decrease toward the edge of the system. From the materials presented in Section 3.2, it also follows that the field distribution of the fundamental mode in such resonators must be described well by the formula for the opticogeometric approximation (5) which satisfies equation (9). The relation between the equations of the diffraction approximation (13) and the opticogeometric approximation (9) is quite obvious. Actually, the factor $\exp[i\pi NM(X' - X/M)^2]$ for large values of $X' - X/M$ oscillates rapidly. Therefore if the product $\rho_1\chi$ is a slowly variable function of X' the magnitude of the integral in (13) is in practice determined only by the behavior of this function in the vicinity of the point X/M (see also Section 1.1). Expanding it near this point in a Taylor series

$$\rho_1(X')\chi(X') = \rho_1\left(\frac{X}{M}\right)\chi\left(\frac{X}{M}\right) + \left(X' - \frac{X}{M}\right)\frac{d(\rho_1\chi)}{dX'}\Big|_{X'=X/M} + \dots$$

and limiting ourselves to the terms written out, after integration we immediately obtain (9) with the aberration function $F(X) = \rho_1(X/M)/\rho_1(0)$ (in the case of an empty resonator $K \equiv 1$).

In order to discover what the mode spectrum of unstable resonators with smoothed edge is, let us consider their properties in the diffraction approximation in the example of a resonator with Gaussian distribution of the mirror reflection coefficient:

$$\rho(x) = \exp(-2x^2/a^2), \quad \rho_1(X) = \exp(-2X^2).$$

This case is especially interesting in that the mirrors with Gaussian distribution ρ can be considered to have an ideally smoothed edge: As a result of reflection of the light beams from them with an amplitude having Gaussian or uniform distribution, the Gaussian beams are generated, the far-field pattern of which does not have additional peaks. In addition, for resonators with such mirrors there is an exact analytical solution [3]. When the transverse dimensions of the mirrors and the diffraction losses are not too small (more

precisely, on satisfaction of the condition $\pi N_{equiv}(M - 1/M) >> 1$), after transition to the normal coordinates this solution acquires the form [151]*

$$u_m(x) \sim u_0(x) H_m\left(2\sqrt{-i\pi N_{equiv}}\frac{x}{a}\right), \quad m = 0, 1, 2, \ldots, \qquad \dagger = \text{equiv} \qquad (14)$$

$$\gamma_m \approx \left(\frac{1}{M}\right)^{m+\frac{1}{2}}, \qquad (15)$$

where $u_0(x) = \exp(-[2/(M^2 - 1)][x^2/a^2])$, $H_m(t) = (-1)^m \exp(t^2/2) \times (d^m/dt^m) \times \exp(-[t^2/2])$ are Hermite polynomials. Inasmuch as $H_0(t) = 1$, the function u directly describes the field distribution of the lowest mode; it is easy to see that it satisfies the opticogeometric equation (9) and can be found using formula (5):

$$u_0(x) \sim \rho\left(\frac{x}{M}\right)\rho\left(\frac{x}{M^2}\right)\ldots \exp\left(-\frac{2x^2}{M^2a^2} - \frac{2x^2}{M^4a^2} - \ldots\right) = \exp\left(-\frac{2}{M^2 - 1}\frac{x^2}{a^2}\right).$$

Now let us consider the Hermite polynomials. All of them contain the term t^m; in the first two polynomials it is unique ($H_0(t) = 1$, $H_1(t) = t$); the rest, in addition to it, also contain the terms of lower orders ($H_2(t) = t^2 - 1$, $H_3(t) = t^3 - 3t$, and so on). These additional terms play a significant role only for small values of the argument H_m; from (14) it is obvious that this occurs in the investigated case of large N_{equiv} only on the small central section of the resonator cross section. Thus, the first two modes on the entire resonator cross section, and the subsequent ones, on the larger part of it are described by the functions $u_0(x)(x/a)^m$ which are solutions of the opticogeometric equation (9) (see the end of Section 3.2). The exponents on x/a actually turn out to be integral, except, in spite of the proposition of Sigmen and Arratun, this does not follow from any conditions on the resonator axis (where the geometric approximation ceases to be valid), but from the requirement of the bounding of $u_m(x)$ at infinity [151].

An example of the field distribution of several lowest modes for M = 2 and $\pi N_{equiv} = 50$ is presented in Figure 3.10. The field amplitude of the fundamental mode (m = 0) decreases on going away from the center of the mirrors by a Gaussian law, the characteristic size of the "spot" in the plane of the mirror is $2a\sqrt{M^2 - 1}$. The fields of the other modes fill the central region of the resonator less uniformly. With an increase in the transverse index m the zone of larger amplitude shifts away from the center. The equiphasal surfaces of the modes with m = 0, 1 naturally coincide with the surface of the spherical wave of the geometric approximation (Figure 3.10, b). In the wave fronts of the higher-order modes near the center of the mirrors noticeable deviations from the spherical shape are observed--it turns out that the Hermite polynomials contain, in addition to t^m, also other terms.

* On comparison with the published data it is necessary to consider that in a number of papers, including [151, 154], the dependence of the field on time $\exp(i\omega t)$ was used and not $\exp(-i\omega t)$ as in the present publication (as a result, the sign on i changes everywhere).

Nevertheless, the most interesting for us now is not the specific form of the solutions in the resonator with Gaussian mirrors, but the fact that in expressions (14), (15) the form of the distribution $\rho(x)$ essentially determines only the factor $u_0(x)$ common to all eigenfunctions (inasmuch as $N_{equiv} \sim a^2$, the value of the argument H_m does not depend on a). It is also remarkable that the eigenvalues in accordance with (15) do not depend on the sizes of the mirrors and coincide with the eigenvalues which were obtained by formal methods in references [158, 159] for resonators with mirrors of infinite dimensions.

We have already seen that within the framework of the opticogeometric approximation the isolation of the factor describing the field distribution of the fundamental mode for any form of aberration function $F(x)$ reduces the corresponding equation to the equation of an ideal resonator (see the transition from (9) to (9a)). By analogy it is possible to propose that in the diffraction approximation the eigenfunctions have the form (14) not only for Gaussian mirrors, but also in the general case of many unstable resonators with well-smoothed edge. The field distribution of the fundamental mode u_0 which figures in (14) here must be considered using (5); the eigenvalues must be equal to the following (see (11))

$$\gamma_m = K(0)\rho(0)(1/M)^{m+1/2}. \qquad (15a)$$

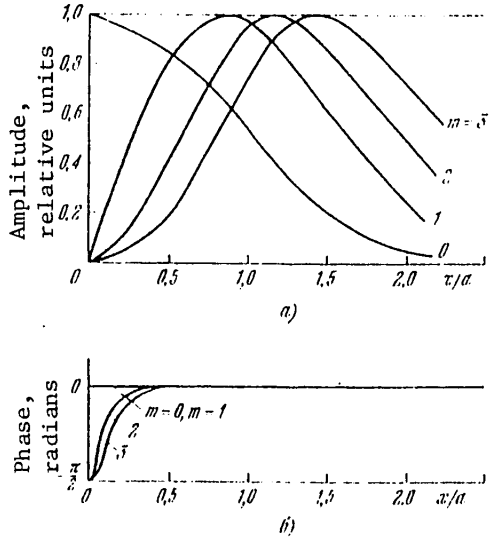

Figure 3.10. Field distributions of the lowest modes in a resonator with Gaussian mirrors ($M = 2$, $\pi N_{equiv} = 50$): a--amplitude distribution; b--phase distribution (the origin is the spherical wave of the geometric approximation).

Then it will be obvious that these arguments formulated in [151] are basically true; however, it is still necessary to become familiar with the properties of resonators, the mirrors of which have regular geometric shape with sharply outlined edge.

Unstable Resonators With Sharp Edge. As we have already mentioned in Section 3.1, in Sigmen's first paper [4] he stated the argument that in unstable resonators with large losses the edge diffraction must influence only the peripheral part of the beam immediately exiting from the resonator. Hence, it follows that the field distribution on the mirrors (or with one-sided output, on the output mirror) and the magnitude of the losses must not noticeably depend on the edge effects; the analogous conclusion regarding the properties of unstable resonators with large losses can also be found in Vaynshteyn ([3], problem No 8 for Chapter 4). However, precise machine calculations performed by Sigmen and Arratun [157] by the iterative method demonstrated that the picture of the properties of unstable resonators with totally reflecting mirrors of finite dimensions is far from simple. It was discovered that the field distribution for oscillations with the least losses does not differ too strongly, but nevertheless, noticeably, from the predictions of the geometric approximation (Figure 3.11). It turned out that the nature of this distribution and the magnitude of the losses depend in a complex way on the transverse dimensions of the mirrors, revealing explicit periodic dependence with variation of N_{equiv} for fixed M. The typical form of the relation calculated in [157] for the losses as a function of N_{equiv} is presented in Figure 3.12, a (the procedure used made it possible simultaneously to find the losses of the two highest Q modes).

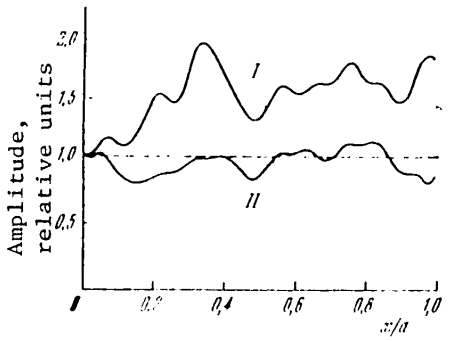

Figure 3.11. Amplitude distribution of modes with least losses near the degeneration point in the resonator with sharp edge (M = 1.86, $N_{equiv} \approx 5$) [157]. Curve I--$N_{equiv} \leq 5$; curve II--$N_{equiv} \geq 5$.

The work by Sigmen and Arratun was a significant contribution to the theory of unstable resonators with a sharp edge; in particular, the parameter N_{equiv} was introduced here. However, the physical meaning of this parameter remained unclear; in addition, when interpreting the calculated data the authors of [157] erroneously considered that the lower "wavy" line GHJ ... corresponds to one mode of the lowest order, and the V-type branches AGB, CHD and EJF ..., another symmetric mode. In reality, as was indicated in [152] and confirmed by the results of the latest machine calculations [160, 161] the apparent periodicity of the variation of the losses is caused by the fact that as N_{equiv} grows, the types of oscillations having the highest Q-factor alternately exchange places (similarly to how this occurs in Figure 2.21). This exchange takes place near

the integral values of N_{equiv} for which the modes turn out to be doubly degenerate with respect to losses (but not with respect to frequencies). Let us note that the configurations of the fields of two adjacent modes near the degeneration point are presented in Figure 3.11.

In Figure 3.12, b, c, a more complete picture of the behavior of the natural oscillations of a two-dimensional resonator [160] and a three-dimensional resonator with circular mirrors [161] is depicted. It is obvious that in the final analysis there are a small number of modes, the losses of which vary with N_{equiv} quasiperiodically so that these oscillations alternately become the highest Q. In the three-dimensional case these laws are also maintained for large N_{equiv} at the same time as in the two-dimensional case, beginning with a defined value of N_{equiv}, the curves cease to intersect--the degeneration of the modes with respect to the losses is removed.

Without going into a detailed analysis of these phenomena, it is possible directly to draw the conclusion that the edge effects in unstable resonators are still manifested although only the central and it would appear, almost undisturbed part of the beam as a result of diffraction is incident on the exit mirror. In order to understand the cause of this, it is necessary to consider that as a result of diffraction, in addition to the undistorted reflected wave, an additional wave also appears, the fictitious source of which is the edge of the mirror (see Section 2.2). Although the amplitude of the additional wave decreases sharply with removal from the direction of the reflected wave (Figure 3.13), some part of the radiation scatters also at large angles, including in the direction opposite to the direction of the incident wave (noted in the figure by the dotted arrows). This radiation gives the beginning of the converging wave, the properties of which were investigated in detail in Section 3.1. Let us remember the basic characteristic feature of the converging wave: at the same time as the intensity of the basic wave decreases on a single pass through the resonator by M or M^2 times, the radiation pertaining to the converging wave remains entirely inside the resonator for many passes. As a result, the converging wave, in spite of its negligible intensity near the edge of the system where it is formed, is amplified as it approaches the resonator axis to such a degree that it has a significant influence on the entire field structure.

The discussed picture, although primitive, nevertheless permits understanding of the role of the parameter N_{equiv} [154]. For this purpose let us return to Figure 3.9. In Figure 3.9 the dotted line depicts the equiphasal surface of the diverging wave moving in the direction of the mirror for the presently investigated case of an ideal resonator (the medium is absent or uniform). It is easy to see that this surface is equiphasal also for a converging wave moving away from the mirror. Therefore the radiation of the diverging wave incident on the edge of the mirror and then forming the converging wave passes between the equiphasal surfaces of these waves a total distance $N_{equiv}\lambda$. Thus, on variation of N_{equiv} by one, the phase difference between the diverging wave and the converging wave occurring as a result of edge diffraction varies by 2π, which also leads to quasiperiodicity of the properties of unstable resonators.

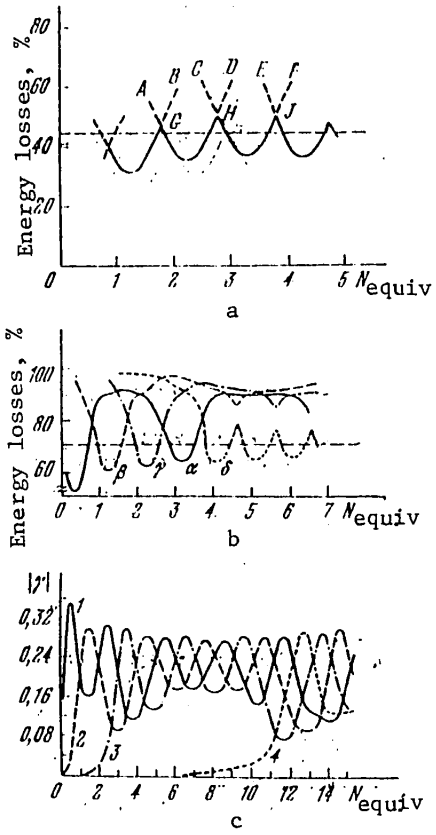

Figure 3.12. Losses and eigenvalues as a function of N_{equiv}: a--losses in the two-dimensional resonator, M = 1.86 [157]; b--losses in the two-dimensional resonator, M = 3.3 [160] (the dotted line is used to plot the losses for the lowest resonator mode with smoothed edge); c--the eigenvalues in the three-dimensional resonator with spherical mirrors, M = 5, the azimuthal mode index is equal to zero (there is no dependence on the azimuthal angle) [161].

Let us note that it is possible always to determine N_{equiv} by the distance between the equiphasal surfaces of the diverging and converging waves near the element bounding the beam cross section in the resonator, whereas the definition of N_{equiv} given in Figure 3.9 sometimes makes no sense. This occurs primarily in ring cavities and also in systems in which the beam cross section is limited not only by the exit mirror, but by the iris placed at a noticeable distance from it.

A more careful investigation of the properties of unstable resonators with a sharp edge can be made by the analytical methods of Vaynshteyn similarly to how this was done in Section 2.2 for the case of a planar resonator. We shall

become somewhat familiar with the mathematical aspect of the question in the following section where there is a discussion of the properties of resonators with central beam hole: the solution in the geometric approximation is in general absent there, and it is not possible to get along without the Vaynshteyn approach. Now we only note that as a result of considering the interference effects the radiation scattered by edge diffraction inside the resonator turns out to be distributed not with respect to all, but with respect to a number of discrete directions. Just as in Section 2.2, one of them corresponds to the wave "reflected" from the edge, and the rest, to the "transformed" waves; only inasmuch as the angle of incidence of the initial wave on the edge of the mirror α (see Figure 2.7) is very large here, among the "transformed" waves there are waves which are scattered not only at angles larger than the "reflected" one (that) is, with $\theta > \alpha$), but also at smaller angles ($\theta < \alpha$). A comparison of Figures 3.13 and 2.7 shows that in the case of unstable resonators, when a divergent wave is incident on the edge, the wave that is "reflected" from the edge is indeed convergent. The approximate calculations made by Lyubimov et al. [162, 163] demonstrated that the above-described complex laws actually are explained by interaction of the fundamental wave with the "reflected" wave and the one or two "transformed" waves closest to it. The radiation scattered in other directions quickly exits from the resonator, and therefore plays no significant role.

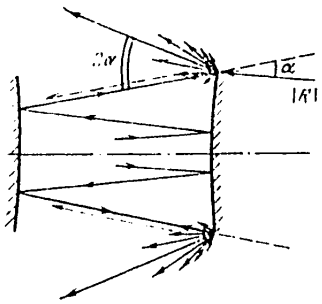

Figure 3.13. The formation of scattered waves during edge diffraction.

Subsequent foreign publications in which the Vaynshteyn methods were still used (see, for example, [164]) do not add anything theoretically new to the results obtained in [162, 163]. It must be noted that in a case of unstable resonators such calculations, especially considering at least one "transformed" wave, require extraordinarily awkward calculations and in the final analysis it is not possible to get around a machine solution of the systems of transcendental equations. Therefore their results are very difficult to see and are not clear. In addition, later it will be obvious that the problem of classification of the natural oscillations in unstable resonators, in general, and in those with a sharp edge, in particular, is primarily of academic interest. In practice only the nature of the behavior of the modes with the least losses turns out to be important, and it is entirely clear from the results of references [157, 152, 160, 161] in which the numerical iterative method was used (see Figure 3.12). Therefore we shall consider this problem in more detail and proceed to a discussion of the properties of real systems.

Specific Nature of Edge Effects Under Actual Conditions. The resonators with significant cross sectional dimensions and not too small $|M| - 1$ are of the greatest interest from the point of view of the problems of divergence of the radiation; obviously for them $|N_{equiv}| \gg 1$ is satisfied. The specific nature of the diffraction effects in such resonators primarily consists in the fact that the fundamental diverging wave is incident on the edge of the mirror at a comparatively large angle α defined by the geometry of the system (see Figure 3.13). From the radiation scattered as a result of diffraction only that part remains in the resonator which is deflected from the reflected beam at angles exceeding α. We have already seen that even in this part of the radiation the primary role is played by the converging wave corresponding to the angle of deviation 2α. It is easy to show that the values of α and N_{equiv} are related by the expression $\alpha = N_{equiv}\lambda/a$. In real resonators of powerful lasers N_{equiv} usually varies from several tens to many thousands (see Chapter 4); here the angles 2α reach several degrees.

At the same time it is known that the intensity of the diffraction scattering of light at large angles depends strongly on the nature of the edge of the mirrors [165]. The above-enumerated theoretical papers in which the effects of the mode degeneration with respect to losses, and so on were observed essentially pertain to the hypothetical case where the edge of the mirrors is ideally sharp and precisely outlined along a straight line or curve with center on the axis of the resonator. Such a model is entirely admissible when we are talking, for example, about the lowest modes of planar resonators which correspond to small angles of incidence of radiation on the edge of the mirror. For unstable resonators it is impossible to neglect the natural "blurring" of the edge and imperfection of the mirror outlines; both of these factors lead to attenuation of the diffraction scattering of the light at large angles and, consequently, to a decrease in the intensity of the converging wave. If this decrease is significant, the degeneration with respect to losses is removed and the eigenvalues approach the values predicted by formula (15).

Let us estimate what the deviations from the ideal conditions should be in order that the intensity of the converging wave decrease sharply. This is done most frequently for the case where the mirror reflection coefficient decreases from one to zero not discontinuously, but over the extent of a zone of finite width d (a similar situation occurs, in particular, when using mirrors with multilayered interference coatings). Actually, significant variation of the amplitude of the beam reflected from the mirror at the characteristic dimension d indicates that in the expansion of the amplitude in a Fourier series there are components present with spatial frequencies of $\sim 1/d$. Inasmuch as the angular distribution of the radiation is the Fourier type of distribution in the near zone (Section 1.1), these components correspond to the angles of inclination of $\sim\lambda/d$. Hence it follows that in order that the light be scattered primarily at angles less than $2\alpha = 2N_{equiv}\lambda/a$, it is necessary to satisfy the condition $d > d_0 \equiv a/2N_{equiv}$ [151]. Let us note that the situation here is entirely the same as in radio engineering where a decrease in the steepness of the pulse front is accompanied by the corresponding constriction of the signal spectrum.

A more careful calculation of the decrease in intensity of the scattered waves can be made as follows. Let us break down the entire "smoothing" zone in a series of sections Δx wide each. Replacing the "smooth" function $\rho(x)$ by a step function, we obtain the set of "steps" of height $-(d\rho/dx)\Delta x$. Each "step" obviously generates edge waves with relative amplitude $-(d\rho/dx)\Delta x$ (see Section 2.2). Adding them in the far zone considering the phase relations and replacing the summation with respect to all "steps" by integration, we find that the intensity of the edge waves scattered at an angle ψ is proportional to

$$B(\psi) \sim \int_{a-d/2}^{a+d/2} \exp\left(i\frac{2\pi}{\lambda}\psi x\right) \times \frac{d\rho}{dx}\,dx \quad [166];$$

let us note that $B(\psi)$ is the angular spectrum of a source of width d with amplitude distribution $-(d\rho/dx)$. If we consider that for $d \to 0$ the value of $B(\psi) \to 1$, it becomes clear that replacement of the sharp edge by a smoothed edge causes a decrease in the amplitude of the radiation scattered at an angle ψ by $1/|B(\psi)|$ times.

The estimates made using these relations in [166] demonstrated that the parameter d_0 introduced above is actually the critical width of the "smoothing" zone, on achievement of which the diffraction "reflection" from the edge turns out to be significantly attenuated. With a further increase in zone width, the intensity of the converging wave continues to decrease rapidly (in some cases experiencing pulsations; the specific form of the dependence of $1/|B(2\alpha)|$ on d/d_0 naturally is determined by the law of decrease of ρ inside the zone).

In the same paper [166], Sherstobitov and Vinokurov performed the corresponding calculations for two-dimensional resonators made of cylindrical mirrors with comparatively small N_{equiv}. The calculations were performed by the numerical method of Fox-Lee; the "smoothing" of the edge was introduced by direct assignment of the form of $\rho(x)$. It was found that smoothing does entail elimination of degeneration of the lowest modes with respect to losses. As an illustration Figure 3.14 shows the losses of the two lowest symmetric modes as a function of N_{equiv} in the resonator in which ρ decreases to zero in a region of width $\sim d_0$ by a linear law. It is obvious that the degeneration is completely removed, and the losses are close to the losses in a resonator with ideally smoothed edge (dotted lines). The field distribution of the basic mode u_0 in this case is excellently described by the formula (5); the distribution of the second mode, although not so good, still satisfactorily coincides with the results of the calculations by formula (14) with substitution in it of the same u_0 (see Figure 3.15).

Let us note that in general on making the transition to the higher-order modes, the effect of the converging wave regularly increases and for elimination of it, a greater and greater degree of smoothing of the edge is required. This is easy to understand if we begin with the field distribution in the resonator with ideally smoothed edge and introduce the partially smoothed edge of a disturbance leading to the formation of a converging wave. The initial field of the high-order modes is comparatively high on the periphery of the resonator and small on its axis (see Figure 3.10). Therefore with an increase in the transverse index,

on the one side, the initial intensity of the converging wave increases, and on the other, its influence on the field structure in the central part of the resonator increases. Hereafter we shall not touch on the problem of higher modes, but limit ourselves to analysis of behavior of modes with the least losses.

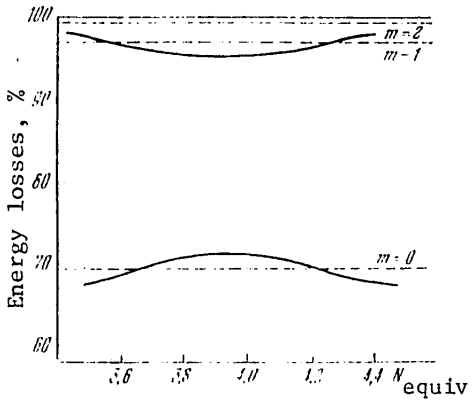

Figure 3.14. Losses of two lowest symmetric modes as a function of N_{equiv} in a resonator with partially smoothed edge [166]; the dotted lines are the values of the losses in the resonator with completely smoothed edge; M = 3.3.

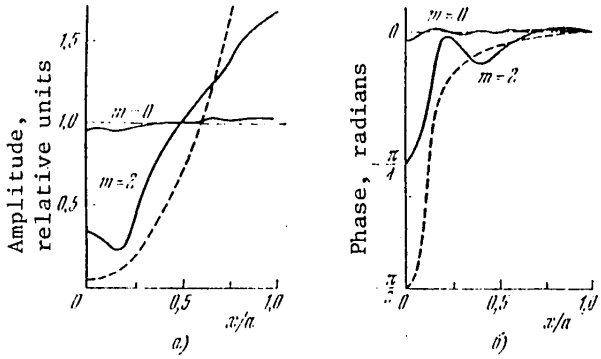

Figure 3.15. Field distributions of the lowest symmetric modes in a resonator with partially smoothed edge for M = 3.3, $N_{equiv} \approx 4$ [166]: a--amplitude distribution; b--phase distribution (the origin is the spherical wave of the geometric approximation). The solid lines represent the machine calculations, and the dotted lines, the calculation by formulas (14), (5).

Thus, for removal of the degeneration of the lowest modes of the two-dimensional unstable resonators with small N_{equiv} slight smoothing of the edge is sufficient (let us remember that for large N_{equiv} the degeneration in the two-dimensional resonators is absent even without any smoothing). This conclusion can be

directly generalized to the case of a three-dimensional resonator with spherical rectangular mirrors, for in such resonators, as we have seen many times in Chapter 2, the variables are easily separated.

In resonators with circular spherical mirrors the edge effects are manifested significantly more strongly: Here, in contrast to the three-dimensional resonators with cylindrical mirrors, a simple increase in N_{equiv} in the presence of a sharp edge does not lead to removal of the degeneration of the lowest modes (see Figure 3.12). The reasons for this consist in the fact that the density of the converging wave increases as it approaches the center more sharply for spherical mirrors than for cylindrical mirrors (it is known that the diffraction structure at the center of the pattern is expressed more strongly with diffraction on a circular hole than on a slit of the same transverse dimension). In references [163, 338], the Vaynshteyn method was used to show that for removal of the degeneration in resonators with circular spherical mirrors it is necessary to decrease the amplitude of the converging wave by comparison with the case of a sharp edge by approximately e $\ln(2\pi N_{equiv})/\ln M$ times. This corresponds to a not so small width of the smoothing zone: for the most favorable decreasing law

$$\rho\left(\rho(r) = \frac{1}{2} - \frac{1}{\sqrt{\pi}}\int_0^{(r-a)/d} \exp\left(-\frac{t^2}{2}\right) dt \right) \quad [166]$$

it will be $(d_0/\pi)\sqrt{1 + \ln[\ln(2\pi N_{equiv})/\ln M]}$, in the case of a linear law and laws close to it [166] it reaches $\sim 0.5 d_0 \ln(2\pi N_{equiv})/\ln M$. Nevertheless, for large N_{equiv} this is only a small portion of the total size of the mirrors.

Finally, the time has come to see what relation the case of the resonator with partially smoothed edge discussed by us has to the properties of the real systems. The parameters of solid-state lasers described in the following chapter correspond to the widths of the smoothing zone required for removal of the degeneration of the lowest modes by losses 0.1-1 mm; this blurring of the edge occurs quite frequently.

There are other factors which can lead to attenuation of the influence of the edge effects. Thus, for the smallest misalignments of the resonator the values of N_{equiv} measured from different sides of the system axis begin to differ from each other; these differences also arise as a result of the influences of aberrations (see Figure 3.9). Finally, the edge of the mirrors can be inexactly outlined. All of this leads to the fact that the waves beginning in different sections of the mirror loop arrive at the axis with different phases and therefore are mutually extinguishing (it is known that using the diaphragm with uneven edge, it is possible completely to blur the diffraction pattern far from the boundary of the geometric shadow). The meaning of the parameter d_0 here becomes entirely clear: For variation of the distance from the axis to the edge within the limits from $a - d_0/2$ to $a + d_0/2$ the value of N_{equiv} varies by one, the phase difference between the diverging and converging waves, by 2π.

Everything that has been stated together with certain other results of the above-enumerated experiments suffices for drawing the following basic conclusion: The degeneration of the lowest modes of real resonators with $N_{equiv} >> 1$, as a rule, is absent, and if necessary it can be reliably prevented by using such simple measures as the application of a bevel to the edge of the mirror (for more information about the suppression of edge effects by this method see [3]), the application of a serrated iris, and so on. Of course, we are talking only about cases where the degeneration is caused by diffraction on the edge of the mirror and not light dissipation in the active medium or on interfaces (the effect of the light dissipation will be briefly considered in Section 4.1).

The removal of the degeneration with respect to losses is accompanied by the fact that the field distribution begins to be described with a high degree of accuracy by the formulas of the opticogeometric approximation (it is only necessary to consider that manifestations of diffraction remain in the peripheral part of the beam leaving the resonator with small smoothing of the edge). The applicability of the opticogeometric approximation in turn indicates that the operation of the laser will be reliably realized on one transverse mode. Actually, the condition of steady-state lasing on the fundamental mode has the form $\gamma = K(0)\rho(0)/|M|^P = 1$ (see (11), (15a)). Hence it follows that the amplification coefficient of the medium on the system axis for any intensity and distribution of the pumping in the free lasing mode is equal to $|M|^P/\rho(0)$, which in accordance with the same formula (15a) is appreciably less than the amplification coefficient required for excitation of the other modes. Thus, the lasing regime can cease to be unimodal only in the presence of such large disturbances that the formulas (14), (15) become inapplicable even for the lowest modes. A special case of such disturbances is, as we have seen, the presence of an ideally sharp and exactly outlined edge of the mirrors.

All of these problems pertaining to edge effects in unstable resonators are of unquestioned cognitive interest. However, from the practical point of view in itself the problem of degeneration of the modes with respect to losses is not so important as can be demonstrated. From the numerical calculations performed in [157, 153, 162] and other papers, it follows that for small N_{equiv} the degenerate modes correspond in practice to the same angular radiation distribution, especially in the case of nontransparent mirrors, although only the outer part of the beam will exit from the resonator (see also Figure 3.11). With an increase in N_{equiv}, the fields of the highest Q oscillations, independently of the presence or absence of degeneration, differ less and less from the spherical wave field of the geometric approximation undergoing single diffraction on the mirror aperture. In addition, even for an ideally sharp edge if N_{equiv} is sufficiently large these differences are of an almost irregular nature (Figure 3.16). Thus, degeneration cannot be essentially felt in the angular divergence of the radiation, and it is undesirable only when constructing single-frequency lasers.

If the transverse dimensions of the cross section of the active medium are so small that N_{equiv} cannot exceed a few units, for achievement of the single-frequency lasing it is possible to select, in accordance with Sigmen's recommendations [167], resonator parameters such that N_{equiv} will be close to the a half-integer. In this case the difference of the losses of the two highest

Q modes turns out to be comparatively large even for a sharp edge (see Figure 3.12). It is only necessary to consider that the field distribution in the resonators with small N_{equiv}, as a rule, is highly nonuniform, which prevents the achievement of the maximum high output parameters of the lasers (for more information see Sections 1.4, 4.1).

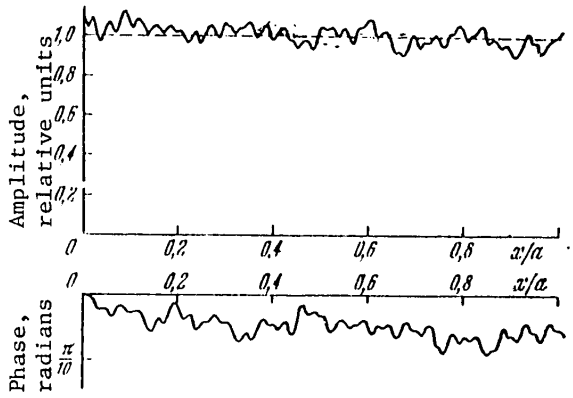

Figure 3.16. Amplitude and phase distribution of the basic mode of a two-dimensional resonator for N_{equiv} = 30, M = 2.38 [166].

In conclusion let us note that the above-discussed arguments were basically stated in [151, 154], and with minimum corrections, they are confirmed by the results of the numerical calculations in [166, 163, 338]. Thus, the problem of suppression of nonuniformity of the field distribution occurring as a result of the edge diffraction, first acquired urgency and found theoretical solution as applied to the problem of optical resonators. Some time later the same problem arose for the creators of powerful laser amplifiers. The fact is that when the density of the amplified radiation approaches the self-focusing threshold occurring under the effect of any factors the nonuniformity of the distribution can lead to the fact that at any point this threshold will be exceeded, and the active element damaged. One such factor can be edge diffraction; for suppression of its effect, the same procedures in essence were used as were discussed in [151] (the so-called anodizing of the aperture).

CHAPTER 4. APPLICATIONS OF UNSTABLE RESONATORS

§ 4.1. Unstable Resonators in Pulsed Lasers with Free Lasing

The basic result of using unstable resonators usually is expected to be the achievement of small angular divergence while maintaining the same energy characteristics of the laser as in the case of using planar or unstable resonators. It is perhaps simplest of all to do this for pulsed lasers using large volumes of active medium that are not too nonuniform. Actually, in the case of pulsed excitation usually high amplification coefficients are achieved; as will be obvious later, this permits the application of resonators with quite large magnification M, which without any of the contrivances of the type described at the end of the preceding chapter have low sensitivity to the effect of optical nonuniformities. If the operating cross section of the active zone is large, the values of N_{equiv} also turn out to be large; therefore the edge effects almost have no influence on the mode structure and have no negative effect on the directionality of the radiation.

Selection of the Type of Resonator and Its Parameters. The most important factors which determine the angular divergence of the radiation were investigated in the preceding chapter. Therefore now we shall primarily discuss the problems pertaining to the energy characteristics of lasers with unstable resonators: in the case of large volumes of the active medium, the problem of efficiency acquires primary significance. As for the efficiency of the lasers during their operation on a single transverse mode, unstable resonators here have explicit advantages over resonators of other types. Actually, it is known that the maximum efficiency of a laser is achieved usually when the laser radiation distribution in general features repeats the pumping distribution (§ 1.4). In planar resonators and, especially in resonators with stable configuration the field of one mode cannot uniformly fill a sufficiently large cross section, the correlation between the forms of distribution of the lasing and pumping fields is very weak (thus, in § 2.5 it was noted that the amplitude aberrations in a planar resonator primarily cause not amplitude, but phase distortions of the wave fronts). Accordingly, in lasers with such resonators usually the multimode oscillation mode is realized with large angular divergence of the radiation (§§ 2.3, 2.4).

Unstable resonators provide incomparably more favorable conditions for achievement of high efficiency in the presence of single-mode oscillation. With a uniform active medium and mirrors with reflection coefficient constant with respect to cross section, the field distribution of the lowest mode is close to Π-type. If the inverse population is nonuniform, then, as was noted in [152], in accordance with formula (5) the lasing field acquires a similar nature of distribution.

However, for realization of the indicated prerequisite it is necessary that a number of conditions be satisfied. First of all, of course, it is necessary that the lasing radiation fill the cross section of the active zone well over its entire length. If this is not so, the output power of the laser decreases, frequently more sharply than in accordance with the proportion of the used volume: the region in which the medium is excited, and the lasing radiation is absent, is a powerful source of luminescence and, as a result of amplification of it (so-called superluminescence [32]) it can significantly decrease the inverse population in the remaining volume.

On the other hand, it is necessary to see that the lasing radiation does not hit the sidewalls of the active element or the cell in which the lasing is realized. In addition to decreasing the efficiency of the system, this can lead to an increase in angular divergence of the radiation as a result of the influence of the scattered light.

Thus, it is necessary that the configuration of the beam propagated to the exit mirror exactly coincide with the configuration of the active element (the beam propagated in the opposite direction has less volume for one-way output). This imposes restrictions on the type of resonator used.

Most frequently, the active zone has a cylindrical shape. In this case the beam going to the exit mirror must be at least close to parallel. If M exceeds one by very little, the given condition is more or less observed even when using the simplest resonator made up of a planar and convex mirrors (see Figure 3.3,a), the beam cross section in which on the path from the plane mirror to the convex mirror increases by $2M/(M + 1)$ times. However, with large losses to radiation, it becomes necessary to use the asymmetric confocal systems depicted in Figure 3.3,c,d. The transverse dimension of the exit mirror must be $|M|$ times less than the cross section of the active element. Here, its shape should obviously be similar to the shape of the cross section of the active zone (from reading the theoretical papers it appears that it must be circular or square; in reality, this is not so at all).

A confocal resonator made of concave mirrors is less sensitive to aberrations (§3.2); in addition, for the same $|M|$ and distance between the mirrors it has $(|M| + 1)/(|M| - 1)$ times larger value of $|N_{equiv}|$ than the telescopic one. On the other hand, it also has a very large deficiency: the center of the spherical wave reflected from the exit mirror is inside the resonator (Figure 3.3,c). As a result, the beam following from the exit mirror fills the resonator cross section worse than in the telescopic one; however, it is still more important that the beam density at the focal point reaches an extremely large value and can easily exceed not only the rupture threshold of the solid active medium, but also the threshold of formation of breakdown in the gas. For the indicated reasons, in the majority of practical applications the theoretical resonator proposed in [185, 152] is used.

Then the question arises of selecting the optimal magnification M. From the point of view of diminishing the effect of large-scale optical nonuniformities it is desirable that M be as large as possible. For this purpose it is expedient to destroy other sources of losses to radiation and use completely reflecting mirrors. Then the admissible value of M is determined by purely energy arguments. In order to understand what these arguments are, let us consider the dependence of the output power of a laser with telescopic resonator on M. Just as in § 1.4, we

shall limit ourselves to the analysis of the simplest case where the pumping is uniformly distributed with respect to the volume of the active medium having a cylindrical shape, the interference phenomena between the radiation fluxes following in opposite directions do not appear, and the relation between the amplification coefficient and the total radiation has the form of (1.33). Introducing the radiation density in dimensionless units $\rho \equiv \alpha I$, let us rewrite (1.33) in the form

$$k_{yc} = k_{yc}^0/(1 + \rho^+ + \rho^-), \quad (1)$$

(a)

Key: a. amplification

where ρ^+ and ρ^- are the flux densities to the exit mirror and in the opposite direction, respectively (Figure 4.1).

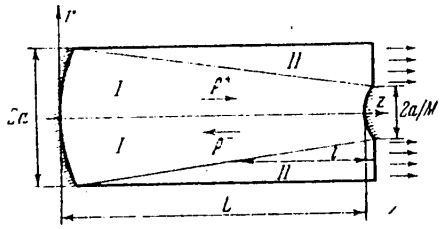

Figure 4.1. Radiation fluxes in a laser with telescopic resonator.

It is easy to see that inside the region I which is filled by the fluxes in both directions, the inverse population and the flux density itself vary only along the length $z(0 \leq z \leq L)$, and these values are constant with respect to cross section. Then for ρ^+ and ρ^- in the indicated region the obvious relations are valid:

$$\rho^+(z) = \rho^+(0) \exp\left\{\int_0^z [k_{yc}(z') - \sigma_0]\, dz'\right\},$$

$$\rho^-(z) = \rho^-(0) \exp\left\{-\int_0^z [k_{yc}(z') - \sigma_0]\, dz'\right\} \cdot \left(\frac{z_0}{z_0 - z}\right)^2, \quad (2)$$

where σ_0 is the coefficient of inactive losses; the factor $[z_0/(z_0 - z)]^2$ describes the decrease in the density of the diverging spherical wave on going away from an imaginary center z_0 coinciding with the common focal point of the mirrors.

Equations (1) and (2) must be solved jointly with respect to $\rho^+(z)$ and $\rho^-(z)$ considering the boundary conditions $\rho^+(0) = \rho^-(0)$ and $\rho^+(L) = \rho^-(L)$. Finding the exact solution in analytical form is impossible. For approximate solution it is convenient to use the fact that according to (2) $\sqrt{\rho^+(z)\rho^-(z)} = \rho(0)z_0/(z_0 - z)$.

Inasmuch as the sum $\rho^+ + \rho^-$ is with an accuracy to several percentages equal to $2\sqrt{\rho^+\rho^-}$ up to values of ρ^+ and ρ^- differing by two or three times (larger differences in practice do not exist) it is possible by the corresponding substitution to convert equation (1) as follows:

$$k_{yc} = k_{yc}^0 [1 + 2\rho(0) z_0/(z_0 - z)]^{-1}. \qquad (1a)$$

The substitution of (1a) in (2) with subsequent integration leads to the equation for determination of $\rho(0)$:

$$2\frac{M}{M-1}\rho(0)\ln\frac{[2\rho(0)+1]M}{2\rho(0)M+1} = 1 - \frac{\ln M + \sigma_0 L}{k_{yc}^0 L},$$

where $M = z_0/(z_0 - L)$, as always, is the magnification of the resonator.

Finding $\rho(0)$, it is possible by using (2) to calculate the distribution $\rho^+(z)$ in the region I. When the part of the radiation flux remote from the axis ($r > a/M$, $2a$ is the diameter of the active element) intersects the boundary between the regions and goes into zone II where $\rho^- = 0$, further amplification of the flux is easily considered by the corresponding formula for the amplifying mode [186], which is a direct consequence of the radation transport equation:

$$\ln\left(\frac{\rho_{\text{(a) вых}}}{\rho}\right) = (k_{yc}^0 - \sigma_0)\, l + \frac{k_{yc}^0}{\sigma_0}\ln\left[\frac{(k_{yc}^0/\sigma_0) - 1 - \rho_{\text{вых}}}{(k_{yc}^0/\sigma_0) - 1 - \rho}\right]_{\text{(b)}},$$

Key: a. out b. amplification

where ρ is the flux density at the entrance to region II; ρ_{out} is the flux density at the exit from the resonator as a function of the distance l traveled by the flux in this region (see Figure 4.1). It is obvious that the value of l, and with it also ρ_{out}, increase with an increase in r.

Figure 4.2 shows the graphs of the density distributions of the radiation leaving the resonator calculated in this way. As is obvious from Figure 4.2, with an increase in M the radiation density at the laser exit decreases, but the width of the radiating zone (a - a/M) naturally increases. For some value M_{opt} the power of the outgoing radiation will be maximal.

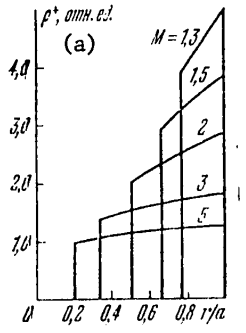

Figure 4.2. Density distribution of outgoing radiation with respect to cross section of the active element for the case $k_{0amp}^0 L = 3.0$, $\sigma_0 L = 0.12$ and different values of M.

Key: a. relative units

The effectiveness of the energy conversion and the resonator X introduced in § 1.4 can be calculated as the ratio of the number of lasing photons leaving the resonator $\int_{(S)} I\,dS$ (integration is performed over the area of the exit aperture) to the total number of acts of filling out the inverse population in the volume of the oscillator $\int_{(V)} P_{pump}dv$. Inasmuch as in the case of a four-level medium with uniformly broadened line and unpopulated lower level of the operating transition $P_{pump} = k^0_{amp}/\alpha$ (see § 1.4), we obtain $X = \left(\int_{(S)} \rho^+ ds\right) \Big/ \left(\int_{(V)} k^0_{yc}\,dv\right)$. In particular, for the case of a circular cylindrical element with uniform pumping

$$X = \frac{2}{k^0_{yc} L a^2} \int_{a/M}^{a} \rho_{вых}(r)\, r\, dr.$$
(a) (b)

Key: a. out b. amplification

Figure 4.3 shows the efficiency of the resonator X calculated using the last formula as a function of the value of M for a number of values of $\sigma_0 L$ and $k^0_{amp} L$ (let us remember that in the case of a four-level medium the ratio k^0_{amp}/σ_0 is the amount the lasing threshold is exceeded in the absence of losses to radiation, that is, for M = 1). The data for a telescopic resonator are compared with the data pertaining to a planar resonator with the same total losses and lasing threshold (the reflection coefficient of the output mirror R' is $1/M^2$).

From Figure 4.3 it follows that the efficiency of the energy conversion in a telescopic resonator in the given case is somewhat less, but it is very close to the efficiency in the corresponding planar resonator. Thus, for a laser with a telescopic resonator, the formulas of § 1.4 can be used under the condition of replacement of R' in them by $1/M^2$. In particular, for $\sigma_0 L$ that is not too large, the value of X can be determined using the expression

$$X \approx \frac{\ln M}{\ln M + \sigma_0 L}\left(1 - \frac{\ln M + \sigma_0 L}{k^0_{yc} L}\right), \tag{3}$$

the optimal magnification of the resonator, by the formula

$$\ln M_{опт} \approx \sigma_0 L\left(\sqrt{k^0_{yc}/\sigma_0} - 1\right), \tag{4}$$
(a)

Key: a. opt

finally, the maximum value of X, just as in the case of a plane resonator is approximately equal to

$$X_{max} \approx \left(1 - \sqrt{\sigma_0/k^0_{yc}}\right)^2. \tag{5}$$

The above-discussed analysis was performed in reference [187], being the first example of calculation of the energy characteristics of lasers with unstable resonators. Later, more complex cases were investigated which require very awkward machine calculations (we shall touch on the methods of performing these calculations

in § 4.2). Thus, in [188] calculations were made of the efficiency for nonuniform distribution of the pumping with respect to cross section and large excesses over the threshold; it turned out that the formulas (3)-(5) remain in force under the condition of substitution of the value of k^0_{amp} averaged over the cross section in them. Analogous laws occur, as is known, also in the case of planar resonators.

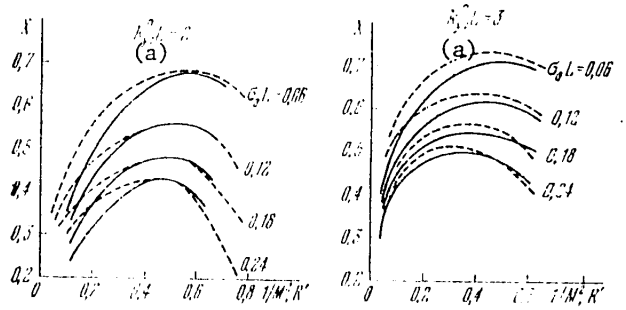

Figure 4.3. Efficiency of the resonator with telescopic (solid curves) and planar (dotted curves) resonators as a function of the values of $1/M^2$ and R', respectively, for $k^0_{amp} L = 2$ and 3.

Key: a. amplification

This similarity of behavior of the telescopic and planar resonators of course is no accident. Its causes consist in the fact that the nature of filling of the cylindrical active element with lasing radiation in these two types of resonators with identical losses to radiation is not so strongly distinguished as it appears at first glance. Actually, with equality of the losses in the medium, identical mean values of the amplification coefficient are established; consequently, the mean radiation densities approximately coincide. Then, along the path from the "blind" mirror to the exit mirror in a planar resonator, the radiation density increases by $1/\sqrt{R'}$ times (§ 1.4), in the telescopic resonator, by M times, that is, in the same ratio. Hence it is obvious that ρ^+ in these two resonators has similar values in the entire volume of the active medium. As for the radiation traveling in the opposite direction (ρ^-), in the telescopic resonator its distribution is less favorable: although the total radiation flux is approximately the same as in the planar resonator it is distributed not with respect to the entire cross section, but only with respect to part of it; worst of all is the filling near the exit mirror. As a result, the total density $\rho^+ + \rho^-$ is distributed over the active volume in the case of a telescopic resonator somewhat more nonuniformly, which leads to insignificant decrease in the efficiency.

Thus, the telescopic resonator insures an efficiency which is close to its maximum value defined by formula (5) if we select the radiation losses $1 - 1/M^2$ such as the optimal planar resonator would have. Moreover, the value of X in the vicinity of its maximum varies very slowly with M, and the variation of M within known limits is not related to a significant reduction in the efficiency of the system. This can be used so that when selecting M the arguments connected with divergence of the radiation are considered. For reduction of the divergence, it is, as a rule, expedient to use resonators with the largest possible M. Here the sensitivity of the resonator to the aberrations decreases (§ 3.2); in addition, the ring

at the exit will become less narrow. However, it is necessary to proceed to values of M significantly exceeding 2 with great caution. First of all, from § 3.3 it follows that single-mode lasing with uniform field distribution is achieved most reliably for large N_{equiv}. If the transverse dimensions of the active element are given, N_{equiv} reaches a maximum for M = 2. A futher increase in M, in spite of some increase in curvature of the mirrors causes a decrease in N_{equiv} as a result of a fast decrease in the transverse dimensions of the exit mirror.

Extremely large values of M can be disadvantageous also in the presence of light dispersion, especially at angles close to 180° (usually all possible interfaces are sources of this light dispersion). It is easy to understand the reason for this if we consider that with an increase in M the proportion of the radiation participating in the "regular" feedback channel decreases, and the light intensity mixedwith it as a result of dispersion of the basic flux remains unchanged; thus, the role of the light dispersion increases.

The proper choice of the resonator parameters even in the case of uniform active medium still does not guarantee that a high axial luminous intensity will be obtained. From the information presented in the preceding chapter it is clear that for this to occur, it is necessary to exclude the formation of converging waves with noticeable initial intensity. In the case of a telescopic resonator, the purely converging wave is formed, as is easy to see, with partial reflection of the basic wave from the plane interfaces perpendicular to the resonator axis; therefore the interfaces existing in the laser (for example, the end surfaces of the rod) must be inclined noticeably.

Results of Experiments with Neodymium Glass Lasers. The above-discussed arguments about the choice of the type and the parameters of an unstable resonator and also a signficant part of the concepts developed in Chapter 3 regarding the properties of unstable resonators were developed during the course of experimental studies of neodymium glass resonators [5, 152, 189, 153, 190, 191, 1968, 192-197], and they were confirmed by the results of these studies. In the example of lasers of the given type a most detailed comparison was made between the characteristics of the lasers with planar and unstable resonators; in practice all of the new versions of the systems based on unstable resonators were tested and studied for the first time. Let us discuss the basic results of the experiments pertaining to the lasers with the simplest two-mirror resonators discussed in this section.

For a diameter of the neodymium rod of 10 mm and length of 120 mm, the application of an unstable resonator led only to a twofold gain in axial luminous intensity by comparison with the case of a planar resonator [152]. In the greater part of the subsequent experiments, a highly efficient laser based on a rod 45 mm in diameter and 600 mm long which was described in [198] was used. It served as a prototype for the series manufactured GOS-1001 lasers and various versions of them. Here the axial luminous intensity on replacement of the planar resonator by an unstable one increased by tens of times. The angular divergence of the radiation measured by the half intensity level decreased from 2' to 15-20"; with respect to the half energy level, from 5' to 40" (Figure 4.4, curve I) [152]. Let us note that this situation is quite characteristic: the larger the laser, the greater the effect from using an unstable resonator in it. The achieved gain in divergence also increases with an increase in optical uniformity of the active medium; in this respect the investigated laser was entirely satisfactory.

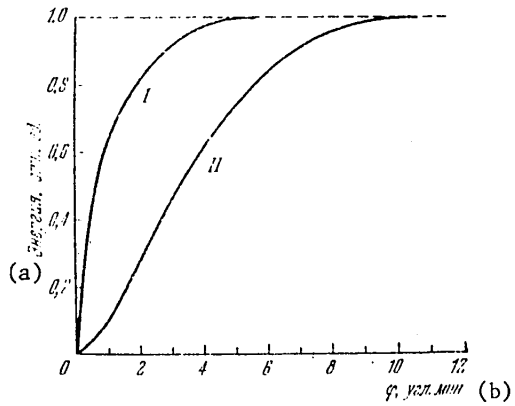

Figure 4.4. Angular distribution of the emission of a solid-state laser with telescopic resonator [152]: I -- resonator without interfaces perpendicular to the axis; II -- a coated glass plate was installed inside the resonator perpendicular to the axis. The proportion of the energy included in the cone with apex angle ϕ is plotted on the y-axis.

Key: a. energy, relative units
b. angular minutes

In the experiments with rods 45 mm in diameter the mirrors were totally reflecting. The losses to emission were equal to the optimal transmission factor for the case of planar mirrors, and they amounted to ~75% (M = 2). The use of a telescopic resonator insured approximately the same radiation energy as in the case of a planar resonator. In the case of a planoconvex system of mirrors, the output energy dropped by 1.5-2 times as a result of worse filling of the active element with the lasing radiation. After these experiments with large losses to emission, only telescopic resonators began to be used everywhere.

Subsequently, the output energy of an emission of a laser of the given type was brought to 4500 joules, and with series installation of two active elements in one resonator with M = 5, to 8000 joules [194]. The angular divergence of the radiation was: with respect to 0.5 intensity level, ~40"; with respect to half energy level, about 1'30".

Let us note the following important fact. In order to realize small angular divergence, in the case of a telescopic resonator it turned out to be necessary to incline the ends of the active element by 2-3° with respect to the resonator axis, which made it possible to avoid the converging waves generated by Fresnel reflection. The necessity for taking such measures was proved by the following demonstration experiment: a glass plate with coated surfaces was installed strictly perpendicular to the axis in a telescopic resonator with active element, the ends of which were inclined; the residual reflection of the coated surfaces did not exceed 0.3%. This turned out to be sufficient that the lasing pattern changed strikingly, and the angular divergence of the radiation increased so much that it approached the value characteristic of a planar resonator (curve II in Figure 4.4) [153]. The corresponding photographs are presented in Figure 4.5, a, b [photos not reproduced].

The mechanism responsible for poor directionality of radiation in such cases was studied in [197, 336]. It turned out that on introduction of a third planar mirror into the telescopic resonator, "spurious" modes appear which correspond to closed beam trajectories. Many passes through the active medium go with one reflection from this mirror. Therefore the "spurious" modes even for the smallest reflection coefficients of the planar mirror have lower excitation thresholds than the fundamental mode of a two-mirror resonator. Inasmuch as these modes, in addition, are characterized by high nonuniformity of the field distribution, some of them are excited immediately with all of the sad consequences following from this. And this is no surprise: in § 3.3 we encountered the situation where the presence of even a negligibly weak converging wave generated by edge diffraction leads to degeneration with respect to losses. Therefore the efforts sometime made to influence the lasing mode (in particular, lower its threshold) by artificial initiation of converging waves obviously always must lead to an increase in divergence of the radiation [336].

However, let us continue the discussion of the properties of lasers with "normal" unstable resonators not having sources of converging waves. Among the discovered peculiarities of such lasers, high stability of their output parameters is remarkable, including the form of the angular distribution of the radiation. Such phenomena characteristic of lasers with planar resonators as variation of the angular distribution from pulse to pulse, a gradual increase in angular divergence during aging of the active element, and so on were not observed. This property of lasers with unstable resonators is to one degree or another inherent in all systems with spherical mirrors, and it is frequently connected with their small criticalness with respect to the alignment precision. As the experiments have demonstrated, small rotations and shifts of the mirrors in the transverse direction cause only small changes in the beam direction. The magnitude of these variations corresponds completely to the predictions of the geometric approximation. The form of angular distribution is essentially distorted only for such large rotations of the mirrors that the axis of the resonator tightly approaches the flat surface of the sample [152] (an analogous cycle of studies for the case of a CO_2 laser was performed later in the paper by Krupke and Suya [199]).

Also in accordance with the geometric approximation, the displacements of one of the mirrors in the longitudinal direction cause variation of the curvature of the wave leaving the resonator. In the case of a telescopic resonator it is possible to use this means of focusing the beam at a given distance $d \gg L$ from the laser, increasing the distance between the mirrors by comparison with the distance L for confocal location of them by the amount $\sim(M + 1)L^2/(M - 1)d$ (focusing at the distance $d \sim L$ is also possible, but it is accompanied by a decrease in the output power as a result of "tapering" of the light beam in the active element).

In reference [152], a study was also made of the spectral and time characteristics of the emission of a neodymium glass laser with unstable resonators. There were no special differences from the characteristics of lasers with planar mirrors: the same random spikes, approximately the same integral width of the spectrum; only the duration of each spike turned out to be somewhat less, and the average time interval between them increased.

The reduction in duration of the spikes arose from the fact that the oscillations in unstable resonators are set up somewhat faster than in planar resonators. The

main reason for this is the presence of some mechanism of forced "spreading" of the emission over the cross section. We shall discuss this question in more detail at the end of this section when we are talking about lasers for which the rate of establishment of the oscillations plays the decisive role. As for the spectral distribution of the radiation, for planar and unstable resonators it is essentially the distribution of the radiation intensity between modes with different axial indices (see § 2.4). Near the axis of an unstable resonator the same interference of two counterflows and the formation of standing waves occur as in a planar resonator. Therefore the mechanism of the spatial competition of the axial modes in resonators of both types is identical in spite of the fact that in the unstable resonator the peripheral part of the active element is filled with radiation propagated in only one direction (see also the discussion of the problem of spectral selection in ring cavities in § 3.5).

The observations of the time expansion of the spatial distribution of the emission [152, 153, 192] demonstrated that during lasing, insignificant shifts of the center of symmetry of the angular disribution of the emission take place. In addition, the angular distribution also in individual spikes differed from the distribution for the ideal emitter. As a result, the integral width of the angular distribution with respect to time for the investigated lasers noticeably exceeded the diffraction limit. Obviously, this was a consequence of thermal deformations of the resonator, the vibrations of the samples, and so on. Taking measures against the effect of these factors led to a decrease in the radiation divergence.

In particular, the results of experiments with a laser based on an active element of great length and with rectangular cross section are indicative [192]. During the pumping pulse the sample underwent noticeable mechanical vibrations along the small dimension of the cross section. Accordingly, the center of gravity of the angular distribution completed complex oscillatory movement in the same direction; the divergence of the radiation with respect to this direction was four times greater than the diffraction limit, and it amounted to ~2'20". The replacement of the concave mirror by a dihedral prism with convex surface turned into the resonator and an edge parallel to the large dimension of the cross section led to complete correspondence to the ideas developed in § 3.5, almost total stabilization of the direction of radiation. The angular divergence decreased in this case to 1'. If a telescopic resonator made of two prisms was used, the degree of stabilization of the direction was somewhat less, and the divergence was ~1'10".

Extraordinarily high selective properties of unstable resonators with large Fresnel numbers were fully manifested in the test experiments performed in [190]. The manifestations of optical nonuniformity of the medium and other similar causes were completely eliminated here. A two-dimensional unstable resonator with M = 2 made of totally reflecting mirrors, one of which was planar and the other, convex cylindrical (Figure 4.6), was used. The active element, just as in the preceding case, was a rectangular parallelepiped, the location of the flashlamps insured high uniformity of distribution of pumping in the direction of the large dimension of the cross section. The curvature of the wave front emitting from the resonator was compensated for by an additional lens.

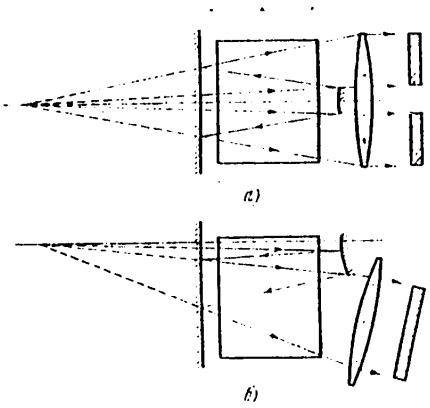

Figure 4.6. Diagram of a laser with rectangular active rod and two-dimensional unstable resonator: a) symmetric, b) asymmetric exit of the radiation (the crosshatched rectangles on the right depict the exit beam cross section).

Two methods of exiting this radiation from the laser were tested which are illustrated in Figure 4.6, a, b; N_{equiv} was ~1700 and ~7000, respectively. In the former case the integral angular distribution of the radiation with respect to pulse time along the direction in the plane of the figure coincided almost with the Fraunhofer diffraction pattern on two rectangular openings (Figure 4.5, c [photo not reproduced]; the long extent of the pattern with respect to the second direction is connected with the fact that in this direction the resonator was equivalent to a planar resonator; in addition, the compensating lens was not cylindrical as should be, but spherical). The band contrast is very close to one, which indicates high spatial coherence of the radiation (let us note that the distance between two beams leaving the resonator was ~120 mm).

Noticeable deviations from the results of the diffraction at the exit aperture of the laser and when using the system depicted in Figure 4.6, b with exit of the radiation in the form of a single beam in one direction from the axis of the resonator were not detected. As a result of increasing the aperture width, in this case the divergence was less than in the first case, and it was 2" or $1 \cdot 10^{-5}$ rad (Figure 4.5, d [photo not reproduced]).

After performing these experiments the thesis that unstable resonators with large N_{equiv} with uniform medium provide single-mode lasing with diffraction angle of divergence of the radiation could be considered proved. It was only left to establish whether departure of the divergence of the radiation of real lasers from the diffraction limit is a consequence of such prosaic causes as imperfection of the elements of the resonator, optical nonuniformity of the medium, or the "high-order modes" sometimes mentioned in the literature are at fault here. According to § 3.2, the wave front of a light beam which is the fundamental mode of an unstable resonator is formed in it just as on transmission of the beam through a multistage amplifier (Figure 3.6). Therefore the best answer to the stated problem can be given by direct experimental comparison of the divergence of the radiation of a real laser with an unstable resonator with divergence at the exit of the multistage amplifier

(see § 2.6) constructed from analogous active elements. This comparison was undertaken in [195].

The basic results of [195] are presented in Figure 4.7. Curve 1 corresponds to the angular distribution at the input of the final stage of amplification, curve 2, at the output of the multistage system. The data for the laser with telescopic resonator are plotted using x's; it is obvious that the multistage system in its "pure" form insures somewhat less divergence of the emission. However, if we cover the central part of the exit aperture of the multistage system so that the beam acquires the same circular cross section as in the case of a telescopic resonator the divergence of the radiation of the devices of both types comes close to coinciding (see curve 3).

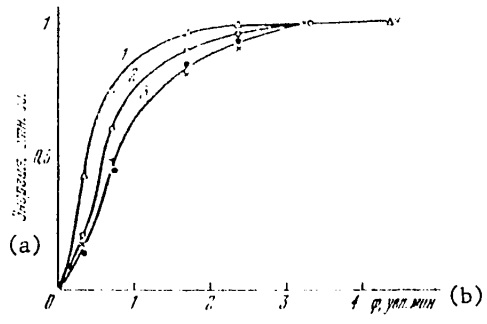

Figure 4.7. Angular distribution of the radiation energy (the proportion of the energy in a cone with apex angle ϕ is plotted on the y-axis): 1 -- at the entrance of the final stage of a multistage system; 2 -- at the exit of a multistage system with circular aperture; 3 -- annular exit of the radiation; x -- telescopic resonator, ● -- multistage system with annular diaphragm.

Key: a. energy, relative units
b. angular minutes

Attention is attracted by the fact that the differences between curves 2 and 3 cannot be explained by purely diffraction phenomena: the halfwidth of the angular energy distribution as a result of diffraction of the plane front in a circular opening was 5" more under the conditions of [195], and in the annular opening, a total of 4" more. Obviously these differences were caused primarily by the fact that the optical uniformity of the central part of the pumped neodymium glass rod is higher than its periphery (information about the nonuniformity induced in such cases is presented in [200]); therefore the addition of the central part to the annular exit aperture also causes a noticeable decrease in the divergence.

From Figure 4.7 it is obvious that preliminary stages and the final amplifier in the given case make similar contributions to the total radiation divergence with respect to magnitude. From the materials of § 3.2 it follows that for a telescopic resonator used in [195] with M = 2 the distortions of the wave front coming as a result of large-scale nonuniformities before the last pass through the active rod and directly in this last pass are also similar with respect to magnitude. The analogy between the multistage system and the telescopic resonator is quite obvious here.

Thus, carefully made unstable resonators are actually capable of insuring the same radiation divergence as multistage circuits (considering obvious corrections connected with the differences in the exit apertures). As will be obvious in §4.3, by using these resonators amplifiers can be constructed which provide enormous amplification of the weak signal in one standard active element (considerable work is required, in particular, in devices consisting of many channels synchronized by a single master oscillator). At the same time, the experience of [195] demonstrated that the problems pertaining to energy efficiency are solved on the basis of unstable resonators much more simply than when using multistage systems (as a result of a significantly smaller number of elements in the optical system of the device). Therefore the sphere of application of the awkward multistage systems primarily remains the rare cases where for the sake of achieving record radiation parameters any means are considered justifiable.

The entire research cycle discussed above which was performed in the example of pulsed neodymium glass lasers with free lasing permitted sufficiently complete discovery of the possibilities connected with the application of unstable resonators in their simplest version. This cycle was preceeded by a total of two articles with reports on experiments with similar resonators. The first of them is the initial paper by Sigmen [4] which we have mentioned many times and in which, in addition to the formulation of a number of the most important theoretical arguments (§ 3.1), the preliminary results of studying a ruby laser with unstable resonator are also discussed; the second is the paper [201] on experiments with a pulsed argon laser having a discharge tube 7 mm in diameter. In both cases it was impossible to obtain any positive effect from transition to the unstable resonator.

Gas Pulsed Lasers with Unstable Resonators. Problem of Setting up the Oscillations. Subsequent foreign publications about the application of unstable resonators in pulsed lasers began to appear only in 1972 [202, 203], and they pertained to the case of CO_2 lasers. No new information about the properties of unstable resonators was contained in these papers, and nothing special was presented on a purely technical level. Actually, among several of the first experiments the highest output parameters were achieved in [203]: for a pulse energy of 3.5 joules, the radiation divergence was $\sim 2 \cdot 10^{-4}$ radians, and the brightness was $\sim 2 \cdot 10^{13}$ watts/(cm^2-steradian). For comparison we mention that in Soviet lasers with telescopic resonator based on neodymium glass long before this the smaller angular divergence was "mastered" with an output energy of $\sim 10^3$ joules, and in 1971-1972 there were already lasers with brightness of $\sim 10^{17}$ watts/cm^2-steradian) [204, 205].

Beginning with that time, unstable resonators began to be used also with invariant success in lasers of almost all types. It is sufficient to mention, for example, the creation of an electroionization laser with a pulse energy of 7500 joules [206]. However, the results of experiments with metal vapor lasers are of the greatest cognitive interest [207]: the specific peculiarities of these lasers forced a new look at some theoretically known properties of unstable resonators. The fact is that the amplification coefficient of the medium is extraordinarily high here; on the other hand, the population inversion here exists for such a short time that during this time the light travels through the resonator only a few times. Since low divergence is desirable at all costs, it is of primary importance for the optical cavity to be capable of rapidly isolating the fundamental mode from noise radiation.

The problem of establishing oscillations in optical resonators was first encountered in 1961 by Fox and Lee [9]: the iterative calculations that they performed to a significant degree simulate the processes occurring in real lasers; the initial field distribution written into the iterative procedure plays the role of the "nucleating center," the source of which in real lasers is spontaneous emission. Then Fox and Lee noted the obvious relation between the rate of establishment of steady oscillations and the differences in the losses of the individual modes: actually, during the time of passage of the light through an empty resonator the intensity ratio of any two modes varies by $(1 - \Delta_1)/(1 - \Delta_2)$ times, where Δ_1 and Δ_2 are their diffraction losses. Obviously the intensity ratio will vary in the same way also in the presence of a medium with uniformly distributed amplification coefficient k_{amp} with respect to volume (the eigenvalues of the integral equation of the resonator turn out to be multiplied by the same coefficient $\exp(k_{amp}\ell)$ in this case, (see § 1.3). If the medium was uniformly excited at the time of beginning of development of lasing from the noise "nucleating center," the situation will be maintained until the lasing power builds up to such a degree that saturation level is reached.

Hence it follows that the more the losses of the individual modes differ, the faster the generation of certain modes against the background of the others will occur; in particular, the oscillations in unstable resonators must be set up much faster than in plane, and especially stable cavities. For these reasons the rate of establishment of the oscillations in the most unstable resonators increases with an increase in $|M|$.

Although all of these facts were well-known, the problem of calculating the time required for the diffraction directed beam to form in an unstable resonator from spontaneous emission was clearly stated only in [207], and it was gradually solved in [207-209]. It is true that the authors of the indicated papers for some reason considering the given situation exceptional tried to get around using the known results and methods of the theory of optical resonators, even such generally used ones as the introduction of the equivalent resonator. Accordingly, for this quite simple problem they obtained a very complex solution, making, in the course of the matter, an entire series of erroneous statements (for more details see [210]). In particular, their advice to select the resonator parameters so that the converging beam will expand to the former cross sectional dimensions invariably in an integral number of passes is meaningless. Therefore it is better to discuss a significantly simpler solution to the same problem presented in [210].

Let the active medium have the cross section 2a × 2a and be placed inside a telescopic resonator (Figure 4.8). Let us follow, for example, the fate of the nucleated radiation which at the initial point in time is emitted near the convex mirror in the direction of a concave mirror. We shall take the spherical equiphasal surface of the diverging wave located on the convex mirror, the center of curvature of which is at the common focal point of the mirrors as the reference surface. The complex amplitude of the nucleation field of one of the polarizations on this reference surface can be represented in the form of the series

$$u(x, y) = \sum_{k,l} u_{kl} \exp\left(k\pi i \frac{x}{a}\right) \exp\left(l\pi i \frac{y}{a}\right), \quad k, l = 0, \pm 1, \pm 2, \ldots$$

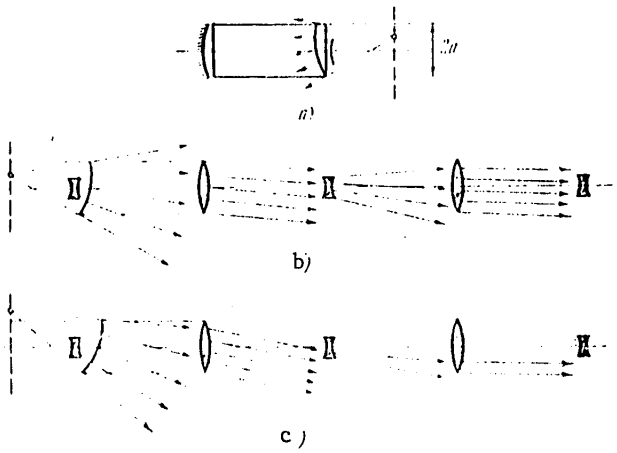

Figure 4.8. Transmission of spherical waves through a telescopic resonator: a) one of the "diverging" waves; b), c) transmission of diverging waves with centers of curvature near the zone 2a wide (b) and outside this zone (c) over an equivalent line.

This series corresponds to the set of spherical waves with randomly distributed amplitudes u_{kl}, the mean value of which can be calculated beginning with the power of the spontaneous radiation for a solid angle $(\lambda/2a)^2$. The centers of curvature of these waves lie in the focal plane and are shifted from the common focal point of the mirrors in two directions a distance $k\lambda f_2/2a$, $\ell\lambda f_2/2a$, where f_2 is the focal length of the convex mirror, k and ℓ are the wave indices. The centers of curvature of the waves, the radiation of which completely covers the concave mirror, fills a zone 2a × 2a in size (see the figure); the number of such waves, consequently, is equal to $(4a^2/\lambda f_2)^2$. As the figure shows, some of the radiation of waves lying near this zone also reaches the range of the laser; however, it very quickly leaves the confines of the optical cavity entirely. Therefore, except for the very earliest stages, the number of waves taking part in the process of lasing onset is $(4a^2/\lambda f_2)^2$, i.e. the spontaneous emission falling in a solid angle of $(2a/f_2)^2$.

Now let us trace the behavior of the waves; this is entirely possible within the framework of the geometric approximation until the divergence tightly approaches the diffraction limit. Obviously after the first reflection from the concave mirror part of the cross section of each wave equal to $1/M^2$ remains inside the resonator; the waves themselves go from spherical to planar with propagation directions inclined with respect to the axis at angles of $(k/M)(\lambda/2a)$; $(\ell/M)(\lambda/2a)$. The width of the entire range of angles, that is, the total divergence of the emission is $\frac{4a^2}{\lambda f_2}\frac{1}{M}\frac{\lambda}{2a} = 2a/Mf_2$. After each subsequent passage through the resonator, the amount of radiation remaining in it decreases by M^2 times. The slopes of all the beams, and with them, also the total angle of divergence, decrease by M times.

Thus, after n passes through the resonator, the proportion of the radiation of all of the waves entering into the "nucleating center" equal to $1/M^{2n}$ remains in it,

and the total "geometric" divergence is $2a/M^n f_2$. The number of passes n_0 during which the "geometric" divergence decreases to $\lambda/2a$ and thus the formation of the diffraction diverging beam (the basic mode) is completed, is defined by the expression $2a/(M^{n0}f_2) = \lambda/2a$ or $M^{n0} = 4a^2/(\lambda f_2)$. By this time the proportion of primary "nucleating" radiation equal to $1/M^{2n0} = (\lambda f_2/4a^2)^2$ remains inside the resonator. It is easy to see that this proportion corresponds to the radiation intensity which initially pertained on the average to one wave.

In spite of the primativeness, the given analysis leads to the same quantitative results which were obtained in [207-209] using somewhat more complex manipulations with the "compressing waves." Using these results, it is entirely possible to undertake specific calculations of the kinetics of such lasers. However, the most important conclusion can also be drawn without performing such calculations. From the above-presented relations it follows that the time of formation of a diffraction-directional beam with fixed dimensions of the resonator decreases slowly and monotonically with an increase in M (inasmuch as $n_0 = \ln [4(M - 1)a^2/\lambda L]/\ln M$). Thus, the thesis that to obtain the smallest possible divergence it is necessary, considering the stipulations made on page 53 to use unstable resonators with the largest possible magnifications, has received another, quite weighty substantiation.

This entire concept was checked experimentally in [207]. When using a telescopic resonator with M = 6 in a copper vapor pulse laser, the calculated time required for fundamental mode lasing turned out to be greater than the time during which the radiation density inside the given laser could grow from the noise density to the saturation level. As a result, the integral divergence with respect to the pulse duration exceeded the diffraction limit by almost an order. For M = 200 (!) this limit was reached, it is true, at the price of a sharp drop in radiation power as a result of the extraordinary rise in the lasing threshold. Probably for intermediate M it would be possible to achieve both small divergence and sufficient radiation energy[1]).

§ 4.2. Unstable Resonators in Continuous Lasers

Survey of Experimental Papers. Somewhat later than in pulsed neodymium glass lasers, unstable resonators began also to be used in continuous gas lasers. Among the first publications only one short, but exceptionally interesting article [211] stands out which to a great extent anticipated the future development of the resonators of gas dynamic lasers; we shall return to this paper later. As for other studies in 1969-1973, their subjects were low-pressure electric discharge CO_2-lasers [199, 212, 213] and chemical lasers [214, 215]. The early paper by Krupka and Suya [199] is isolated here. In this paper a telescopic resonator was used in practice for the first time; as a result of the carefulness of the experiment and the high optical uniformity of the active medium the authors were able to observe the diffraction structure of the distribution in the far zone with full width of the central peak on the order of 1' ($3.5 \cdot 10^{-4}$ radians)[2].

---

[1] This was done in the recent experiment [332].

[2] In this paper an analysis was made for the first time of the consequences of misalignment and variation of the curvature of the mirrors in two types of confocal unstable resonators.

It must be noted that in all of the enumerated studies except [211] not only the goals, but also the conditions differed sharply from the conditions of the experiments with neodymium lasers, primarily by the fact that in view of the modest dimensions of the resonator cross sections and the long wavelength, the Fresnel numbers N were quite small. The theoretical limit of the angular divergence of these lasers, on the other hand, was not small. Thus, in the same paper by Krupka and Suya, the width of the radiation ring at the exit from the laser was ~1 mm; the angle into which half the energy went, although it was not measured, must have been equal to $5 \cdot 10^{-3}$ radians under these conditions. This divergence could be completely achieved also using a planar resonator. Therefore the basic positive result of the mentioned experiments is not the achievements in the field of angular selection, but experimental testing of a number of conclusions of the theory of unstable resonators pertaining to the magnitude of the losses, the nature of their dependence on N_{equiv}, and so on. A detailed summary of the results of testing the theory is available in the highly substantial survey by Sigmen [216]. It is of interest that although the majority of researchers, in accordance with the recommendations of Sigmen [167], have carefully selected the resonator parameters so that N_{equiv} will be close to a half integer, no article contains data indicating that this choice actually is useful from the point of view of angular divergence of the emission.

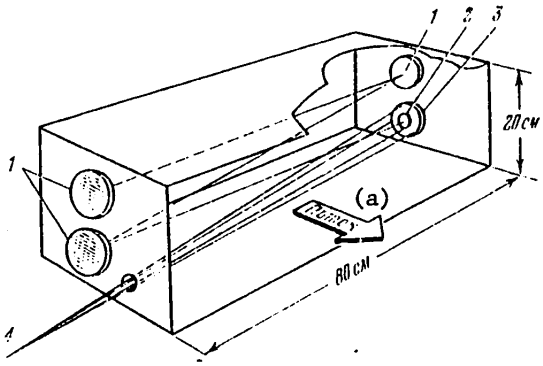

Figure 4.9. Schematic representation of the active zone and resonator of a powerful gas dynamic laser [211]: 1 — planar mirrors, 2 — convex exit mirror, 3 -- external concave mirror, 4 -- exit beam.

Key: a. flow

Now let us more carefully consider the results of [211]. This article is devoted to experiments with a powerful gas dynamic laser; the schematic representation of the active zone with the resonator borrowed from [211] is presented in Figure 4.9. As is obvious from the figure, the resonator is installed so that the lasing radiation will pass through the gas flow perpendicularly to the direction of motion of the flow itself. This arrangement of the cavity, which is called transverse, is adopted because the high average powers require large flow rates of the gas mix, and organization of uniform gas flows with large flow rates is possible only in the case where the resonator elements are beyond the limits of the flow cross section (in electric discharge lasers the same thing occurs also with the electrode assemblies).

Tests were run on a gas dynamic laser in [211] with resonators of two types. The first type was a stable resonator made of two large metal mirrors, in one of which a system of many holes 1.5 mm were made, the total area of which was on the order of 6% of the total area of the mirror. This procedure does not withstand any criticism from the point of view of divergence of the radiation (§ 2.5), but it permits realization of a resonator with given small losses to emission, and, as the experience of [211] shows, it can be used for experimental optimization of the energy characteristics of the laser. With this resonator the output power was 55 kilowatts.

The second type resonator is depicted in Figure 4.9. It was formed by four mirrors and was already unstable. One of the mirrors was convex, it served as the output mirror, and accordingly was smaller in diameter than the others. The beam passing near it fell on the additional concave mirror and was focused on the hole in the wall of the cavity through which it was taken outside. The use of a system with three passes through the active medium permitted, in spite of small amplification per pass, operation of the laser with magnification of the resonator M = 1.6; the output power was 30 kilowatts.

An almost twofold reduction in lasing power by comparison with the case of a stable resonator indicates that the achievement of the maximum efficiency of energy conversion in the gas dynamic laser resonator is not such a trivial problem as for pulsed lasers. It is necessary to consider that such a resonator consists, as a rule, of several carefully aligned (or even equipped with an automatic alignment system, see [217]) cooled mirrors and is, together with the fastenings, the aligning slides, and so on, a quite complicated device. It is part of a still more complicated engineering structure which is the fast-flow laser as a whole. Inasmuch as the purely empirical selection of the optimal resonator under such conditions becomes too thankless, the theoretical methods of analysis have been widely developed, the investigation of which we shall proceed with.

Methods of Calculating the Efficiency of Flow Lasers. It is necessary to distinguish two cases immediately. Whereas the fast-flow laser operates in the frequency mode where the excitation of the medium is realized by individual, periodically repeating pulses, the procedure for calculating its energy characteristics does not differ in any way from the procedure for calculating the efficiency of the resonator of ordinary pulsed lasers. Actually, one pumping pulse lasts, as a rule, 10^{-6} to 10^{-4} seconds; the medium during this time can travel such a short distance that it can be considered stationary during the pulse (the flow velocity in the frequency lasers usually does not exceed 100 m/sec. In pulsed lasers, as we know from §1.4, the state of the active medium in any elementary volume of it under the given pumping conditions is uniquely defined by the density of the lasing radiation passing through this volume. This makes it possible to talk not only about the efficiency of the laser as a whole, but also about the efficiency of energy conversion in any part of its volume, which significantly facilitates the understanding of the basic laws (§ 1.4). The local nature of the dependence of the amplification coefficient on the radiation density leads to significant simplification also of the quantitative calculations of lasers with unstable resonators. First, the equations describing the state of the medium themselves are simple in this case. Secondly, it is very easy by using the threshold condition to find the radiation density on the axis of the resonator before finding the distribution in the entire volume (see § 4.1), which greatly accelerates the convergence of the ordinarily used iterative procedure.

In continuous-action flow lasers the situation is quite different. The concept of local efficiency here cannot exist in general: the previously excited active medium flows through an entire beam of generated radiation, and the number of atoms reacting with the beam can be calculated only beginning with knowledge of the radiation distribution as a whole. It is also more difficult to calculate the radiation density in advance on the system axis inasmuch as the inverse population on the axis depends not on this density, but on the entire history of the medium reaching here, in particular, the field density on its entire path.

Similar laws occur also in the case of side optical pumping of induced Raman scattering lasers frequently called Raman [combination] lasers or VKR[1]-converters[218]. On the other hand, the amplification coefficient of the lasing radiation on the combination frequency is proportional to the pumping radiation density on the initial frequency. On the other hand, the attenuation of the pumping radiation on passage through the medium is almost wholly determined by its interaction with the generated radiation -- without lasing, the primary pumping radiation is poorly absorbed by the medium. It is easy to see that the pumping light density in Raman lasers is, from the point of view of resonator theory, the complete analog of the inverse population density in flow lasers; the residual absorption in the Raman laser medium corresponds to a decrease in the inverse population down stream with respect to the gas as a result of spontaneous relaxation of the active medium of the flow laser.

In 1968 Alekseyev and Sobel'man [219] pointed out that the application of a planar resonator in a Raman laser with side pumping is fraught with highly unpleasant consequences. Inasmuch as the amplification coefficient near the edge of the resonator from the side of which the pumping is realized, usually noticeably predominates over the losses on the combination frequency in the mirrors and the medium, the lasing radiation density here turns out to be extraordinarily high (if its growth does not prevent the beginning of lasing on subsequent combination frequencies, for which the radiation on the first combination frequency is itself pumping). At the same time, with an increase in the density of the converted (Raman) radiation, the attenuation coefficient of the primary radiation increases -- the region of powerful lasing screens the remaining volume from the pumping radiation. Thus a tendency shows up for the lasing region to contract into a very narrow zone, and this is difficult to eliminate. Analogous phenomena must occur also in flow lasers although usually not in such sharply expressed form (we shall discuss the causes of this somewhat later).

In the case of an unstable resonator, independent development of lasing on the periphery of the converter or the flow laser is impossible, for the lasing radiation must come from the central section of the cross section. Extraordinary growth of the lasing radiation density on the axis of the system is impossible, for it causes rapid growth of the density also on the periphery, which leads to a decrease in the amplification on the axis. As a result, the regime turns out to be self-balanced; the lasing radiation fills the resonator cross section, its density is established on a level such that the number of pumping quanta reaching the axis in the Raman laser or excited atoms in the flow laser insures exact satisfaction of steady state conditions.

---

[1] The first letters of the Russian words that mean induced Raman scattering].

These arguments are formulated in [154], and they were confirmed by the experimental data of the above-quoted reference [211] (the nonuniformity of the intensity distribution observed there with respect to cross section of the unstable resonator did not exceed ±50%). In all of the subsequent theoretical papers devoted to estimation of the efficiency of the continuous lasers, a study is made of the self-balanced lasing regime on the lowest transverse mode.

It is true that in the experiment of [220] with defined resonance, a mathematical model of a flow laser was proposed from which it follows that the lasing regime must be not steady, but autooscillatory with an oscillation period on the order of the drift time of the gas flow through the resonator zone. If this model were correct, the autooscillations would be characteristic of even a broader class of lasers than the authors of [220] themselves proposed[1]. However, the medium was considered single-component in [220], the speed of light was considered infinite, and the geometric approximation, valid, even under the conditions where the properties of the medium vary sharply over the extent of small sections of the resonator cross section near its axis. Judging by the results of [221], it is sufficient to do away with the proposition of single-component mixture so that the trend toward the autooscillations will decrease sharply (and in real lasers, as a rule, mixtures are used which contain more than one component). Consideration of the fact that for the light to pass through the resonator takes a finite time is extremely important and must also lead to damping of the oscillations (from the papers at the beginning of the 1960's devoted to the kinetics of solid-state lasers it is known that neglecting this fact usually leads to absurd results). Thus, the deep autooscillation mode is hardly widespread. As for the ordinary and unavoidable oscillations of intensity caused by fluctuations of the resonator Q-factor, and so on, they can hardly lead to significant departure of the energy parameters of the laser averaged over a large time interval from the calculation results in the quasistationary approximation (see § 1.4).

In itself the calculation of the efficiency of a laser operating in the steady state mode in the general case reduces to finding a self-consistent combination of distributions of the amplification coefficient and the lasing field. The equations describing the dependence of the amplification coefficient distribution on the excitation conditions and the lasing field depend on the peculiarities of the medium and are quite different. As for the lasing field distribution, for it it turns out most frequently to be sufficient to use the geometric approximation. Actually, we have already discussed the causes by which it is possible to neglect the effect of the edge diffraction in lasers with large M_{equiv} (§ 3.3). The consideration of large-scale nonuniformities of the active medium does not require diffraction approximation (§ 3.2). Moreover, if the medium is not too nonuniform, it is possible also to take the path of the beams the same as would occur in an ideal resonator. Hence, it follows that weak optical nonuniformity of the active medium, just as the edge diffraction, can in general not be considered in the energy calculation. On the other hand, inasmuch as the angular divergence of the radiation depends primarily on the phase distribution at the laser output, and the nonuniformity of

[1] At the end of the indicated article, an additional factor is erroneously introduced to describe the phenomena of amplification saturation, at the same time as consideration of these phenomena is already built into the initial equations.

the intensity distribution influences it weakly, the amplification saturation phenomenon must be felt little in its magnitude; this conclusion follows from the materials of § 1.1 and is confirmed by the results of sometimes undertaken specific calculations (for example, [222]). Therefore the width of the radiation pattern can be estimated in the first approximation without calculation of the energy characteristics of the laser.

In order to find the self-consistent solution most frequently an iterative method is used. The simplest iterative procedure used in the 1960's to study the phenomena of amplification saturation in planar and stable resonators [100, 90, 109] consists of the following. An initial field distribution (usually uniform) is taken; this distribution is substituted in the equations of the medium; the latter are solved, and the spatial distribution of the amplification coefficient is found. Then the new field distribution is calculated as a result of single passage of the initial beam through the resonator with the active medium. The newly obtained field distribution is substituted in the equations of the medium, and so on. As applied to the calculations of lasers with unstable resonators in a weakly nonuniform medium performed in the geometric approximation, the given procedure can be written as follows: $F_{n+1}(r) = f[u_n(r)]$, $u_{n+1}(r) = F_n(r)u_n(r/M)$, where F is the aberration function calculated considering the distribution of the amplification coefficient (see § 3.2), and the index denotes the number of the iteration. The calculations are quite tedious, for although only the field distribution at the exit mirror u(r) figures in the above formulas, for the calculation of F(r) it is necessary to deal with the amplification coefficient distributions (and, consequently, the field distribution) in the entire volume of the laser.

As was noted above, the convergence of the iterative procedure can be accelerated significantly by preliminary calculation of the radiation density and inverse population on the resonator axis. In the case of lasers considered in the preceding section, it was sufficient for this purpose to consider the conditions on the axis itself. Later it will be obvious that this problem is also solved for flow lasers, it is true, using more complex calculations. The data obtained on the magnitude of the field under the state of the medium on the resonator axis are used in the subsequent calculations; here the condition of stationarity of the regime turns out to be automatically satisfied in all phases of the iterative procedure. Finding the amplification coefficient distribution next, this makes it possible for us to not limit ourselves to single "transmission" of the beam through the resonator with the medium and to find the steady state field distribution corresponding to the given picture of the state of the medium. The iterative procedure acquires the form $F_{n+1}(r) = f[u_n(r)]$, $u_{n+1}(r) = u(0)F_n(r)F_n(r/M)F_n(r/M^2)\ldots$, where u(0) is the previously found field amplitude on the axis. As a result, the volume of the calculations is reduced noticeably, especially for complex mathematical models of the medium. The calculations of pulsed lasers with nonuniform optical pumping mentioned in § 4.1 [188] and the calculations of gasdynamic lasers discussed below were performed by approximately the same method.

Other procedures are also used which permit reduction of the volume of the calculations both when finding the field distribution by the given parameters of the resonator and state of the medium and for calculations of lasers as a whole. Although the authors of each of these procedures present very convincing arguments in its favor, it is now difficult to determine which of them is actually more

effective. Therefore those who desire to familiarize themselves in more detail with the method of the calculations are referred to numerous corresponding articles [222-227, 188, 156], and so on); at the same time we shall limit ourselves to the fact that we shall explain some peculiarities of the calculations and the behavior of flow lasers in the example of gas dynamic lasers with two-mirror telescopic resonator investigated in [188, 228]. All of the basic laws here are the same as in the case of resonators of the type depicted in Figure 4.9 (if, of course, we compare lasers with identical amplification not on the beam width, but on the entire path from one terminal mirror of the resonator to another). Lasers with resonators, the axis of which is "broken" not across, but along the direction of the gas flow behave differently; we shall not consider them.

Simplest Model of a Gas Dynamic Laser Medium. Procedure and Results of Energy Calculations of Gas Dynamic Lasers with Twin-Mirror Resonator. In the overwhelming majority of gas dynamic lasers the inverse population is created, by the proposal of Konyukhov and Prokhorov [229], by adiabatic expansion of a gas mixture consisting primarily of CO_2 and N_2. These two components also play the primary role in the lasing process. CO_2 molecules are characterized by a comparatively short oscillatory relaxation time; the laser transition is also realized in them. Fast loss of the oscillatory energy reserves in this component is frequently compensated for by resonance transmission of excitation from the N_2 molecules on collision with them.

The relative molar concentration 1 - c of the second component of the mixture is larger than the first (c) and the majority of the total oscillatory energy reserves is concentrated in the second component, N_2, which is, therefore, a type of energy "reservoir." As a result of the long natural oscillatory relaxation time of the molecules of the second component, the energy from this reservoir is consumed primarily for excitation of molecules of the first component.

Although the atoms located on a quite large number of oscillatory levels of both components participate in the operation of the laser in one way or another, Konyukhov [230] proposed limiting ourselves to a system of a total of two equations for description of the relaxation processes of the medium occurring in the resonator zone. These equations, being reduced to the maximum convenient form for calculations of the resonators, have the form [188]

$$\frac{dk_1(x, z)}{dx} = \frac{ck_2 - (1-c)k_1}{h} - \frac{k_1}{h_1} - (\rho^+ + \rho^-)k_1,$$

$$\frac{dk_2(x, z)}{dx} = -\frac{ck_2 - (1-c)k_1}{h} - \frac{k_2}{h_2}.$$

Here k_1 is the amplification coefficient of the laser radiation; it is proportional to the oscillatory energy reserves in the first component (the population of the lower laser level is considered equal to zero, which usually does not lead to large errors); k_2 is the value having dimensionality (but not meaning) of the amplification coefficient and characterizing the oscillatory energy reserves in N_2; ρ^+ and ρ^-, just as in the preceding section, are the densities of the lasing radiation fluxes directed in opposite directions in the corresponding units; the designations of the coordinates are presented in Figure 4.10; h_1, h_2 are the distances during the time of passage of which by the flow of mixture oscillatory relaxation of the

individual components will occur in the absence of resonance energy exchange; finally, h is the distance during the time of passage of which the processes of resonance energy exchange, neglecting processes of other types (oscillatory relaxation, induced emission), cause relaxation of the ratio of the energy stored in the components k_1/k_2 to the equilibrium value of $c/(1 - c)$ (it is considered that on collision of two different molecules the probability of exchange of excitation does not depend on which of the molecules is excited before collision). Let us note that as a result of the fact that the energy exchange between the components is realized with finite velocity ($h \neq 0$), the total oscillatory energy reserve in the medium cannot decrease too rapidly with as high a density of the generated radiation as one might like. This should attenuate the manifestations of the mentioned trend toward "constriction" of the radiation in the case of a planar resonator.

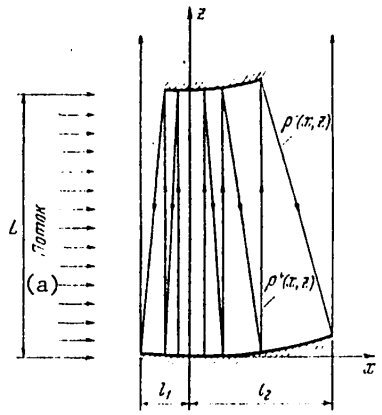

Figure 4.10. Diagram of a telescopic resonator in a flow laser.

Key: a. flow

It is possible to demonstrate that the transition from the density of the output radiation ρ^+ in the adopted units to the resonator efficiency X defined as the ratio of the number of quanta of output radiation to the total number of excited molecules at the entrance to the resonator should take place according to the formula

$$X = \int \rho^+(s)\, ds \left\{ \int [k_1(s') + k_2(s')]\, ds' \right\}^{-1},$$

where the first integral is taken with respect to the exit optical aperture of the resonator, and the second with respect to the flow cross section surface at its entrance to the resonator.

In spite of simplicity of the given model, its application insures satisfactory precision of the energy calculations of the gas dynamic laser in a defined range of variation of composition and parameters of the gas mixture [231]. In the greater part of the specific calculations performed with its help, the results of which will be discussed below, the following initial data standard for gas dynamic lasers were used: mixture composition 15% CO_2, 83.5% N_2, 1.5% H_2O; gas flow

velocity 1500 m/sec; gas pressure in the vicinity of the resonator 0.1 atm, temperature in the flow 350 K. These data correspond to the following values of the parameters which figure in the equations of the medium: $c = 0.15$, $h = 0.1$ cm, $h_1 = 4$ cm, $h_2 = 250$ cm. Let us also present the value of such an interesting characteristic of the active medium of the flow laser as the length H on which independent relaxation of the excitation is realized in the absence of the lasing field. As is known, any multicomponent mixture, the energy exchange rate between the components of which significantly exceeds the rates of the remaining processes, has such a unique relaxation length. For our medium this condition is satisfied ($h \ll h_1, h_2$); the total relaxation length is $H = [(c/h_1) + (1 - c)/h_2]^{-1} \approx 25$ cm.

At the entrance to the resonator the active medium was considered excited uniformly over the flow cross section and in equilibrium ($k_1^0/k_2^0 = c/(1 - c)$), the total magnitude of the application coefficient of the entrance to the resonator $k_1^0 L$ varied from 0.3 to 0.6 (L is the flow width of the medium). For maximum energy pickup for the location of the mirrors depicted in Figure 4.10, their shape obviously must be rectangular, which was assumed in the calculations. The reflection coefficient of each mirror was considered to be 98%.

The calculations were performed for resonators both made of cylindrical mirrors and made of spherical mirrors. In the first case the calculations were not too complicated inasmuch as all of the distributions are essentially two-dimensional. However, the resonator made of cylindrical mirrors can insure angular selection only with respect to one direction. In the case of spherical mirrors which in practice is more important the calculations are greatly complicated: the gas flow alternately intersects the planes passing through the axis of the resonator at different angles to the direction of motion of the flow, and the solutions in these planes turn out to be dependent on each other. Therefore when constructing the solution in the entire volume it is necessary in all steps of the iterations to manipulate the total three-dimensional field distributions and amplification coefficient distribution. The only exception is one plane passing through the resonator axis on which the solution can be found without constructing distributions in the remaining volume -- the plane in Figure 4.10. The solution of the corresponding two-dimensional problem permits the field on the resonator axis to be found immediately, which greatly facilitates subsequent calculations.

It also turned out to be convenient to divide the resonator by the axial plane $x = 0$ into two parts having in the general case different lengths ℓ_1, ℓ_2, (see Figure 4.10) and to proceed with calculations of the distributions in the right-hand side only after the solution on the left-hand side has been completely constructed.

For optimization of the resonator, its magnification M, the widths of the left and right-hand sides ℓ_1 and ℓ_2 were varied. In addition to the effectiveness of the resonator X, for each version the values of the relative losses characteristic of flow lasers were also calculated -- relaxation in the volume X_{rel}, removal from the resonator X_{rem} and absorption in the mirrors $X_{mir} = 1 - X - X_{rel} - X_{rem}$. Let us remember that X is the ratio of the number of quanta leaving the laser in the form of useful radiation to the total number of excited molecules entering the resonator at the same time; the relative relaxation and removal losses are

fractions of this total number lost as a result of the processes of deactivation by collisions and as a result of removal of excited molecules that have incompletely interacted with the radiation from the resonator; the meaning of X_{mir} is entirely clear.

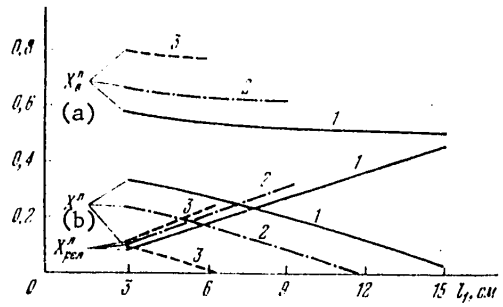

Figure 4.11. Efficiency of the left-hand side of the resonator X^m, the relative relaxation losses in its volume, X^{ℓ}_{rel} and the removal from it X^{ℓ}_{rem} as a function of the length of the left-hand side ℓ_1 for M = 1.33: curves 1, 2, 4 -- for $k_1^0 L$ = 0.6, 0.5 and 0.4, respectively.

Key: a. X^{ℓ}_{rem} b. X^{ℓ}_{rel}

Let us proceed with the investigation of the results of the calculations pertaining to the case of the resonator with spherical mirrors. The relations are presented in Figure 4.11 for the efficiency of the left-hand side of the resonator X^{ℓ} and relative losses X^{ℓ}_{rem}, X^{ℓ}_{rel} as a function of the width of this part with respect to the flow ℓ_1. As is obvious from the figure, with a decrease in ℓ_1 the losses to relaxation are reduced approximately proportionally to ℓ_1 at the same time as the losses to removal vary slowly; as a result, the efficiency X_{ℓ} increases. The meaning of these laws becomes clear if we consider the following peculiarity of the solution for the left-hand side. On the axial plane x = 0 separating the left and right sides of the resonator, the distributions and densities of the field and, what is especially important, the amplification coefficient turned out to be quite uniform in all of the calculated cases. Thus, over the extent of the left-hand side of the resonator the amplification coefficient with respect to the entire flow cross section decreases from the initial value of k_1^0 approximately to the threshold value k_1^{π} = (In M - In R')/L (R' is the mirror reflection coefficient). It is necessary to add to this that for the selected mixture the energy exchange between components was so fast that the present radiation field could not significantly disturb the equilibrium ratio between the number of excited molecules CO_2 and N_2. Hence it follows that the losses to removal from the left-hand side of the resonator for any width must in the given case be close to k_1^{π}/k_1^0.

On the other hand, the less the width ℓ_1 becomes, the greater the fields must be insuring such a decrease in the amplification coefficient. This leads to an increase in the role of the induced radiation processes by comparison with the role of the relaxation processes, that is, to an increase in X^{ℓ} as a result of a decrease in X^{ℓ}_{rel}.

Now let us proceed to the right-hand side. As we have seen, the state of the medium at the entrance to it can be considered in the first approximation uniquely defined by the resonator losses. Therefore the only parameter which depends on the conditions in the left-hand part of the resonator subject to variation when investigating the right-hand part remains the radiation flux density on the axis $\rho(0, 0)$; this makes it possible significantly to reduce the number of variants of the calculations of the right-hand side.

The construction of the solution in the right-hand side offers the possibility of calculating its efficiency X^{π} defined as the proportion of the excited molecules "processed" into outgoing radiation left after passage through the left-hand side. The results of the calculations X^{π} for M = 1.33 and three values of $\rho(0, 0)$ are presented in Figure 4.12. It is obvious that the dependence of X^{π} on ℓ_2 differs with respect to nature from the similar dependence for the left-hand side: with an increase in ℓ_2, the efficiency first increases rapidly, then more and more slowly and, finally, it reaches an extraordinarily gently sloping maximum. This is explained by the fact that on passage of the active medium through the right-hand side of the resonator the oscillatory energy reserve of the molecules is completely exhausted; as a result of a decrease in field density down stream this process takes place more and more slowly. The maximum efficiency is achieved when the amplification in the medium becomes so small that it compares with the losses on the mirrors. Of cours, it is possible in practice to limit ourselves to a significantly smaller width of the right-hand side, losing very little in efficiency, and on the other hand gaining significantly in size of the mirrors. For the above-indicated parameters of the medium, the value of $\ell_2 \sim 15$ cm (see [228] and also Figure 4.12) can be used which is also used in the subsequent calculations.

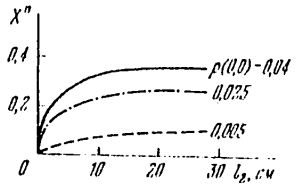

Figure 4.12. Efficiency of the right-hand side of the resonator as a function of its length ℓ_2 for M = 1.33 and three different $\rho(0, 0)$.

Now it is possible to proceed with investigation of the properties of the resonator as a whole. In Figure 4.13 we have the relations for its efficiency $X = X^{\ell} + X^{\ell}_{rem} X^{\pi}$ as a function of the magnification M and width of the left-hand part for $\ell_2 = 15$ cm. It is obvious that the given relation coincides with respect to nature with the analogous function for the left-side only (see Figure 4.11). This is also understandable: for small M and ℓ_1, $\rho(0, 0)$ increases, and as a result the efficiency not only in the left-hand side, but also the right-hand side increases, and together with them, the efficiency of the resonator as a whole. The growth of X with a decrease in M and ℓ_1 continues in the entire investigated range of parameters, slowing only in the case of $k_1^0 L = 0.6$ for $\ell_1 \sim 3$ cm and M ~ 1.3; at this time

X already reaches 60%. It makes no special sense to investigate the region of still smaller values of M and ℓ_1: for ordinary sizes of the active zone of a gas dynamic laser the geometric approximation ceases to be valid there, and therefore the direction of the radiation must become worse.

Thus, in order to achieve high efficiency of energy conversion it turns out to be sufficient to select a total resonator width which is not too much less than the relaxation length of the medium (let us remember that H = 25 cm), the width of the left-hand side is selected approximately an order less, and the resonator losses such that the threshold value of the amplification coefficient is approximately half the value at the entrance to the resonator. This choice has quite clear meaning and may fail to give the desired result only in case of inadequate energy exchange rate between the components of the mixture. Actually, then the total oscillatory energy reserve will not be able to keep up with the gain reduction in the presence of the field, and the losses to removal must increase.

In [228] a series of the corresponding calculations were made for mixtures with the compositions 5% CO_2, 90% N_2, 5% H_2O and 8% CO_2, 90% N_2, 2% H_2O; in both cases the value of k_1^0L was 0.8, the pressure was taken equal to 0.05 atm, and the remaining parameters were the same as in the above-investigated case. The energy exchange rate between the components for these mixtures was noticeably less (primarily as a result of reduced pressure). The calculations demonstrated that for analogous selection of the position of the axis and the dimensions of the mirrors, the efficiency on the order of 0.6-0.7 was achieved only when the threshold value of the amplification coefficient was less than the input value by 3 or 4 times. From the procedural point of view the following is networthy. Although the amplification coefficient in the plane x = 0 is as before close to threshold, the content of the excited molecules N_2 here also depends on the field density. Inasmuch as, in turn, in the entire indicated plane the field density is close to $\rho(0, 0)$, the value of $\rho(0, 0)$ even for mixtures with small energy exchange rate remains the only parameter subject to variation for calculations of the right-hand side.

Problem of the Formation of Uniform Field Distribution with Respect to the Flow Laser Resonator Cross Section. The above-investigated example is quite typical; it is clear from it what arguments must be and are being taken into account when selecting the resonator for a fast-flow laser. It is also obvious that even the

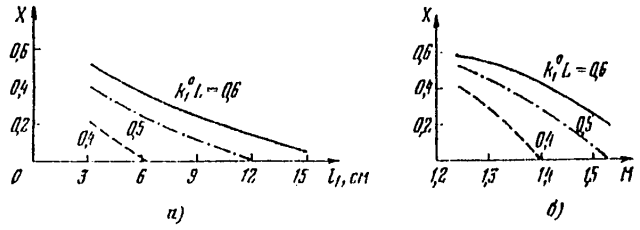

Figure 4.13. Efficiency X of a resonator as a whole as a function of its parameters with a length of the right-hand side ℓ_2 = 15 cm: a) dependence of the magnitude of X on the length of the left-hand side for M = 1.33; b) the value of X as a function of parameter M for ℓ_1 = 3 cm.

simplest unstable laser made up of spherical mirrors with accurate selection of its parameters can entirely insure satisfactory efficiency of the energy conversion. However, for practical applications it is almost as important to have more or less uniform distribution of the radiation intensity with respect to cross section (otherwise the local thermal loads of the mirrors and angular divergence of the radiation will increase). Although with uniformity of field distribution in the unstable resonators of this type things go better than in planar resonators, they are not sufficiently good. Thus, in Figure 4.14 we have the intensity distribution on a concave spherical mirror (curve 1) for the very case where efficiency of 60% ($k_1^0 L$ = 0.6, ℓ_1 = 3 cm, M = 1.3) was achieved for a mixture with a pressure of 0.1 atmosphere. Here the graph is also plotted for a two-dimensional resonator (curve 2) for the same parameters of the medium, losses and position of the axis (let us note that under these conditions it has approximately the same efficiency). From the figure it is obvious that the field distribution is quite nonuniform, especially in the more important case of spherical mirrors (in the diffraction approximation a sharp distribution "peak" can smooth off somewhat, but the total nonuniformity will still be clearly noticeable). A more favorable form of distribution is observed only in versions with low efficiency, primarily with excessively large M when the field inside the resonator turns out to be insufficiently intense. This type of situation obviously occurred in the above-described experiments using a gas dynamic laser [211], which is indicated by the low efficiency of the resonator with satisfactory uniformity of distribution.

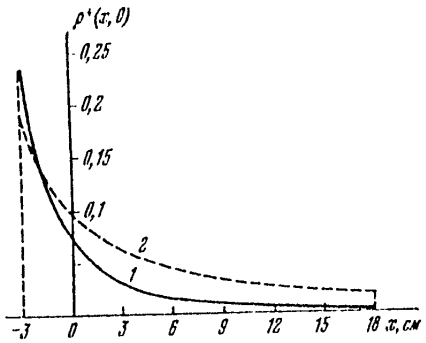

Figure 4.14. Field density distribution in a concave mirror: 1 -- for spherical mirrors, M = 1.3; 2 -- for cylindrical mirrors, M = 1.69.

The use of multipass systems of the type depicted in Figure 4.9 permits a sharp increase in M. As a result of the complication of the system, a noticeable positive effect is achieved, in particular, the compactness of the exit aperture increases, and its filling factor γ increases (see §§ 1.1, 3.6; Figure 1.3, a b corresponds to the single pass and one of the possible versions of multipass systems). However, it is still not possible to achieve a combination of high efficiency with high uniformity of the field distribution here.

In order to solve this most important problem it is possible to consider the prism resonators investigated in § 3.5 in which the effect of wave aberrations of odd order was significantly attenuated by comparison with the ordinary telescopic resonater. The effect of the amplification coefficient gradient directed across the

axis is identical to the influence of the gradient of the index of refraction (wedge) and the wave phase, and it must be attenuated to the same degree.

It is true that in the far infrared range where the greater part of the flow lasers operate, transparent total internal reflection prisms analogous to those used in solid state lasers are hardly realizable. However, for low magnifications M which are characteristic of the flow lasers with single-pass resonators, the application of a confocal resonator becomes mandatory inasmuch as satisfactory filling of the operating cross section with lasing radiation is also achieved in a resonator made up of planar and slightly convex mirrors (see also § 4.1). Replacing the planar mirror by a dihedral 90-degree reflector made up of two planar mirrors, we obtain the desired resonator. For equalizing the intensity distribution, the edge of the reflector must be oriented obviously perpendicular to the plane of Figure 4.10.

This possibility was investigated experimentally in the example of the flow-type CO_2-laser of comparatively smaller power in reference [232]. The systems discussed above were tested (Figure 4.15, a, b); for convenience of selecting the optimal parameters of the resonator, the convex mirror was not spherical, but cylindrical with regulated curvature [233] so that the unstable resonator would be two-dimensional. For the same purpose the radiation was coupled out by two auxiliary mirrors, the position of which could be adjusted. The preliminary recordings of the radiation patterns of the amplification coefficient with respect to the resonator cross section [234] demonstrated that the medium in the given laser relaxes quickly, and the conditions are quite typical for continuous flow systems.

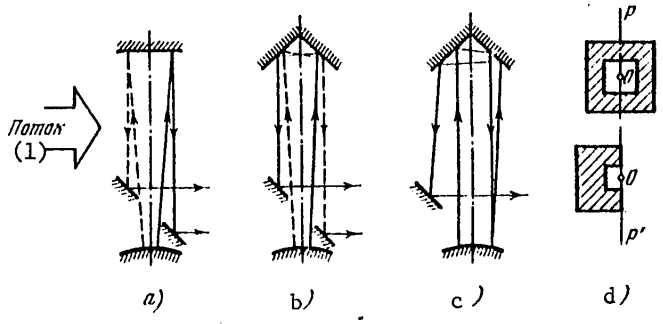

Figure 4.15. Unstable resonators in the flow-type lasers: a) resonator made of planar and convex mirrors; b), c) resonator made of a corner reflector and convex mirror; b) symmetric; c) asymmetric radiation output; d) various versions of the type of projection of the exit aperture on the plane perpendicular to the resonator axis; the axis passes through the point O, the line PP' is perpendicular to the plane of the figure; a) to c).

Key: 1. flow

The results of the experiments turned out to be highly hopeful. When using the system depicted in Figure 4.15, a a tenfold decrease in intensity downstream was observed inside the generated beam. The differences between the intensities and the left and right halves of the resonator with corner reflector (Figure 4.15, b) did not exceed 25%. Another interesting possibility is connected with the application of the corner reflector: in order to increase the compactness of the exit

aperture it is sufficient to resort to asymmetric output of the radiation. In the case of a three-dimensional resonator this is done using an output mirror, the possible versions of the shape and arrangement of which are explained by Figure 4.15, d. In the two-dimensional resonator it is possible simply to remove one of the two output mirrors (Figure 4.15, c). Then the radiation which was incident earlier on this mirror and immediately left the resonator now makes an additional pass through the resonator and leaves from the opposite side. The width of the output zone approximately doubles, the radiation distribution in the far zone becomes more favorable.

From the results of the experiments and rough estimates [232] it is also possible to draw some conclusions relative to the energy characteristics of the flow lasers in which an unstable resonator with corner reflector is used. If we select magnification M and the width of the left-hand side the same as in the case of an ordinary resonator, the average radiation density here will remain as before; the efficiency of the left-hand side almost does not change. As for the right-hand side, its width in the systems with beam "inversion" is automatically close to the width of the left and, as a rule, falls far short of the optimal width of the right-hand side of the ordinary resonators. However, as a result of much greater radiation density the efficiency of the right-hand side also remains approximately on the former level. Thus, it is possible to hope that resonators with corner reflectors will permit insurance of the same efficiency of energy conversion as ordinary resonators with noticeably less width of the operating zone and greater compactness of the exit aperture.

The confocal unstable resonators made of two concave mirrors must have similar properties (see Figure 3.3, c), where "inversion" of the light beam is also realized. However, their use in many cases can cause undesirable phenomena at the common focal point of the mirrors where the radiation density reaches an enormous value.

On the other hand, the great prospectiveness of the application of unstable resonators investigated in § 3.6 with field rotation in continuous-action lasers is unquestioned. The quite recently published results of the corresponding experiments [235, 333] completely confirm the correctness of the arguments discussed in this regard in § 3.6. The introduction of the operation of rotation of the cross section actually cardinally equalizes the intensity distribution in the near zone. Sensitivity to astigmatism decreases so much that the latter is weakly manifested even when the corner reflectors forming the linear resonator include spherical mirrors, the angles of incidence of the light on which are, therefore, $\pi/4$. Finally, the use of a sectional output (see Figure 3.28) instead of annular not only increases the compactness of the exit aperture, but also leads to a significant decrease in divergence of the outgoing radiation without reducing its power.

It only remains to mention that sometimes reports appear in the literature and resonators, the elements of which have the shape of a surface differing sharply from spherical -- conical, toroidal, and so on (see, for example, [236]). The possibility of obtaining a small angular divergence of the emission in this way still is far from obvious and we shall not analyze properties of such systems.

§ 4.3. Unstable Resonators in Lasers with Controlled Spectral-Time Radiation Characteristics

Simplest Types of Lasers with Control Elements. For many practical applications it is necessary that the stimulated emission have not only small divergence, but

also given time-spectral characteristics. Their achievement usually is insured by the fact that the corresponding control elements are located inside the resonator.

The first publication on the creation of a monopulse laser with unstable resonator belongs to the year of 1969 [189]. This was a solid state neodymium-doped glass laser; a passive shutter covered the entire cross section of the active element. The output energy was ~20 joules, the peak power was $\sim 1.5 \cdot 10^9$ watts, the angular divergence with respect to 0.5 intensity level was ~4"($2 \cdot 10^{-5}$ radians), but a significant part of the energy went to the "tails" of the angular distribution as a result of light dissipation in the shutter liquid. As a result of rapid "spread" of the emission over the cross section of the unstable resonators the pulse duration turned out to be noticeably shorter than when using a planar resonator.

Subsequently, monopulse lasers with unstable resonators have always been constructed by one of two circuits depicted in Figure 4.16; here the shutter does not cover the entire cross section of the active element, but only the exit mirror. This leads to significant improvement of the output characteristics: the peripheral part of the beam running "to the exit" from the laser, bypasses the shutter and does not undergo additional absorption and dispersion in it [204]. In addition, possibilities are created for controlling the radiation flux having larger area using a small shutter. If we consider that the optically improved fast-acting shutters usually have small aperture, the prospectiveness of using such systems to construct spikeless, monopulsed and other controlled-Q lasers becomes obvious. Thus, at the beginning of the 1970's highly improved monopulse neodymium-doped glass lasers were built with radiation brightness of $\sim 10^{17}$ watts/(cm^2-steradian) [204, 205]. Let us also note the achievement of the quasisteady lasing mode of an analogous laser in [237].

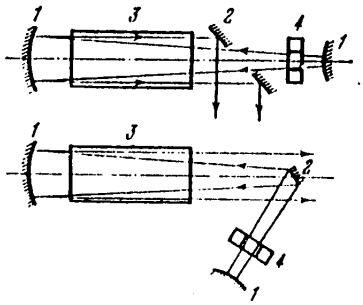

Figure 4.16. Diagrams of lasers with modulated Q-factor: 1 -- resonator mirror, 2 -- additional mirror, 3 -- active sample, 4 -- shutter

The entire resonator cross section or its exit mirror can be covered, of course, not only by the shutter, but also the spectral selector. It is necessary, however, when installing any controlling elements to deal with the specifics of unstable resonators which impose restrictions on the types and methods of placement of these elements. First of all it is necessary to take steps to prevent the occurrence of a converging wave. If the resonator is telescopic, the flat surfaces of the controlling elements must be also inclined with respect to the resonator axis just as any other interfaces (see § 4.1; in the light of this fact Figure 4.16 is provisional).

Another important characteristic of unstable resonators complicating the problem of controlling their emission is the fact that the introduction of a small optical wedge does not lead to sharply exceeding the lasing threshold, just as in a planar resonator, but it causes only a shift of the optical axis. As a result, it is necessary to depart from a number of traditional methods of control based on the application of an optical wedge which varies in time or depends on the wavelength. Thus, the placement of a dispersion prism inside an unstable resonator leads not to spectral selection of the emission, but only to the fact that the radiation spectrum will be expanded in the corresponding direction -- in the far zone instead of one spot the spectral distribution image appears. Efforts to modulate the Q-factor using a rotating prism can hardly lead to good results.

Thus, in monopulse lasers with unstable resonators it is necessary to use predominately passive or electrooptical shutters[1]; for spectral selection primarily the Fabry and Perot etalons are suitable, on passage through which the value does not change its direction. However, even here it is necessary to consider the fact that in any linear, unstable resonator, not a plane wave, but a spherical wave will be propagated in at least one of the two opposite directions. Under these conditions the introduction of the etalon will not cause intensity modulation with respect to the resonator cross section except in the case where the angular width of the maximum transmission of the etalon will exceed the angle of opening of the spherical wave. The angular width of the maximum transmission of the etalon in turn is equal to the angular distance between adjacent rings divided by the number of inferfering beams N which depends on the reflection coefficient of the working surfaces of the etalon. As a result, we arrive at the following condition imposed on the magnitude of the etalon base t [196]:

$$t \leqslant \frac{\lambda}{2N \sin \varphi \Delta\varphi} = \frac{M}{M-1} \frac{\lambda L}{2ND \sin \varphi}, \qquad (6)$$

where D is the diameter of the transverse cross section of the active element; M and L are the magnification and the equivalent length of the resonator; ϕ is the angle between the normal to the etalon surface and the resonator axis; finally, $\Delta\phi = (M - 1)D/ML$ is the angle of opening of the diverging beam in the telescopic resonator (when deriving (6), the inequality $\phi >> \Delta\phi$ which usually is satisfied was considered to be valid).

Multiple beam reflection in an inclined etalon also leads to some "blurring" of the position of the resonator axis, which in turn can cause an increase in the radiation divergence. The corresponding calculations indicate that the condition of smallness of this increase by comparison with the diffraction angle again reduces to formula (6). Inasmuch as the etalon base determines the width of the region of its dispersion ($\Delta\lambda = \lambda^2/2t$), consequently the expression (6) limits the minimum width of the spectrum reached in the laser with direct placement of the selecting etalon in the telescopic resonator.

---

[1]Self-Q switching of unstable resonators described in [238] and a number of subsequent papers is realized only in the smallest lasers and leads to output parameters which are hardly recorded even for this class of laser.

Lasers with Three-Mirror Resonator. Further improvement of the methods of controlling the emission of lasers with unstable resonators is connected with the idea formulated and experimentally substantiated in [153] of the effect on the central section of the resonator cross section, from which the radiation "spreads." For normal course of the beams this section is the analog of the master oscillator, and the remaining part of the cross section, a multipass amplifier. In order to realize this idea, it is sufficient to make an opening at the center of one of the mirrors and install an auxiliary mirror behind it; the control elements of very small size can be conveniently placed in the narrow "appendix" formed in this way. This three-mirror resonator and the scheme equivalent to it without an opening in the mirror are depicted in Figure 4.17.

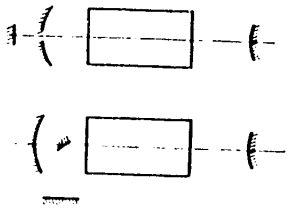

Figure 4.17. Diagrams of resonators with radiation control in the central section of the cross section.

The possibility of efficient radiation control using the given procedure is limited by the fact that, as follows from the materials of § 3.4, a laser with unstable resonator is capable of lasing even with a completely shielded central section of the cross section. Therefore, if in the "appendix," for example, the shutter and the axial section are "blocked" at a given point in time and the lasing threshold increases insignificantly, independent lasing which is not controlled, will develop in the remaining volume. Hence, it is clear what important practical significance the nature of the dependence of the lasing threshold on the dimensions of the covered central segment of the cross section has.

The results of the measurements of this relation performed in [191, 168, 193, 196] turned out to be entirely in correspondence to the theoretical representation developed in § 3.4. In the case of two-dimensional resonators the threshold increases with an increase in hole sizes (more precisely, the slit width) extraordinarily sharply. Thus, the shielding of the central section ~3 mm wide has approximately tripled the threshold intensity of the pumping of the laser described in § 4.1 based on a rectangular large active element with resonator made of planar and cylindrical mirrors (Figure 4.6) [168]. Therefore the control of the radiation characteristics of lasers with two-dimensional unstable resonators is realized without special difficulty. In particular, the use of the simplest disc modulator has made it possible to convert the mentioned laser to the regular "spike" mode with repetition of these spikes from 25 to 50 kilohertz [168]. In reference [193] special selection of the radiation of the same laser without a noticeable decrease in its output power was successfully produced by the introduction of the Fabry and Perot etalon into the "appendix."

Lsers with resonators made of spherical mirrors behave entirely differently. Their lasing threshold increases very slowly with the size of the central circular

opening. Thus, in a laser with active neodymium doped glass element 45 mm in diameter and a telescopic resonator with magnification M = 2 for a hole diameter in the concave mirror of 4 mm, the pumping threshold intensity increased by 1.3 times; for a diameter of 8 mm, it approximately doubled by comparison with the case where the hole was absent. Even the presence of a hole with a diameter of 20 mm and almost reaching the diameter of the convex mirror (22 mm) caused only a triple increase in the self-excitation threshold [191].

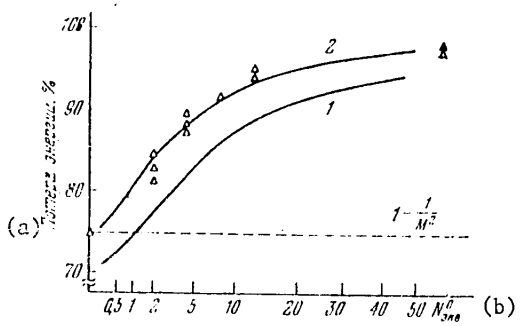

Figure 4.18. Losses of the lowest modes as a function of the size of the coupling hole in a three-dimensional resonator with circular mirrors (M = 2, N_{equiv} = 60). The dots represent the experimental data; 1 -- the calculation for the case of a sharp mirror edge; 2 -- analogous calculation in the presence of "smoothing" of the edge ($|R_{refl}|$ decreased by four times).

Key: a. energy losses, %
b. N_{equiv}

In Figure 4.18, the data on the dependence of the losses of the lowest mode on the size of the coupling hole calculated by the results of experimental observations and by formulas from § 3.4 in [168] are compared. As is obvious from the figure, the experimental points lie noticeably above curve 1 obtained on substitution of the value of the coefficient of diffraction reflection from the edge R_{refl} calculated by the formula for an ideally sharp edge (3.25) in expression (3.24). In order to achieve comparison of the calculated and the empirical data it is necessary to decrease the value of $|R_{refl}|$ substituted in (3.24) by four times (curves 2). For this decrease $|R_{refl}|$ in the given case there was sufficient "smoothing" of the edge (see § 3.3) in a zone ~0.1 mm wide, which, apparently, are curved in the experiment.

Inasmuch as the shielding of the small axial section here only causes an insignificant increase in the self-excitation threshold, the possibilities for controlling the radiation turn out to be more limited than in the case of two-dimensional resonators. In particular, it is explicitly impossible, when placing the controlling elements only in the "appendix" to realize monopulse lasing or a lasing mode close to it. If the operating transition line is broadened nonuniformly, the spectral selection of the radiation is also complicated. Actually, in the loop

of this line with intense single-frequency lasing a "trough" arises, and the amplification coefficient on the side frequencies becomes noticeably larger than on the frequency at which lasing occurs. Therefore the isolation of one frequency using the selector in the "appendix" cannot prevent self-excitation of the lasing on the side frequencies in the remaining volume.

Nevertheless the problem of spectral selection in unstable resonators with spherical mirrors frequently can be solved even in the case of a nonuniformly broadened line. According to [196] it is necessary to try to install one etalon having a small base directly between the primary mirrors of the resonator so that it covers the entire operating cross section. The purpose of this etalon must be to isolate the band, the width of which does not exceed the width of the "trough" in the line contour. If this can be done without violating condition (6), for further constriction of the spectrum it is possible to use the "appendix."

The favorable situation actually occurred when performing the experiments described in [196] with a neodymium-doped glass laser with the active element 45 mm in diameter and 600 mm long. The telescopic laser had magnification of M = 2; the output power without spectral selection was 500 joules per pulse. The preliminary constriction of the spectrum from the width usual to neodymium lasers equal to several nanometers, to a value of ~0.5 nm was carried out using an etalon having a base of only 0.05 mm. Insmuch as all of the conditions were satisfied which were initially discussed, the introduction of this etalon did not cause any changes in the form of the angular distribution (its width with respect to the 0.5 intensity level was $8 \cdot 10^{-5}$ radians). Here the output power dropped to 400 joules. Subsequent introduction of the etalons with bases appreciably larger than in the first one into the "appendix" caused only further decrease in the width of the spectrum, reaching, in the final analysis, 0.003 nm; not only the radiation divergence, but also the output power remained constant.

The following is of interest. In these experiments the width of the opening beyond which the "appendix" with additional etalons was located and amounted to a total of 3 mm. The overlap of this small section of the cross section exceeded by only 10% the self-excitation threshold of the entire laser. In the central section taken separately, the lasing threshold, considering all of the introduced etalons, unconditionally would be higher. This demonstrates that the above-mentioned division into the "master oscillator" and "amplifier" is purely arbitrary inasmuch as the radiation control of the "amplifier" is realized when the self-excitation threshold of the latter was below the threshold in the "master oscillator." The fact is that, as the experiments demonstrated, with the "oscillator" and "amplifier" spatially combined in the three-mirror system, the radiation arrives not only from the first to the second, but also as a result of diffraction, from the second to the first. This increases the radiation density in the "appendix" especially for a small diameter of the appendix, and the role of the "appendix" turns out to be quite large.

The uniform part of the line broadening that determines the width of the "trough" was rather extensive in the silicate neodymium glass used in Ref. 196, which made it easier to pick out the precontraction etalon without violating condition (6). It might not be possible to pick out such an etalon in lasers based on media with a narrower uniform broadening band. What to do in such cases is still unclear; it is possible that it remains only to do away with the linear and resort to the unidirectional annular resonators for which condition (6) loses its force.

Ending with three-mirror resonator lasers, let us note that if there is too much absorption in the "appendix," its role can be significantly strengthened by placement of an additional small-cross section active element in it. It would appear that it is possible to achieve an analogous effect on introducing a special deflector (or orienting one of the interfaces perpendicular to the resonator axis) to produce a convergent wave that "overflows" to the center, but this leads to a sharp increase in the radiation divergence (see [196] and also § 4.1).

External Signal-Controlled Lasers. Now let us proceed to another method permitting the use of the special role of the central segment of the cross section of an unstable resonator. This method was proposed in 1969 [239], and it consists in the fact that radiation from an external source is input to the laser with unstable resonator through the central coupling hole. The properties of such a laser depend decisively on the relation between the amplification of the medium and the losses of the resonator with the coupling hole. If this relation is such that self-excitation of the system does not occur in the absence of an external signal, we are dealing with a "pure" amplifier capable of operating in the slave mode and thus, suitable for effective amplification of powerful short pulses and other purposes. If the self-excitation threshold is low and turns out to be exceeded, it is more correct to talk not about an amplifier, but about a laser controlled by an external signal. Let us first consider the latter case.

The control of laser radiation by an external signal is a well-known method of obtaining the given spectral-time characteristics. This method was used successfully in planar resonators (see, for example [240-243]), where the "nucleating center" from an external source was introduced, as a rule, immediately over the entire cross section of the resonator. Inasmuch as in unstable resonators the radiation quickly "spreads" from the central region, for such effective control here it is obviously sufficient to introduce a beam from an external source only into the region which permits us to go on with quite low power of it. Unfortunately, a comparison of the results achieved in practice obtained when using planar and ustable resonators is almost impossible inasmuch as these results pertain to entirely different cases. For planar resonators, a study was primarily made of the spectrum control mode of a giant pulse by injection of the "nucleating center" at the beginning of its development. As for unstable resonators, for them the control of the spectral-time characteristics of the emission was still realized only under conditions close to quasistationary although the possibility of controlling monopulse lasers also raises no doubt.

In order to obtain the same output power for a controlled laser operating in the quasistationary mode as for an ordinary laser it is obviously sufficient to use an unstable resonator for it with the same M and introduce radiation with the same density into the coupling hole which is developed inside the standard lasers without the coupling hole. However, for more reliable control it is expedient either to increase the density of the controlling signal (which both in the pulsed and in the flow lasers leads to a decrease in amplification on the axis) or noticeably increase M or, finally, do both. Then the system with the supplied external signal turns out to be significantly below its self-excitation threshold, which improves its controllability -- in essence, the amplification mode occurs. It is only necessary, by increasing M_i, to see that this does not lead to a large decrease in the output power. This may occur especially quickly in flow lasers with low amplification. As for pulsed lasers using highly amplifying media, the parameters of their resonators can, as a rule, vary entirely "painlessly" within the broad

limits, especially in the presence of a quasistationary controlled signal (we shall discuss the causes for this somewhat later).

Let us touch on the problem of selecting the size of the coupling hole. The losses of resonators made of spherical mirrors and the radiation density required from an external source to prevent self-excitation depend very slightly on the dimensions of the hole. Hence, it follows that the required control signal power is in the first approximation proportional to the area of the hole. Therefore it is advantageous to use quite small holes; however, they must not be so small that the resonator axis can go beyond their limits as a result of alignment errors, vibrations, and so on.

Beginning with these arguments, the parameters of an unstable resonator were selected for the first laser of the given class built in [191]. This laser, just as in many experiments described above, was built on the basis of an active element made of neodymium-doped glass 45 mm in diameter and 600 mm long. The telescopic resonator had magnification of M = 5 instead of the usual M = 2; the diameter of the coupling hole was determined by the precision of the alignment and it was 3 mm. The external master oscillator operated in the mode of random radiation "spikes" which is usual for solid-state lasers; its output power was more than two orders less than the output power of the basic laser which was several hundreds of joules for a pumping pulse duration of ~1.5 milliseconds. Although the presence of intervals between the "spikes" does not at all promote control reliability, complete synchrony of the "spikes" at the output of the master oscillator and the system as a whole was observed.

In [191], the requirements on the required accuracy of mutual alignment of the external oscillator and the control laser were also discovered, and it was demonstrated that they are not at all extraordinary: The admissible magnitude of the angle between the direction of the beam from the external oscillator and the axis of the powerful laser was in the given case ~1'.

One and a half years later a report appeared on work of a similar nature in the field of CO_2-lasers: under the effect of a weak signal introduced in the axial section with frequency corresponding to one of the rotational transitions of the CO_2 molecule, a powerful laser with unstable resonator began to generate on this frequency although without the input of the external signal it operated on another rotational transition [244]. In the same paper the argument was stated of the possibility of feeding the control beam not to the central but to the peripheral section of the cross section so that a converging wave amplified as it approached the axis was formed. Using this procedure, the required spectral characteristics probably can be obtained, but there will hardly be small divergence of the radiation simulataneously with this.

Now let us discuss one of the most remarkable peculiarities of pulsed lasers with unstable resonators operating under the effect of radiation from an external source. We are talking about the extraordinarily weak dependence of their output power on the resonator parameters and the control signal intensity if the latter was present. In this respect the results of the calculations of the energy characteristics of a controlled laser the parameters of which are typical of powerful neodymium-doped glass lasers performed in [245] are indicative. The diameter of the coupling hole in a concave mirror of a telescopic resonator was taken equal to the diameter of the convex mirror or less than it by M times so that the beam from the external

source during its expansion to filling the exit aperture completed three or five passes through the medium, respectively (if the given laser was not capable of self-excitation in the absence of an external signal it would be a "pure" three or five-pass amplifier). The value of M varied from 2 to 20 (M = 2 corresponded to the optimal value of the magnification calculated by formula (4) for an ordinary laser constructed on the given active element).

The calculations demonstrated that as M increases with fixed power of the external signals falling within reasonable limits, the efficiency of the controlled laser decreased monotonically, but noticeably more slowly than the efficiency of ordinary lasers. This is understandable: when M is so large that the lasing in an ordinary laser is completely curtailed, the laser with coupling hole operates as a multipass amplifier, and on supplying the external signal it has a finite output power frequently commensurate with maximum.

The efficiency of a controlled laser depends still less on the power of the external signal. It is sufficient to present the following data: in the entire above-indicated range of variation of M, the variation of the controlling signal power by more than three orders did not lead to a decrease in the efficiency below the level equal to 40% of its maximum value. This also has a simple explanation: it is known that the relative fluctuations of the power at the output of any laser amplifier operating in the quasistationary mode is always significantly less than the relative power fluctuations at its input as a result of amplification saturation. Here, as a result of the presence of several radiation passes through the medium, the given effect appears still more rarely.

The results of [245] permit some conclusions to be drawn which pertain to the properties not only of controlled but also ordinary lasers with unstable resonators. It happens that any disturbance on the central section of the cross section strongly reduces the losses of an empty resonator, and with them, the lasing threshold of the corresponding laser. Thus, the presence of even weak small-scale nonuniformities easily leads to the formation of local "stable" resonators near the axis with all of the consequences following from this [246]. It can be demonstrated that a significant reduction in the threshold arising from such causes must cause a significant increase in the lasing power. However, in reality the variation of the conditions on the small axial section can sharply influence the output power only in the case where the laser was quite close to the lasing threshold before this. If the threshold is greatly exceeded, the output parameters have little sensitivity to variations of the radiation density on a small segment of the cross section independently of whether these variations were caused by the influence of local disturbances or the radiation is supplied, as in a controlled laser, from an external source.

Multipass Amplifiers. In conclusion, let us briefly discuss the "pure" multipass amplifiers, the unstable resonators of which have such large losses that the self-excitation does not occur even in the absence of an external signal. Most frequently these amplifiers are constructed on the basis of a telescopic resonator; then they are called (at least in Soviet literature) telescopic. The possible versions of telescopic amplifiers are presented in Figure 4.19. As a result of the presence of several passes through the medium, one such amplifier is capable of replacing several single-pass amplifiers with telescopes between them (see §2.6, Figure 2.28) [239].

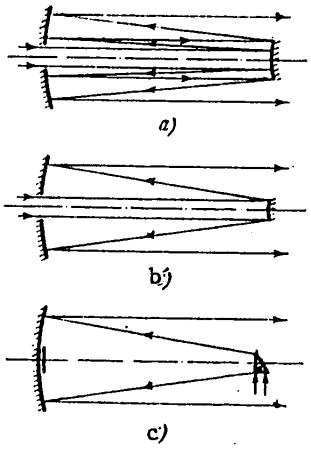

Figure 4.19. Telescopic amplifiers: a) multipass, b) three-pass, c) two-pass amplifiers; in the last amplifier the hole in the mirror is replaced by an absorbing screen.

As a rule, amplifiers with unstable resonators are used in the intermediate stages of powerful monopulse lasers (e. g. [247, 248]; simple single-pass amplifiers are often preferred for the final stages, as they have greater radiation strength through elimination of the output mirror and concomitant radiation in the reverse direction). Therefore, the important thing here is not so much efficiency as it is the weak-signal gain, which preferably should be maximized.

The amplification of the weak signal in the n-pass amplifier is equal to K^n, where K is the amplification on one pass of the active medium. Therefore for the given K it is necessary to strive for the largest possible n; this promotes the achievement not only of high amplification but also satisfactory energy efficiency of the device.

If K is small, multipass systems of the type depicted in Figure 4.19, a can be used; let us begin with them. We shall consider that the radiation is fed through the coupling hole in a concave mirror as depicted in the figure; here n is odd, the beam cross section expands inside the amplifier by $M^{(n-1)/2}$ times. Hence it follows that $n = 1 + 2 \ln (D/d)/\ln M$, where d and D are the beam diameter at the input and the output of the amplifier, respectively. In order to obtain a large n it is obviously necessary to use a resonator with the lowest possible magnification M and minimum coupling hole diameter d.

Inasmuch as the self-excitation threshold of a laser with small coupling hole is almost equal to the lasing threshold of an ordinary laser which is achieved for K = M, the least admissible value of M is equal to K. As for the diameter of the coupling hole, it is limited from below, as we have already pointed out, by the precision of the alignment. The latter, it is true, depends not only on the overall dimensions of the resonator, but also on M, but for the large M characteristic of the amplifiers this relation is very weak. Therefore we shall consider the minimum hole diameter fixed and equal to d_0.

Thus, the maximum n is $n_{max} = 1 + 2\ln(D/d_0)/\ln K$. Here amplification of the weak signal is achieved by $K^{n_{max}} = K(D/d_0)^2$ times [249] (exactly the same power transformation coefficient occurs also in controlled lasers operating in the quasistationary mode [191]). From the condition $n_{max} \geq 5$ we obtain the criterion of applicability of multipass systems: $K \leq \sqrt{D/d_0}$.

For large K three-pass systems can be used (Figure 4.19 b) insuring a general amplification coefficient K^3. Inasmuch as here M = D/d, even without considering the increase in the threshold as a result of the presence of the coupling hole, self-excitation should not begin until K = D/d. If we consider that the coupling hole diameter is no smaller than the convex mirror diameter and if necessary can be made as shown in the figure larger than the convex mirror diameter (at the price of insignificant decrease of output power), the admissible value of K increases as a result of a corresponding increase in the self-excitation threshold to values on the order of $(D/d)^{1.5 \text{ to } 2}$ [249]. Hence it follows that the criterion of applicability of three-pass systems has the form $K \leq (D/d_0)^{1.5}$.

In essence the two-pass system does not contain a resonator (Figure 4.19, c) and can be used for K as high as one might like. In order better to "decouple" the two-pass amplifier with the master oscillator, it is expedient to create a hole in the concave mirror with diameter equal to or somewhat larger than the diameter of the input beam (holes for the analogous purpose not in the concave mirror but in the convex mirror can also be made in the case of the systems depicted in Figure 4.19, a, b).

As all these estimates show, if the ratio D/d_0 is sufficiently large, extraordinarily high total amplification coefficients of the weak signal can be achieved in a wide range of variation of the amplification in one pass. Let us consider an experiment: in reference [249] indirect measurements were made of this parameter in the case of a powerful three-pass neodymium-doped glass amplifier; they led to a value of $2 \cdot 10^5$.

It is necessary, however, to consider that the amplification of any laser amplifier depends exponentially on the excitation energy stored in it, and it decreases extremely rapidly with depletion of the latter (a different, still sharper dependence is observed only in regenerative amplifiers). For example, it is sufficient that the inverse population be cut in half and the amplification coefficient of the weak signal will become equal to the square root of its initial value (under the conditions of [249], $4.5 \cdot 10^2$). Therefore when feeding a pulse with energy sufficient for removal of a significant part of the stored inverse population to the amplifier input, the amplification at the end of the pulse will become very small, and the pulse energy ratio at the output and input turns out to be much less than the initial amplification coefficient of the weak signal (hence it is obvious that the role of the latter should not be overestimated).

In spite of this fact, the telescopic amplifiers do not in practice provide large amplifications even in the case where they are measured with respect to the pulse energies. Thus, in [247], a pulse with an energy of 0.12 joules was fed to the input of the three-pass neodymium-doped glass amplifier; the output power was 15 joules. In [248] the analogous amplifier had an output power of 18 joules for an

energy at the input of 0.03 joule (600 fold amplification with respect to energy). Let us again emphasize that in all the experiments with telescopic amplifiers (just as with controlled lasers) small divergence of the radiation characteristic of lasers with unstable resonators was observed.

In conclusion, let us note one deficiency of multipass systems which consists in the following. If the telescopic amplifier is assembled, for example, by the five-pass system, then thanks to the diffraction, the scattering of the light at the interfaces, on nonuniformities, and so on, some part of the radiation reaches the limits of the exit aperture, completing only three passes with respect to the active medium, and some, even a total of one pass. Thus, the scattered light arrives at the output of the amplifier before the basic flux. If we consider that the first "lots" of the radiation are subject to especially large amplification, this scattered light can turn out to be not so weak by comparison with the basic signal.

This deficiency can complicate (but not make impossible) the application of telescopic amplifiers in specific lasers for research in the field of thermonuclear fusion. There, the admissible radiation power incident on the target before the arrival of the basic pulse is extremely low. It is true that it not excluded that these phenomena are not so dangerous as it appears: the scattered radiation theoretically has a quite different radiation pattern and can simply not hit the target.

There are times when it may also be undesirable that part of the output cross section of telescopic amplifiers is covered by the convex mirror and not filled with radiation, which is detrimental to uniform exposure of the target in laser-driven fusion. However, even though telescopic amplifiers may not be used in such cases, in many other applications they may be extremely useful.

We conclude with this very interesting example of the use of unstable resonators for the construction of amplifying systems with unique properties. The materials of this chapter indicate that the most varied problems of laser engineering can be successfully solved using such resonators.

CHAPTER 5. OPTICAL NONUNIFORMITY OF ACTIVE MEDIA AND METHODS OF CORRECTING WAVE FRONTS

In the preceding sections of the book we are talking primarily about the search for optical systems that permit realization of the limiting energy and angular characteristics of laser emission for the given properties of the active medium. When such systems are found, the following result depends only on these properties. If the medium is optically nonuniform, the maximum small divergence of the radiation at the laser output in the general case is unattainable; it is only possible to decrease the effect of some of the simplest types of aberrations if their existence can be predicted in advance (see, for example, § 3.5). Therefore simultaneously with improvement of the optical systems -- and on a much larger scale -- studies were made of optical nonuniformities of various active media, and efforts were made at a comprehensive decrease in the these nonuniformities. At the same time, a persistent search was made for the universal methods which would permit us to obtain narrowly directional radiation also with arbitrarily nonuniform active medium. A brief discussion of the experiments on this level will be the subject of this chapter.

The most important cause of optical nonuniformity of active media is the fact that the process of excitation of the medium is always accompanied by the dispersion of a significant amount of energy in it which is spent on heating the medium, the formation of shock waves in it, and so on. The nature of the nonuniformities depends on the peculiarities of the medium and the method of its excitation; their value increases quickly with the laser power.

As for high-power gas lasers, the methods of excitation of certain gases and the types of induced optical nonuniformities are extremely varied. In pulsed electric discharge lasers the active medium at the time of occurrence of discharge is heated intensely, its subsequent expansion is accompanied by the formation of shock waves; nonuniformities caused by nonuniformity of the discharge itself are added to this. In pulsed chemical lasers nonuniformities can be manifested which are caused by nonsimultaneity of the occurrence of the reactions in the entire volume of the active medium, and so on.

The sources of aberrations of optical channels of high-power continuous-action gas lasers are highly varied. The thermal deformations of the mirrors, phase distortions in the windows used for output of the radidation from the resonator are added here to the specific phenomena occurring on transmission of light through fast gas flows (scattering on turbulent pulsations, and so on). In powerful flow lasers operating not in the continuous, but in the frequency-periodic mode,

powerful sound waves caused by "pulsating" energy input are superposed on the already complex gas flow pattern.

This entire enormous complex of various phenomenon has still been studied very little, and it is almost impossible to classify the data available in the literature. Only one thing is clear -- the most favorable situation is the one with optical nonuniformities in low-pressure gas lasers.

The situation is entirely different with regard to the problem of optical nonuniformities in solid-state lasers. The excitation method in practice in all types of them is the same -- optical pumping -- therefore the deformation pattern of the resonators is not distinguished by special variety; in addition, it is quite simple. If it is considered that the systematic work in this area started in the first half of the 1960's, it is no surprise that for a number of types of solid-state lasers the given problem has already been solved to a significant degree.

In the example of solid-state lasers it is quite obvious how large a variety of procedures there are which can be used to decrease the resonator deformations; at the same time what difficulties are caused by the solution of the problem of induced nonuniformities even in such a comparatively simple case is highly instructive. We shall limit ourselves to this example.

§ 5.1. Theoretical Deformations of the Resonators of Solid-State Lasers

Origin and Magnitude of Thermal Aberrations in the Presence of Circular Active Rods. In § 2.3 we have already mentioned the thermal deformations of a resonator which occur as a result of nonuniform heating of the active element by pumping radiation. These aberrations are for the majority of types of solid-state lasers one of the main obstacles on the path to achievement of diffraction divergence of radiation, and for the most widespread glass lasers, they are in practice the only obstacle.

In the single pulse mode, the thermal deformations are a consequence of nonuniformity of distribution of heat release with respect to the volume of the sample, which occurs even when using the most modern illumination systems. In particular, for standard active elements of circular cross section, in the best case more or less axisymmetric pumping distribution can be achieved. The nonuniformity of distribution with respect to radius is in practice always present. Its nature is determined in the final analysis by two opposite factors. One of them is attenuation of the pumping radiation on approaching the axis as a result of absorption in the medium, the other one is "fine focusing" of this radiation on the axis as a result of refraction on passage of the active element through the cylindrical side surface. Depending on which of these factors predominates, the pumping radiation density on the axis can be both less than and greater than the density on the lateral surface [47, 48].

The heat release process in the medium takes place with almost zero lag; therefore the thermal deformations build up smoothly during a single pumping pulse, reaching imposing values in the case of high-power lasers (see, for example, [200]). Together with the deformations, the radiation divergence also increases by the end of the pulse.

As was noted in the same § 2.3, the thermal deformations of the resonators of continuous and frequency lasers are especially large. The thermal flux in the

quasistationary mode here has entirely defined direction -- from the axis of the element to its lateral surface, through which heat removal is realized. Therefore the steady-state temperature distribution in lasers of this type is of a quite regular nature even with noticeable nonuniformity of heat release. On going away from the axis the temperature decreases approximately by a quadratic law. The total temperature gradient with respect to the cross section usually approaches close to the limit after which the rupture of the material by the thermal stresses begins; in the majority of lasers of this type this limits the power of the pumping radiation introduced into the active element and, with it, the output lasing power.

Let us consider the phenomena occurring on transmission of light through a nonuniformly heated active element of circular cross section. We shall consider the temperature inside the element dependent only on the distance to its axis: $T(r, \phi, z) = T(r)$. In order not to deal with awkward tensors, we shall limit ourselves to the case of isotropic material, which glass also is.

The thermal deformations of the resonator are a consequence of the dependence of the index of refraction of the medium on the temperature and on the magnitude of the thermal stresses occurring in the active element:

$$n(T, \sigma_{\parallel}, \sigma_{\perp}) = n_0 + \beta(T - T_0) + C_1\sigma_{\parallel} + C_2\sigma_{\perp}, \tag{1}$$

where T_0 and n_0 are the average temperature of the medium and the index of refraction corresponding to it; $\beta = dn/dT$ is the thermal coefficient of absolute variation of the index of refraction in the absence of stresses; $C_1 \equiv \partial n/\partial\sigma_{\parallel}$ and $C_2 \equiv \partial n/\partial\sigma_{\perp}$ are the so-called photoelastic constants [250]; $\sigma_{\parallel}$ are the normal stresses on the polarization direction, $\sigma_{\perp}$ is the sum of the normal stresses with respect to two other directions (the normal stresses are the diagonal elements of the stress tensor; the positive sign is assigned to the tensile stress). As applied to our case

$$n_{r,\varphi}(r) = n_0 + \beta[T(r) - T_0] + C_1\sigma_{r,\varphi} + C_2(\sigma_z + \sigma_{\varphi,r}), \tag{1a}$$

where $n_{r,\phi}$ is the index of refraction for light polarized in the radial or tangential directions, respectively; σ_r, σ_ϕ, σ_z are the radial, tangential and longitudinal stresses.

Elasticity theory leads to the following expressions for the distribution of the thermal stresses inside a rod of unlimited length for axisymmetric distribution of the temperature [251]:

$$\begin{aligned}
\sigma_r &= \frac{\alpha E}{2(1-\mu)}[T_0 - T_{\text{ср}}(r)],\\
\sigma_\varphi &= \frac{\alpha E}{2(1-\mu)}[T_0 + T_{\text{ср}}(r) - 2T(r)],\\
\sigma_z &= \frac{\alpha E}{1-\mu}[T_0 - T(r)].
\end{aligned} \tag{2}$$

(a)

Key: a. average

Here α is the coefficient of thermal expansion, E is the Young's modulus, μ is the Poisson coefficient which fluctuates within the limits of 0,25 to 0,3 for the majority of materials; T_0 is the average temperature of the rod; $T_{ave}(r) = \frac{2}{r^2}\int_0^r T(r')r'dr'$ is the average temperature of the medium in the zone of radius r adjacent to the axis.

The substitution of (2) in (1a) leads to the known formulas for variations of the index of refraction inside the circular cylindrical active element first published in [70, 71]. Let us write out these formulas in the form in which they usually are used at the present time:

$$n_{r,\varphi}(r) = n_0 + P[T(r) - T_0] \pm Q[T(r) - T_{cp}(r)], \qquad (3)$$

where $P \equiv \beta - \frac{\alpha E}{2(1-\mu)}(C_1 + 3C_2)$, $Q \equiv \frac{\alpha E}{2(1-\mu)}(C_1 - C_2)$ are the laser thermal optical constants introduced in [200]. From (3) it follows that the value of P characterizes the variations of the index of refraction average with respect to both polarizations, Q characterizes birefringence. As will be obvious later, these two constants remain meaningful and are sufficient for complete description of the resonator deformations also in the important case of active elements with strongly elongated rectangular cross section uniformly illuminated from both lateral surfaces.

The expediency of introducing new thermal optical constants arose from the following causes. Before lasers, optics dealt primarily with parts free of large internal stresses; their temperature could slowly vary with time, remaining, however, approximately identical throughout the entire volume. If the light beam travels a distance ℓ through such a part, on variation of the temperature of the entire part by ΔT the optical length of path inside it varies by $\Delta(n\ell) = n\Delta T \cdot \alpha\ell + \ell\Delta T \cdot \beta$. Inasmuch as the path traveled by the beam outside the part decreases in this case by $\Delta\ell$, the total increment of the optical path is $\Delta(n\ell) - \Delta\ell = W\ell\Delta T$, where $W \equiv \beta (n - 1)\alpha$ is the thermal optical constant which was used earlier in optical instrument making [252].

In order not to return again to the question of thermal optical constants, let us note that already at the beginning of the 1970's some researchers preferred to be guided by the values not of P and Q, but W when selecting the optimal composition of the neodymium glass (for example, [253, 254]). This was frequently caused by the fact that for many laser glasses the numerical values of W and P are close to each other, and frequently by the fact that the authors [253] created a procedure for measuring W simpler and more convenient than the procedures developed in [200, 255, 256] for direct measurement of P and Q. However, numerous specific data [256, 257] indicate that the correlation between W and P on variation of the compositions of the glasses turns out to be not at all ideal. Therefore now in almost all of the papers devoted to the creation of the so-called athermal glass, only P and Q are used as the criterial thermal optical constants (for more details see [258]).

Let us continue the investigation of thermal deformations of resonators with circular cylindrical elements. Formula (3) describes the variations of the index of refraction inside an unlimited long rod. It is necssary to consider the possible role of the edge effects in real rods of finite length. This problem is nontrivial and is a source of numerous errors; therefore let us discuss it in somewhat more detail.

The nature of the distribution of the longitudinal normal stresses and edge effects in problems of this type is explained by Figure 5.1. Let us first imagine that a rod of length ℓ having flat ends in the unheated state is part of the freely supported (unreinforced) monolithic rod of unlimited length (Figure 5.1, a).

Now we shall heat the entire infinite rod uniformly over the entire length; for determinacy we shall consider the temperature monotonically decreasing on going away from the axis. From the arguments of asymetry it is clear that any cross section perpendicular to the axis which was planar in the unstressed rod of unlimited length remains planar also on axisymmetric heating of it. The two isolated cross sections separated by a distance ℓ do not constitute an exception. Hence, it follows that in the given case all of the layers of the rod located at different distance from the axis acquire the same relative elongation along the z-axis corresponding obviously to the average heating temperature. For cold layers this elongation is excessive, and for hot layers, it is insufficient, from which we have the distribution pattern σ_z depicted in Figure 5.1, a described by formula (2).

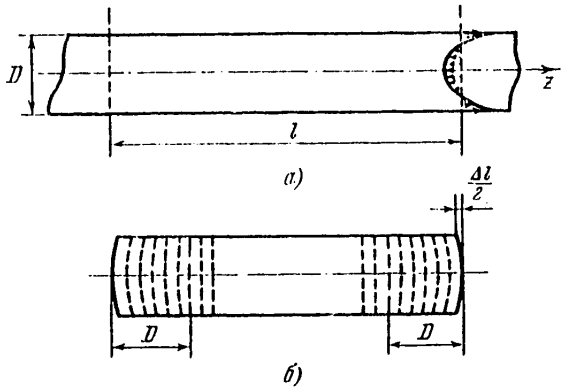

Figure 5.1. Distribution of longitudinal normal stresses and edge effects in an active element with axisymmetric temperature distribution: a) circular cylindrical rod of infinite length; b) rod of finite length.

Let us make sections through the isolated cross sections and thus produce our rod of finite length. Before this, a system of forces depicted in Figure 5.1, a was applied to both ends of the rod from the outside, which kept them flat in spite of nonuniform heating. Now these forces are removed and the ends are deformed. The magnitude of the deformations obviously will be the same as if we applied the same system of forces in the opposite direction (Figure 5.1, b) to each end of the unstressed rod. The results of these forces from each side is equal to zero; therefore in accordance with the Saint-Venant principle which is known in elasticity theory [251], they are capable of causing noticeable deformations only in the sections directly adjacent to the ends, the length of which does not exceed the rod diameter D. As a result, the total picture of longitudinal deformations of the rod acquires the form provisionally depicted in Figure 5.1, b (in reality, in addition to everything else not only the ends are distorted, but also the sections of the lateral surface of the rod adjacent to them). The cross sections which were flat in the unheated rod remain flat also after nonuniform heating of it over the extent of almost the entire length. Only small sections near the end freely expand in

accordance with their individual temperature. Therefore the difference $\Delta\ell$ between the lengths of the rod obtained for measurements along the axis and along the generatrix (Figure 5.1, b) is not $\alpha\ell\Delta T$, as can be demonstrated, but a many times smaller value $\sim\alpha D\ \Delta T$ where ΔT is the total temperature gradient.

Although the conclusion obtained with the help of elasticity theory and confirmed by direct measurements that the amount of sag of the ends is nearly independent of ℓ and is very small, was published in 1966 [74] it was not possible at that time completely to do away with the invalid ideas of thermal deformations. As an example let us mention the paper [259] in which the estimate of the sag of the ends and analysis of the consequences following from this were performed beginning with the formula $\Delta\ell = \alpha\ell\Delta T$. Apparently, the same error prompted the authors of [253] to include the term $\alpha(n-1)\ell\Delta T$ which should not be there in the initial formula for the resonator deformations.

It is possible to sum up the results. The stress and strain pattern in a rod of finite length differs from the pattern in an infinite rod only in small sections of length near the ends of the rod where the state of material is less stressed. If we consider that the mean variations of the optical path on transmission of light through the unstressed and thermally stressed parts are described by constants W and P that are not too different with respect to magnitude, it becomes clear that the edge effects in the given situation play a special role. Actually, in reference [200], they were not manifested noticeably even for $\ell/D \sim 4$. Thus, the deformations of the resonator with axisymmetrically heated rod of length ℓ can be found by simple multiplication of the equality (3) by ℓ. Then, however, we deal with the case where analogous edge effects will play a larger role.

Consequences of Aberrations and Efforts to Correct Them. From formula (3) it follows that for any form of T(r), except the trivial T(r) = const, changes also take place in the average index of refraction for two polarizations of the index of refraction and birefringence. What the presence of an index of refraction gradient leads to, we already know from Chapters 2-4. For quadratic dependence of T on r which is characteristic of the frequency and continuous lasers, the average index of refraction is also a quadratic function of r -- a powerful thermal "lens" is manifested. If this lens is in no way compensated for, the angular divergence of the radiation turns out to be very large. On introduction of the corresponding quadratic phase corrector into the resonator, the divergence decreases [54, 260].

This lens-like nature of a specimen is frequently observed also in the single flash mode. Its compensation naturally has the same effect on the angular divergence [261, 262]. However, the possibilities of this method of controlling the thermal "lenses" should not be overestimated. Actually, the dynamic correction of any distortions, including arbitrary "lenticularity" is a very difficult problem. Technically complicated correction methods which will be discussed in the next two sections have been developed only in very recent times, and they will be used obviously only in highly critical cases. If we are talking about comparatively simple means, it remains only to place the previously selected corrector inside the resonator, adjust the resonator, considering the subsequently manifested "lenticularity" (this is what was done, in particular, when creating the monopulse master oscillator in [129]), and so on. In this situation any variations of the thermal regime of the active element and pumping conditions are sufficient for compensation to be disturbed. Satisfactory correction in the powerful single pulse mode of free lasing where the magnitude of the deformations changes

significantly under the effect of the pulse is highly problematic. One of the many attempts to create an element capable of compensation for a thermal lens coming during the pulse was undertaken in [263]. This element was a mirror that absorbs a small portion of the lasing radiation incident on it in its mass and undergoes, therefore, thermal deflection. The mirror was successfully tested outside the resonator, but no special applications were found.

Double refraction also leads to highly unfavorable consequences. It is known that the results of transmission of planopolarized light through an isotropic medium, the optical axis of which is perpendicular to the direction of propagation essentially depends on the mutual orientation of the optical axis and the plane of the initial polarization. If they are parallel or perpendicular to each other, the light remains planopolarized. In all the remaining cases the polarization becomes elliptic -- a second linear component appears, and, as is said, the beam depolarizes. In a circular rod with axisymmetric temperature distribution, the local optical axes of an anisotropic medium as a result of the stress effect are directed along the radii. Therefore the depolarization with respect to passage through this element takes place in all sections of the cross section except the ones adjacent to the two straight lines passing through the axis of the element, one of which is parallel to the polarization plane of the initial beam, and the other is perpendicular to it (Figure 5.2, a).

If the resonator contains elements realizing the complete or partial polarization of the radiation, the double refraction leads to the highly characteristic "cross" pattern of the distribution of the polarized components with respect to the cross section. This picture was investigated theoretically and experimentally in [264, 265] for the case of weak double refraction in planar and telescopic resonators (in a telescopic resonator it turned out to be more favorable). However, even without detailed investigation it is clear that the depolarization of such resonators leads to a reduction in the lasing power inasmuch as the radiation of the newly appearing polarization component is output in one way or another from the resonator, making no contribution to the useful signal. In the case of large-scale double refraction the degree of depolarization and power losses become significant (lasing can even be curtailed). It is possible to avoid this, using the system proposed in [266], the meaning of which reduces to the fact that the resonator for emission of undesirable polarization "is blocked" -- this radiation returns, not reaching the part of the optical system which contains the shutter and the output mirror (Figure 5.2, b).

Even in cases where double refraction does not lead to power losses (in particular, in the absence of polarizers), a number of undesirable effects still remains both in the oscillators and in the amplifiers. In particular, the natural oscillations of the resonator with axisymmetric anisotropic medium cannot have a polarization state identical with respect to the entire cross section. As a rule, this leads to a sharp decrease in the spatial coherence of the generated radiation; in the best case the laser begins to operate on modes, the direction of the polarization of the radiation of which in each segment of the cross section is oriented along the radius or tangentially [267, 268]. From § 2.2 it is known that such polarization states are obtained only as a result of superposition of higher-order modes than zero (see Figure 2.14). In laser amplifiers the double refraction even in the single pulse mode can lead to nonuniform distribution of the radiation intensity with respect to cross section [269, 270]; it prevents the creation of highly efficient multipass amplifiers "decoupled" with respect to polarization [271].

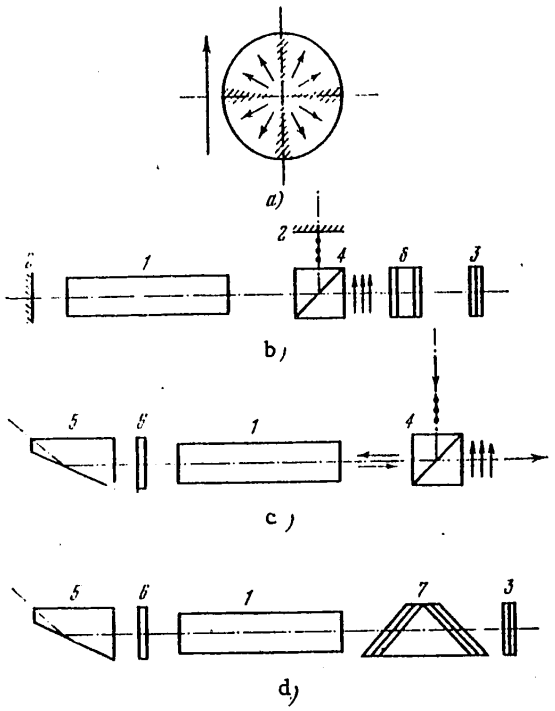

Figure 5.2. Birefringence in lasers based on circular active elements with axisymmetric temperature distribution: a) direction of local optical axes inside the active element (the zones are crosshatched in which the plane-polarized light with the direction of polarization indicated to the side by the large arrow does not undergo depolarization); b) the resonator for the plane-polarization radiation laser in which double refraction does not lead to energy losses; c) diagram of the double-pass amplifier with compensated double refraction; d) diagram of an analogous laser; 1 -- active element in the form of a circular cylinder, 2 -- completely reflecting mirror, 3 -- output mirror (stacked), 4 -- Glan prism (radiation of one polarization passes without losses, the other is reflected from the diagonal splicing plane), 5 -- tetrahedral reflecting prism, 6 -- quarter-wave phase plate, the principal direction of which is 45° with the plane of the figure, 7 -- polarizer (conventional representation), the principal plane of which makes an angle of 45° with the plane of the figure, 8 -- electrooptical shutter.

All of these phenomena greatly complicate the construction of single-mode laser systems with small radiation divergence. Therefore the efforts to completely avoid the consequences of double refraction are of unquestioned interest, realizing 90-degree rotation of the polarization plane on the path between the two identical active elements. Then the radiation having r-polarization in the first element will have ϕ-polarization in the second element, and vice versa. Obviously, the phase shifts between the different polarization components in the two active elements are compensated for here, and the manifestations of double refraction

disappear [272]. It is possible to achieve the analogous effect also for one active element, rotating the polarization plane on the path from the element to the mirror and back (which can be achieved, for example, using a 45-degree Faraday rotator of the polarization plane installed between the element and the mirror).

A detailed analysis of the possible diagrams of two-pass amplifiers and lasers with compensated double refraction, two of which are presented in Figure 5.2, c, d, was performed in [273]. The experiments performed there demonstrated, on the one hand, that when using these systems, the double refraction actually does not lead to such a sharp decrease in power as in ordinary lasers; on the other hand they demonstrated that the required accuracy of all of the optical elements and their mutual orientation here are far from simply achieved. In addition, the compensation of the double refraction still turns out to be incomplete inasmuch as the beams pass through the active element nonparallel to its axis as a result of the presence of the same thermal aberrations.

Let us mention such a characteristic method of compensation of the thermal deformations as the creation in the active element of the correspondingly selected preliminary stresses by quenching it [274], and let us proceed to the efforts to decrease the deformations themselves.

Different Methods of Decreasing the Resonator Deformations. The most natural method of decreasing the thermal deformations of the resonator is the adoption of all possible measures to insure the maximum uniform temperature field with respect to the active sample. In the single pulse mode the decisive role is obviously played by uniformity of the pumping distribution with respect to the volume of the active element. Inasmuch as ideal uniformity is still not achieved, sometimes a temperature gradient is created in the active element which is inverse to the gradient occurring as a result of pumping. This can be achieved, varying the temperature of the coolant in time according to a given law [275] or heating the sample by an additional pumping pulse and waiting a defined time until the required temperature distribution is established in the cooling process [271]. In frequency lasers operating in a series of pulses, obviously it is best of all to cool the active element only in the gaps between the series, offering it the possibility of being freely heated during the series itself, which insures the minimum temperature gradients with respect to cross section [276].

From this list alone, the necessity for more radical methods of eliminating thermal deformations is clear. Actually, such methods exist. One of them consists in the fact that the lateral surfaces of the active element are made planar, and the light flux passes through the sample inclined to these surfaces and undergoes total internal reflection on them. Here each ray of the parallel beam crosses through all of the layers of the sample with different temperature and index of refraction, which leads to equalization of the optical paths, that is, the absence of thermal deformations.

The generation of radiation beams experiencing reflections from the side walls of the active elements of rectangular and octagonal cross sections was first observed by Vanyukov, et al., in 1963-1964 [18]. The different systems of lasers and amplifiers with total internal reflection in the active element were subjects of lively discussion in 1965-1968 [277, 139, 140]; two of them borrowed from [139, 140] are presented in Figure 5.3. It is true that the creators of these systems primarily pursued the goal of using sharp dependence of the reflection coefficient on

the angle of incidence near the critical angle of total internal reflection for angular selection of the radiation (see § 2.6, Figure 2.24, d), but it turned out that the problem of thermal deformations is also solved simultaneously 140].

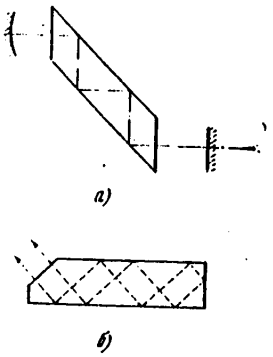

Figure 5.3. Diagrams of lasers with total internal reflection in the active element: a), b) diagrams proposed in [139, 140], respectively.

Finally, in 1970 attention was again attracted to this area by the papers of Mikaelyan and D'yachenko [278], who did not try to use the mentioned dependence of the reflection coefficient on the angle of incidence, but were only interested in the problem of thermal deformations. They classified the resonators which they called wave guide resonators and demonstrated the possibility of eliminating the thermal deformations experimentally. However, lasers of this type did not become widespread as a result of difficulty of manufacturing the active elements, complexity of their cooling and other similar causes.

The method consisting in transmission of plane-polarized light through active elements again inclined with respect to the plane side surfaces but at the Brewster angle so that the light is not reflected, but on the contrary, passes through the surfaces almost without losses turned out to be more vital. This method is used when constructing frequency lasers (for example, [279]) and also powerful output stages of the monopulse lasers [280, 281]. In the frequency lasers the elements are in a coolant, the presence of which decreases the Brewster angle and reduces unavoidable losses on transmission of the light through the surfaces to an extraordinarily small magnitude. This, in turn, creates the possibilities for placement of a large number of active elements in one resonator to which the form of thin disks is assigned (Figure 5.4, a). Small thickness of them implies a sharp decrease in the temperature gradients and promotes an increase in the uniformity of the pumping distribution.

In the terminal amplifiers of monopulse lasers the cooling or immersion liquids are not used as a result of the low self-focusing threshold characteristic of them. Therefore such amplifiers are capable of operation only in single-pulse modes. There is a positive side here -- the thermal loads for small, and the thickness of the active elements can be made sufficiently large; thus, in [281] it was 30 mm. This permits us to limit ourselves to a moderate number of elements. The diameter of the light aperture here usually is very large and frequently reaches 200 mm [281]. Therefore it is necessary to realize the pumpings through the same lateral surfaces through which the amplified radiation is

transmitted and locate the element so that they do not shield each other from the pumping source (Figure 5.4, b). In spite of its unique characteristics, the disc amplifiers are used only in exceptional cases as a result of enormous dimensions and large labor consumption of manufacture.

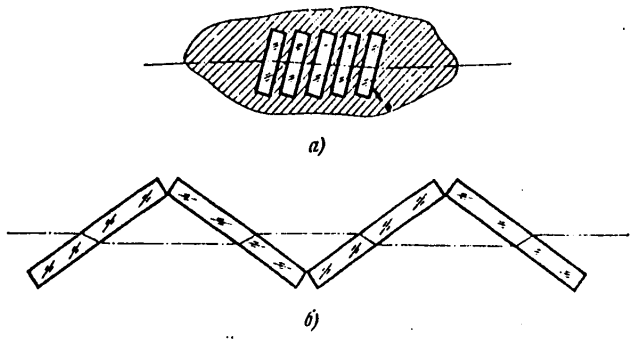

Figure 5.4. Diagram of the arrangement of the active elements: a) disc elements in the coolant (frequency laser); b) flat plates in the air (monopulse laser).

The most fruitful idea pertaining to the methods of controlling thermal operations in the resonator and amplified channels lies in a somewhat different area. It was first stated by Spitzer [71]; it pertains only to loss lasers and reduces to the fact that the thermal deformations can be significantly decreased by the selection of the glass composition. The fact is that the variations of the index of refraction as a result of the temperature gradient itself and the stresses arising here in practice are always in opposite directions — in the formula for P the terms with dn/dT and $\partial n/\partial\sigma$ are subtracted from each other ($\beta < 0$, $C_1 + 3C_2 < 0$). This is easily explainable: a decrease in the index of refraction with an increase in temperature is connected to a significant degree with reduction of the density of the medium, and the thermal stresses always prevent redistribution of the density in the nonuniformily heated part (see Figure 5.1 and the comments to it). At the same time the thermooptical properties of the medium depend, of course, not only on its density (which is indicated at least by the presence of double refraction), and there is a certain possibility of independent variation of some of the parameters entering into (1), (3). The thermal coefficient of the index of refraction β can vary within especially broad limits, and P also with it.

The experiments in this area quickly led to impressive progress in the field of neodymium glass lasers. Over the course of several years an entire series of so-called athermal laser glasses appeared in which one linear combination or another of thermooptical constants P and Q reduce to zero. In order to understand what the developers of laser glasses are striving for, let us return to expression (3).

The optimal version is, of course, equality of P and Q to zero. In this case the thermal deformations must be absent for any form of $T(r)$. In recent years it was actually possible to create glass in which P and Q are extremely small at room temperature [282] (the stipulation with respect to the temperature arose from the fact that the constants P and Q themselves are slowly varying functions of it [283], and athermalness is insured only in a narrow temperature range). However, such

response can be achieved only for phosphate glass having much lower chemical stability and thermal strength than the most widespread silicate glasses. As for silicate glass, in different types of it, the value of Q is in practice the same; only P is subject to variation.

If $Q \neq 0$ the thermal deformations cannot be avoided for arbitrary form of T(r). When the temperature distribution is of a regular nature, some possibilities appear in this respect. In particular, for quadratic dependence of T on r characteristic of frequency and continuous lasers, formula (3) acquires the form

$$n_{r,\varphi} = n_0 + P\Delta T/2 - (P \pm Q/2)\Delta T(r/a)^2,$$

where ΔT is the total temperature gradient between the axis and the side surface, and a is the radius of the rod. Hence it follows that for $P \pm Q/2 = 0$ the thermal deformations for the r or ϕ polarization radiation are absent [284]. For frequency lasers $P - Q/2$ usually approach zero; the divergence of their radiation actually is sharply reduced as this value is decreased (see, for example, [257]). However, as has already been pointed out, double refraction in circular active elements prevents plane-polarized radiation lasing; therefore the maximum small divergence still remains unattainable.

Lasers Based on Active Elements of Elongated Rectangular Cross Section. From everything that has been discussed it follows that even defined possibilities for controlling thermoelectrical characteristics of glass do not permit complete solution of the problem of thermal deformations in lasers based on traditional active elements of circular cross section. It is also obvious that the primary causes of all of the difficulties here are the following: 1. The form of the stress distribution near the circular element in the general case does not repeat the form of the temperature distribution (see (2)); therefore exact compensation for the variations of the index of refraction caused by its dependence on temperature and on the stresses it is possible only for certain specific forms of T(r). 2. Local optical axes of the anisotropic medium from which the circular axisymmetrically stressed rod consists are oriented along the radii and their directions are therefore different in different sections of the cross section which prevents plane-polarized radiation lasing.

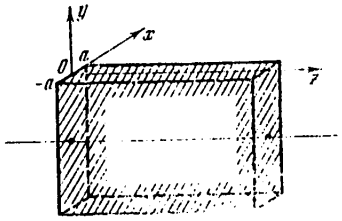

Figure 5.5. Active element in the form of a flat plate.

The origin of both of these phenomena is organically connected with the circular shape of the cross section, and on variation of the type of symmetry of the cross sections they can disappear. Actually, let us consider the optical properties of

glass plate bounded by the planes x = ±a and heated symmetrically with the plane x = 0 (Figure 5.5). Obviously the local optical axes inside this plate together with the temperature gradient have the same direction in the entire volume. In addition, from elasticity theory it is known that the shape of the stress distribution in the absence of external forces here completely repeats the form of the temperature distribution [251]:

$$\sigma_x = 0, \quad \sigma_y = \sigma_z = \frac{\alpha E}{1-\mu}[T_0 - T(x)],$$

where $T_0 = \frac{1}{a}\int_0^a T(x)\,dx$ is the average temperature. Substituting these formula in (1) and considering that the light is propagated through the plate along the z-axis, we obtain the following relations [200]:

$$n_{x,y} = n_0 + (P \pm Q)[T(x) - T_0], \tag{4}$$

where $n_{x,y}$ is the index of refraction for light polarized along the x and y-axes, respectively, n_0 is as before the index of refraction in the medium without stresses at a temperature of T_0.

Hence the obvious conclusion follows immediately: if the plate made of glass with P + Q = 0 or P - Q = 0 is used as the active element, the deformations of the resonator for plane-polarized radiation with one of the two directions of polarization must be absent for any temperature distribution. Let us only remember that this distribution must always remain symmetric with respect to the x = 0 plane; if this is not so, the plate will bend, and for description of the resonator deformations, a much more complex expression is required in which W will figure in addition to P and Q.

It remains only to discuss the edge effects and the polarization characteristics of the generated radiation. Let us begin with the simpler problem of edge effects. In exactly the same way as in the case of a circular cylinder, the width of the region adjacent to the edges of the plate inside which the stressed and strain pattern differs significantly from the pattern in an infinite plate does not exceed the plate thickness (which is confirmed by the results of the corresponding calculations [285]). However, here in contrast to the circular elements, this region borders the plate on all four sides (crosshatched in Figure 5.5). Whereas the zones adjacent to the ends of the element do not play a special role (for the same reasons as for circular rods), the situation is somewhat different with regard to the zones adjacent to the sides -- the light passes crosswise through them, and the effect turns out to be significant along the entire length. Hence it follows that for large temperature gradient the radiation passing near the sides will deviate significantly from the rectilinear direction and will not make a contribution to the central peak of the radiation pattern. Thus, from the point of view of thermal deformations it is desirable that the thickness of the plate determining the width of the edge zones be as small as possible; on the other hand, as the thickness decreases, the vibrations of the active element [192] and its heating at pumping time increase.

Now let us discuss the problem of the polarization of the generated radiation. Inasmuch as for $Q \neq 0$ the resonator deformations can be reduced to zero only for plane-polarized radiation with completely defined direction of polarization, it is necessary in some way to achieve a situation where the laser will operate on this radiation. Double refraction is not dangerous in this case: the required direction of polarization is parallel or perpendicular to the direction of the optical axis of the medium. The data of [264] and subsequent experimental papers indicate that certain other theoretically important reasons which could cause the decrease in power in the case of intraresonator polarization selection of the radiation are absent in the case of neodymium glass lasers.

Thus, the transition to elements with strongly elongated rectangular cross section permits the use of comparatively simple means to avoid thermal deformations without lowering the lasing power. Even the use of a polarizer is not mandatory in this case: it is possible to select conditions such that the "harmful" polarization component will be suppressed automatically. Let us explain this in the example of the single pulse mode.

In the case of symmetric two-sided illumination of the planar element, the minimum pumping density always falls to the central plane ($x = 0$); in the single pulse mode, the temperature obviously is normal at the pumping time. Let the composition of the glass be such that $P - Q = 0$; inasmuch as usually $Q > 0$, $P + Q$ in this case also turns out to be positive. From formula (4) it follows that in this case for radiation polarized along y, the index of refraction gradient is absent, and for the other polarization component the element is equivalent to a scattering lens. In planar or telescopic resonators this necessarily leads to an increase in losses; therefore the x-component can be present equally with the y-component only at the very beginning of the pumping pulse until a noticeable temperature gradient appears.

Spontaneous polarization of the laser emission with planar active elements must occur under certain other combinations of conditions and be actually observed in practice [284].

In spite of individual hopeful experiments with planar active elements to $40 \cdot 204 \cdot 600$ mm^3 in size [192], lasers of this type still have not become especially widespread. The reason for this is that for now for the majority of solid state lasers an effort is being made to consider the possibility of Q-switched operation. The large-cross section planar active elements are not too suitable for monopulsed lasers -- this configuration is highly unfavorable from the point of view of superluminescence which plays an extraordinarily important role in the "slave" operating mode. As for glass lasers with high output energy in the free lasing mode, the procedure discussed above for constructing them obviously is optimal [194].

In conclusion, let us briefly touch on the problems of thermal deformations of the liquid laser resonators. The value of dn/dT here is very large and as a result of the absence of static stresses is not compensated for any way; therefore the variations of the index of refraction turn out to be very large. The always available mixing of different layers of liquid leads to the fact that the temperature field is unstable, and the nonuniformities are irregularly distributed with respect to volume. For these reasons small angular divergence of the powerful liquid lasers almost unattainable. Therefore the liquid media are widely used only in

small lasers with tunable frequency, on the angular divergence of the emission of which as a rule special requirements are not imposed.

§ 5.2. Phase Correction of Wave Fronts. Dynamic Holography and Induced Scattering

Inasmuch as in the optical channels of lasers usually all possible nonuniformities are present, even an insignificant decrease in which frequently is extremely complicated, there is a natural effort to find methods permitting insurance of high output characteristics even when such inhomogeneities are present. A brief discussion of research for this purpose makes up the content of this and the following sections.

Optical-Mechanical Correction Systems. Let us begin with the possibilities which are related to purely mechanical displacements of certain elements with respect to the channel. First of all, the systems for automatic adjustment of laser resonators which are gradually entering into practice deserve attention. Their function is adjustment of the mutual arrangement of the mirrors in order to optimize any laser parameter. Without going into the technical details, let us only discuss the most theoretical problem of selecting a parameter, the magnitude of which is subject to optimization.

The output parameter of the laser which is quite "sensitive" to the resonator geometry and at the same time most simply controlled is its power. Therefore it is easy to create a self-adjustment system which maintains the maximum high level of output power. However, this operating algorithm can be far from always used: the pursuit of an insignificant gain in power can easily become enveloped in the large fluctuations in the position of the resonator axis, and, along with it, also the direction of the generated radiation. In addition, cases are possible where the shift of the resonator axis leading to an increase in power is accompanied not only by "drift" of direction, but also other undesirable consequences. We encountered one such example in § 4.2 — as the resonator axis of the flow laser approaches the point of entrance of the flow of medium into the resonator which is advantageous from the point of view of efficiency, the nonuniformity of the radiation distribution with respect to cross section of the lased beam and, consequently, the divergence increase sharply. Finally, it is necessary not to forget that the systems based on measuring output power can realize adjustment of the resonator only some time after lasing has started. Therefore for the overwhelming majority of pulsed lasers such systems are disadvantageous. It is also difficult to use them for certain continuous-action lasers, at the time of starting of which frequently such large misalignments occur that the laser in general does not begin to lase without resonator tuning.

For all these reasons, the most efficient operating algorithm for the autoadjustment systems is maintenance of the resonator axis in the given position. It is possible to deal with this problem by using the radiation of a low-power external source which will permit adjustment of the laser without beginning of its lasing.

A system for autoadjustment of unstable resonators investigated in the already-mentioned paper [217] was constructed by the same principle; the radiation of the auxiliary helium-neon laser is input to the resonator here along its axis through a small opening in the center of one of the mirrors. Undergoing multiple reflections, this radiation then "spreads" over the entire cross section. If the resonator was misaligned, the intensity distribution with respect to cross section turns out to be asymmetric, which is used for generating the error signal

putting the corresponding automation circuits into operation. The system described in [217] permits insurance also of satisfactory precision of adjustment of the errors (~5") and "capture" of the initial misalignment (5'-7') in a sufficiently large range of angles. The application of an auxiliary laser and the receivers of its radiation operating on a frequency differing from the frequency of the basic laser permits possible interference caused by the lasing process in the latter to be avoided. The system with introduction of the auxiliary laser through the central opening is also convenient in that this radiation passes through the adjusted resonator on the same path as the generated radiation; therefore it can be used so that the radiation will be directed at the measuring devices and so on visually or automatically.

A further step in improving the methods of mechanical automatic tuning of lasers is the application of the so-called adaptive optical system. Linnik's idea [286] about the possibility of autocompensation of phase distortions of the wave front caused by a turbulent atmosphere and interfering with the observation of remote objects marked the beginning of this area of study. The typical method of solving this problem by the methods of adaptive optics consists in the following: one of the elements of the optical channel of the transceiving system, for example, the mirror objective of the shaping telescope is made up of many more small mirrors having the possibility of insignificant translational displacements. By using these displacements, compensation of the large-scale phase distortions is also insured.

When creating such devices it is most complicated to deal with the generation of error signals. Let, for example, the problem of the formation of a beam with divergence as small as possible be solved. The recording and analysis of the form of the intensity distribution in the far zone with invariant arrangement of the individual parts of the composite mirror still do not permit judgment of which of their displacements are needed to improve this form. Actually, the same distribution in the far zone can be observed for different forms of the wave front; thus, in § 1.1 we are dealing with the fact that the beams distinguished by the sign of the curvature of the spherical wave front had identical divergences.

In order to obtain the required information about the deviation of each individual mirror from its optimal position corresponding to the maximum axial luminous intensity of the devices as a whole, it is simplest to use the following fact. The dependence of total axial luminous intensity F on the coordinate of one of the mirrors x measured along the axis perpendicular to its surface is depicted in Figure 5.6. If this mirror undergoes oscillations with of amplitude h much shorter than a wavelength nears its optimal position x_0, the axial luminous intensity as is obvious in the figure, remains almost constant. If the average position of the mirror is shifted to any point x_1 noticeably remote from x_0, the magnitude of the axial luminous intensity begins to fluctuate with the same frequency as the mirror. The relation between the phases of these two fluctuations will obviously depend on the direction from optimal that the average mirror position is shifted.

Now, leaving only one of the mirrors stationary, let us force each of the remaining ones to oscillate with its individual frequency and let us carry out spectral expansion of the time dependence of the axial luminous intensity. Obviously, the presence in this expansion of components with frequencies equal to the frequencies of the oscillations of individual mirrors will indicate that the positions of the

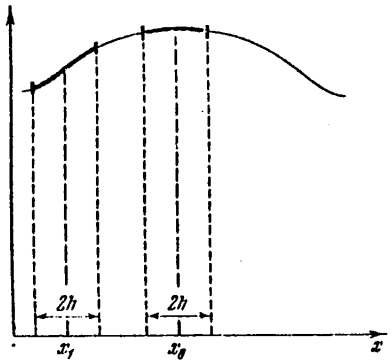

Figure 5.6. Axial luminous intensity as a function of the position of one of the parts of the composite mirror.

given mirrors are subject to adjustment. The phase relations provide information about the direction of the required shifts.

This principle was also proposed and realized in the known papers [287, 288]. In the first of them an adaptive system of seven elements was manufactured and successfully tested; in the second, a system of 18 elements. Later the possibilities of adaptive optics were unconditionally expanded. Instead of the set of individual mirrors now single flexible mirrors are beginning to be used -- this corresponds to the transition from "step" approximation of the given phase distribution to more improved approximation using continuous functions. The number of independently adjustable parameters will also increase; familiarization with [334] gives a sufficiently good idea about the paths of development of adaptive optics.

In spite of all of these prospects it is difficult to count on broad application of adaptive optics directly in the laser resonators: the creation of a low-inertia adjustable mirror capable of operating under high beam load conditions is a highly complicated problem. In addition, the small phase aberrations and unstable resonators, as we have seen in Chapters 3, 4, cannot lead to either multimodal lasing or to large reduction in the output power, and they only cause phase distortions of the wave front of the generated radiation which can be entirely compensated for also outside of the resonator. Therefore the optimal location of the complex adjustable mirrors is the exit of the shaping system where the density of the radiation usually is many times less than the density inside the oscillator. As for resonators, among their mechanical correction devices probably only the simplest autoadjustment systems have become widespread which can be supplemented by very useful and not too complex systems for automatic compensation of the second-order wave aberrations which are variable in time (lenticularity).

Other methods of conversion of the wave front form are also of great interest. The most universal and common of them is obviously holography.

Holographic Correction Principles. Usually two mutually coherent light beams participate in the recording of the hologram depicted in Figure 5.7, a. In the case of standard use of holography for recording the image of real objects one of

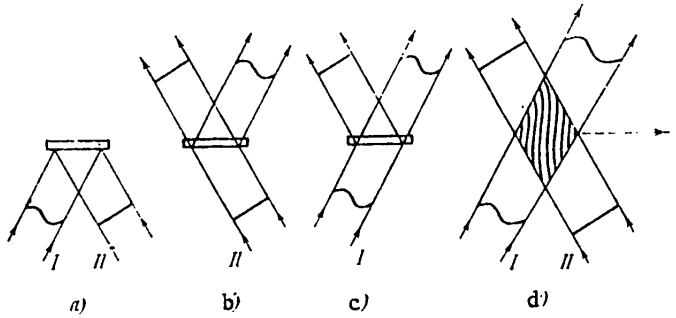

Figure 5.7. Problem of holographic corrections: a) recording of a thin hologram; b), c) reproduction of one of the beams on illumination of a hologram by the others; d) beams and three-dimensional hologram.

these beams -- I -- is the light scattered from the object illuminated by the coherent radiation; its wave front has a complex shape which carries information about the image of the object. The beam II -- the reference beam -- has a regular, for example, planar shape of the wave front. When the hologram, which is an imprint of the interference pattern between these two beams is made and then illuminated by the reference beam itself II, the light scattered from it in the direction of one of the diffraction orders has, as is known, the same structure as the beam I has during the recording, that is, as before, it is the carrier of all of the information about the image of the object (Figure 5.7, b). However, the light beams of I and II are theoretically entirely equivalent. If the hologram is illuminated not by the reference beam, but by the object beam I the light scattered in the corresponding direction will have the same structure as beam II has during the recording, that is, it will have regular (planar) shape of the wave front. The given process is also depicted in Figure 5.7, c.

This property of a holograph also provides the basis for holographic methods of correcting the wave front of the wave emission first realized by Soskin, et al. [289]. The functions of the object beam of I here are performed by the laser radiation, the shape of the wave front of which is subject to correction. The coherent reference beams II with flat wave front can be formed, for example, from part of the same emission transmitted through an angle selector.

When using holography to decrease the convergence of the laser emission, the decisive role is played where the density of the efficiency of conversion -- the fraction of the power of the beam illuminating the hologram which pertains to the required diffraction order. The lowest efficiency not exceeding a few percentages occurs for thin amplitude holograms which are obtained on ordinary processing of thin-layer photographic material. Bleaching converts the metallic silver to a transparent compound with a different index of refraction than for the emulsion gelatin, and the hologram is converted from an amplitude hologram to a phase hologram -- the peaks and the minima of the recorded interference pattern on the hologram made correspond to sections of different optical thickness. The efficiency of thin phase holograms can theoretically approach 30%; such holograms were used when investigating the possibilities of the given correction method used by the same group of authors in 1969-1972 [289-291].

Among the other results contained in the mentioned papers, the realization of phase correction of the radiation of the helium-neon laser generated on one transverse mode of the stable resonator TEM_{02} [290] deserves to be noted. Before correction, the lasing beam had a flat equiphasal surface in the hologram zone and just as the radiation of any nonzero mode of a stable resonator, it had sign-variable amplitude distribution (see § 2.1). It is possible to interpret the change in sign of the amplitude as a phase shift by π; as a result of the holographic correction such phase shifts disappear, and the wave front becomes genuinely planar (although the amplitude distribution naturally remains nonuniform). Under the conditions of [290] this has led to a fourfold decrease in divergence, and the axial luminous intensity increased noticeably although the energy efficiency of the conversion was a total of ~10% [291][1].

No less interesting experiments were performed with a ruby laser operating in the ordinary "spike" free lasing mode [291]. Here the gain in the divergence turned out to be still more significant. The possibility of realizing the correction itself in the free lasing mode which is more frequently multimodal when using a planar resonator is, generally speaking, connected with two facts. First, in the case of an optically nonuniform active medium the general distortion of the wave front caused by aberrations of the resonator characteristic of different transverse modes can prevail over the differences in the shape of the wave fronts of the individual modes (which, probably, occurred also in [291]). Secondly, although the spatial field distributions can vary from spike to spike, the peaks of these distributions naturally do not coincide; therefore the overlap of the holograms recorded by the radiation of the individual "spikes" is only partial. However, partial superposition of the holograms must lead to a reduction in energy efficiency of conversion; under the conditions of [291] it was a total of 3%.

The successful performance of the individual experiments could not free the given method of holographic correction of the serious deficiencies organically inherent in it. The use of thin-layer photographic materials alone immediately imposes rigid restrictions on the working wavelength and on the admissible radiation flux densities and, finally, the energy efficiency of conversion. It is still more important that the correction using the previously manufactured holograms is generally possible only in rare cases where the laser operates under exceptionally stable conditions, and the shape of the wave front of the generated radiation remains the same.

All of this dictates the transition to dynamic volumetric phase holography based on reversible changes in the index of refraction of certain nonlinear media in the radiation field; as a result of the presence of the known Bragg condition, the light incident on the three-dimensional hologram is scattered predominately in one diffraction procedure, and the efficiency of conversion can theoretically reach 100%.

All of the subsequent studies in the given field have proceeded along this path. The system which is used for correction by the methods of dynamic three-dimensional holography is depicted in Figure 5.7, d. The volumetric interference between two

---

[1] Having high energy efficiency, although less elegant, the procedure for realizing the correction in such cases with the help of a stationary phase plate was described after several years in [292].

coherent light beams leads to the fact that a holographic phase lattice is formed in the nonlinear medium consisting of alternating layers with different index of refraction. If such a lattice is fixed in some way and then illuminated by one of the beams participating in the process of its formation, as a result of reflection from the lattice it acquires the structure of the second beam entirely similarly to how this occurs in the case of a thin hologram (see Figure 5.7, a-c). Reflection takes place without loss of intensity if the absorption in the medium is quite low, the lattice is sufficiently thick (the number of its periods along the direction of the incident beam must be significantly greater than one), and the condition $\Delta n/n \ll 4 \sin^2 \theta$ is satisfied [293, 294], where Δn is the modulation amplitude of the index of refraction, 2θ is the angle between the initial beams (see Figure 5.7, d). The meaning of the last condition reduces to the fact that the reflection from one lattice period taken separately must be quite small; only then does the three-dimensional nature of the lattice acquire a genuinely important role. Otherwise the light, just as with a thin lattice will be scattered also in other directions. Hereafter we shall consider that the conditions of three dimensionality are satisfied, and the scattering of the light in other directions is absent.

Now let us consider a real situation where both light beams exist simultaneously together with the three-dimensional hologram created by them. As a result of the interaction of each of these beams with the hologram, scattered (or, if one likes, reflected from the hologram) radiation appears. However, inasmuch as the shape of the wave front of the scattered radiation coincides with the shape of the wave front of another beam, the structure of the initial two beams remains unchanged; only redistribution of their intensities can occur.

The idea of the dynamic holographic correction is connected with this redistribution: if it actually occurs, the possibility appears for transmission of the energy of a powerful light beam, the shape of the wave front of which is subject to correction, to a reference beam with small initial intensity and plane wave front. This method of obtaining (more precisely, amplifying) narrowly directional irradiation is obviously applicable when the shape of the wave front of the powerful beam varies in time; it is only necessary that these changes be sufficiently small during the lattice relaxation time.

Conditions of Realizing the Process of Holographic "Transfer" and Its Energy Efficiency. "Transfer" on Thermal Lattices. In spite of the apparent "transparency" of the above-discussed idea of using dynamic holography, in reality it is not so simple. A more careful analysis indicates that under steady conditions and in an isotropic nonlinear medium redistribution of the energy between beams of identical frequency does not occur whatever the initial ratio of their intensities [295]. The reason for this is the following. Strictly defined phase relations exist between any of the two light beams and the radiation scattered in its direction as a result of interaction of the second beam with the volumetric hologram. These relations depend on how the holographic lattice is arranged relative to the interference pattern between the beams. Under the above indicated conditions the positions of the lattice and the interference pattern coincide — the extrema of the index of refraction are matched with the extrema of the total field intensity. It turns out that in this case the scattered radiation is phase shifted by $\pi/2$ with respect to the radiation of the beam to which it is added, and therefore it does not cause a change in its intensity. The phase shift and together with it the result of the interaction of the beams with the hologram, becomes different only when the holographic lattice is shifted for certain reasons by a fraction of a period in the transverse direction with respect to the interference pattern.

Initially we shall consider the hypothetical case where the radiation absorption in a nonliear medium is absent. For derivation of the corresponding equations let us represent the total field of two beams in the form

$$E(r) = A_1 \exp(ik_1 r) + A_2 \exp(ik_2 r),$$

where A_1 and A_2 are the complex amplitudes of beams I and II, k_1 and k_2 are the wave vectors of these beams where $k_1 = k_2 = k_0 = 2\pi n_0/\lambda$ where n_0 is the index of refraction of the nonlinear medium in the absence of a field. The index of refraction in the presence of the two beams will be considered equal

$$n = n_0[1 + \alpha|A_1 \exp(ik_1 r) + A_2 \exp(ik_2 r)\exp(i\delta)|^2]. \quad (5)$$

The value of the index of refraction averaged with respect to the lattice period obviously is $n_{mean} = n_0[1 + \alpha(|A_1|^2 + |A_2|^2)]$, and the modulation amplitude $\Delta n = 2|\alpha A_1 A_2|$. The introduction of the factor exp (iδ) in one of the terms in the right-hand side of (5) leads, as is easy to see, to the fact that the holographic lattice described by this formula is shifted with respect to the interference pattern by a fraction of a period equal to $\delta/2\pi$; the direction of the shift for $\delta > 0$ is shown in Figure 5.7, d by the dotted arrow. If the conditions are steady state, and the medium is isotropic, $\delta = 0$; then the formula for n acquires a standard form $n = n_0(1 + \alpha|E|^2)$.

The calculation of the interaction of light beams with a nonlinear medium reduces to the solution of the wave equation $\nabla^2 E + k^2 E = 0$ considering the dependence of k^2 on the radiation field. Inasmuch as the terms with α play the role of a small correction in the formulas for n, the following approximate formula is valid for $k^2 = k_0^2(n/n_0)^2$:

$$k^2 \approx k_0^2[1 + 2\alpha|A_1 \exp(ik_1 r) + A_2 \exp(ik_2 r)\exp(i\delta)|^2].$$

Substituting this formula and the expression for E in the wave equation, as a result of the calculations analogous to those discussed in the known paper by Kogel'nik [296] by the theory of three-dimensional holograms we obtain the following differential equations relating A_1 and A_2:

$$\frac{1}{A_{1,2}}\frac{dA_{1,2}}{dl_{1,2}} = i\frac{2\pi}{\lambda}(n_{cp} - n_0) + ik_0\alpha|A_{2,1}|^2 \exp(\mp i\delta), \quad (6)$$

where $l_{1,2}$ are the distances along the directions of propagation of beams I and II, respectively.

The equations obtained have obvious meaning. The first terms in their right-hand sides are identical and do not depend on the lattice shift parameter δ; they describe the phase incursion occurring as a result of the fact that the average index of refraction n_{mean} in the presence of a field differs from n_0. The origin of the latter is explicitly related to the reflection from the lattice. This is

indicated primarily by the presence of the "shift" factor exp ($\pm i\delta$). In addition, inasmuch as $\Delta n \sim |A_1 A_2|$, the amplitude of the radiation scattered in the direction of beam I must be proportional to $|A_1 A_2^2|$, and in the direction of the second beam $|A_1^2 A_2|$; this dependence is also contained in (6).

From equations (6) it follows that for $\delta = 0$ the scattered radiation leads only to additional phase variations which turn out to be greater for the less intense beam. When $\delta \neq 0$ (the lattice is shifted) in addition to the imaginary terms real terms also appear in the right-sides of (6). Accordingly, the intensity of one of the beams begins to decrease as it is propagated and the other, to increase -- so-called energy "transfer" takes place. The direction of the "transfer" is defined only by the sign of the product $\alpha \sin \delta$ and does not depend on the relation between the intensities of the interacting beams; therefore the energy of one of them can be transferred entirely to the other.

We have succeeded in drawing this optimistic conclusion after the authors of [294] only because, just as in [294], we introduced the lattice shift purely formally, not analyzing the natural situations in which it could really occur. Nevertheless, it will be seen later that the "transfer" will be realized in its classical version (the interacting beams have the same frequency) primarily in the presence of significant linear absorption in the medium. The corresponding theoretical analysis was performed in [297]. In the case of linear absorption (that is, when the absorbed power is proportional to the field intensity) the term $-\sigma/2$ is added to the right-hand side of each equation of system (6) where σ is the absorption coefficient. After transition from amplitudes to intensities $I_1 \equiv |A_1|^2$, $I_2 \equiv |A_2|^2$ the system acquires the form

$$\frac{1}{I_{1,2}}\frac{dI_{1,2}}{dl_{1,2}} = \pm 2k_0\alpha I_{2,1}\sin\delta - \sigma. \qquad (7)$$

Hereafter, for determinacy we shall consider that $\alpha < 0$ (which is characteristic of the thermal lattices investigated later) and $\sin \delta > 0$. In this case the beam I is the donor, and the second is amplified. From (7) it is obvious that $-k_0\alpha I_1 \sin\delta$ has the meaning of the amplification coefficient in a medium for a second beam in the presence of the first. The density of the amplified beam increases while the condition $I_1 > I_0 \equiv \sigma/(2k_0|\alpha| \sin\delta)$ is satisfied.

It follows immediately from this that for maximum use of the energy of the donor beam it is desirable that its density decrease in the zone of interaction of the beams to a value of I_0. In the most favorable case where the densities of the two beams at the entrance to the medium I'_1, I'_2 are constant with respect to cross section, this condition can be satisfied by using the flat layer of the medium (Figure 5.8), the thickness of which must be correspondingly selected. In Figure 5.9, a, b, the data obtained by solution of the system (7) on the optimal thickness of the layer of medium for the cases depicted in Figure 5.8, a, b when the beams enter into the layer from one or different sides are presented[1]. Although for the same I'_1, I'_2 the optimal thickness of the layer in these two versions does not coincide, the attained density of the amplified beam $I_{2\,max}$ turns out to be the same;

[1]The calculations for the second of these cases were performed by V. D. Solov'yev.

the data on it are presented in Figure 5.9, c. It is obvious that high energy efficiency of the "transfer" (on the order of 50% or more) can be achieved only

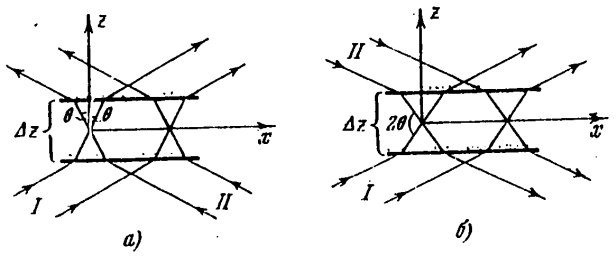

Figure 5.8. Geometry of the interaction of beams during "transfer" in a flat layer of medium: a) one-sided incidence of the beams on the layer; b) counterbeams.

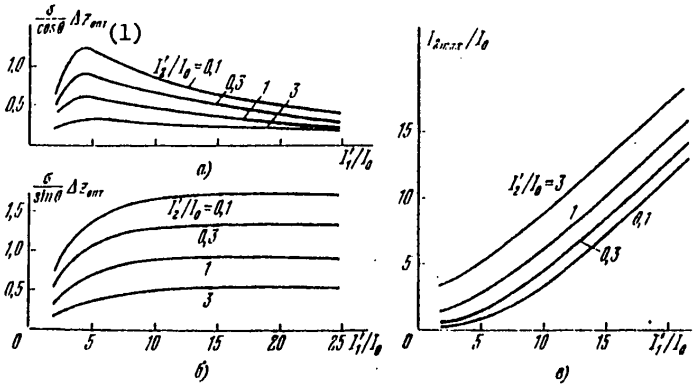

Figure 5.9. Optimal thicknesses of the layers of the medium and maximum attainable density of the amplified beam during "transfer": a), b) dependence of the thickness Δz of the layer of medium in the initial values of the beam densities I'_1, I'_2 in the diagram in Figure 5.8, a, b, respectively; c) dependence of the maximum attainable density of the amplified beam $I_{2\ max}$ I'_1, I'_2.

Key: 1. opt

when the initial density of the donor beam exceeds I_0 by at least several times; the initial density of the amplified beam also must not be too small.

Such is the theory of the interaction of beams with the holographic phase lattice created by them in the quasistationary mode in general outlines. Now we shall discuss the causes of the lattice shift with respect to the interference pattern required for energy "transfer."

In individual cases the shift occurs as a result of a natural anisotropic medium in which the hologram is created. The classical example of this is described in the well-known paper by Shtebler and Amodeya [298] devoted to the investigation of phase lattices in a lithium niobate crystal. On illumination of this material

charge carriers are relaeased in it, which is the cause of local changes in the index of refraction. As a result of anisotropy of the given material, the drift of the free carriers here is directed in an entirely defined direction which also causes a shift of the lattice recorded in the presence of two coherent beams. The authors [298] observed noticeable redistribution of the beam intensities. It is true that they used the given phenomenon not for correction of the wave front, but for discovery of the previously unknown sign of the free charge carriers which can be established by comparing the direction of the energy transfer process with the direction of conductivity of the given crystal. This phenomenon can hardly be exemplary of the dynamic correction -- the setup times here are tens of seconds.

In the general case of an isotropic medium a defined lattice shift can be obtained directly during interaction of the beams, obviously continuously shifting the medium in the direction perpendicular to the lattice planes. The shift must appear as a result of unavoidable inertia of the processes of recording and erasing it. Later it will be seen that it is possible to obtain the desired result in practice using this procedure only when using such comparatively slow recording mechanisms as thermal recordings. According to [297] let us consider this version.

For the geometry of the interaction of the beams depicted in Figure 5.8, a, the density of the thermal power dissipated as a result of absorption in the medium is $\sigma[I_1 + I_2 + 2\sqrt{I_1 I_2}\cos(2\pi x/\Lambda)]$, where $\Lambda = \lambda/2n \sin\theta$ is the period of the interference pattern, and the remaining notation was as before. The origin of the coordinates is matched with one of the peaks of the interference pattern (it is possible to neglect its small distortions along the Y and Z axes in the given investigation). A simple analysis shows that in the case of stationary medium the dependence of the temperature on x in the presence of such peak release sources has the form $T = T_{mean} + 2\sqrt{I_1 I_2}\frac{\sigma}{\kappa}\times\left(\frac{\Lambda}{2\pi}\right)^2\cos\left(\frac{2\pi x}{\Lambda}\right)$ with setup time of the spatial modulation $\tau = \frac{c\rho}{\kappa}\left(\frac{\Lambda}{2\pi}\right)^2$, where T_{mean} is the mean temperature of the medium slowly increasing with time, κ is the coefficient of thermal conductivity, c is the heat capacity and ρ is the density of the medium. This leads to the occurrence of the phase lattice with modulation amplitude $\Delta n = 2\sqrt{I_1 I_2}\frac{\sigma}{\kappa}\left(\frac{\Lambda}{2\pi}\right)^2\left|\frac{dn}{dT}\right|$.

If the medium is shifted continuously along the x-axis with a velocity V, the lattice setup time remains as before; its stationary position turns out to be shifted by $\Delta x = (\Lambda/2\pi)\operatorname{arctg}\omega\tau$, the depth of the modulation of the temperature and the index of refraction decreases in the ratio $(1 + \omega^2\tau^2)^{-1/2}$, where $\omega \equiv 2\pi V/\Lambda$. A comparison of these data with (5) indicates that the parameters of the "transfer" theory under the investigated conditions assume the values

$$\alpha = \frac{\sigma}{\kappa}\left(\frac{\Lambda}{2\pi}\right)^2\frac{1}{n}\frac{dn}{dT}(1 + \omega^2\tau^2)^{-\frac{1}{2}}, \quad \delta = \operatorname{arctg}\omega\tau.$$

As the velocity of the medium increases, δ increases, approaching the optimal value of $\pi/2$ from the point of view of the "transfer," and on the other hand $|\alpha|$ decreases rapidly. From (7) it follows that the intensity of the energy transfer process from beam to beam is defined in the final analysis by the value of $|\alpha \sin\delta|$. This value reaches the maximum equal to $\frac{1}{2n}\frac{\sigma}{\kappa}\left(\frac{\Lambda}{2\pi}\right)^2\left|\frac{dn}{dT}\right|$, for $\omega_0 = 1/\tau$; thus, the optimal

speed of the meium is $V_0 = \left(\frac{1}{\tau}\right)\left(\frac{\Lambda}{2\pi}\right) = \frac{4\pi n}{\lambda}\frac{\varkappa}{c\rho}\sin 0$. The density of the "donor" beam for which the amplification of the second beam as a result of "transfer" compensates for its absorption in the medium; for V_0 is equal to

$$I_0 = 4k\varkappa \sin^2 0 \Big/ \left(\frac{1}{n}\left|\frac{dn}{dT}\right|\right). \qquad (8)$$

All of the relations derived above are also valid for the case of "counter" beams (Figure 5.8, b) except here the index of refraction is not modulated along the x-axis, but along the z-axis; movement of the medium must be realized in the same direction.

Relation of the Idea of Dynamic Holography to the Phenomena of Induced Scattering. Lasers Based on Various Forms of Induced Scattering. Finally the time has come to explain what the logical development of the idea of holographic correction has led us to. For this purpose it is sufficient to compare two facts. First, when investigating the above-described "transfer" process in the coordinate system which is stationary with respect to not the interference pattern but the medium, the interacting beams acquire a defined frequency difference as a result of the Doppler effect. Its magnitude, as is easy to see, is ω, which explains why in this coordinate system the interference pattern is shifted at a velocity -V. Secondly, as follows from (7), the differential amplificaiton coefficient of the radiation with respect to beam II does not at all depend on its intensity and is completely determined by the density of beam I. Therefore when the latter has sufficient power that the "transfer" process takes place, in its presence not only the specially formed radiation is subject to application, but also the randomly scattered or "noise" radiation of proper frequency and direction.

The phenomenon consisting of the fact that on illumination of the proper medium by a powerful coherent beam amplification of the radiation takes place with frequency usually somewhat shifted with respect to the initial frequency is, as is known, called induced scattering of light. A specific amplification mechanism was described above connected with variation of the index of refraction as a result of heating of the medium during absorption of light. This type of induced scattering is actually known. It was discovered in 1967 and since that time has been called induced thermal scattering (ITS) [299, 300]. In accordance with the above-presented calculations, the maximum amplification of the scattered radiation occurs on a frequency shift with respect to the initial frequency in the antistokes direction (that is, larger) by ω_0. The ITS threshold on this frequency is defined by the formula (8); for other frequencies the threshold increases proportionally to $|\alpha \sin \delta|_{max}/|\alpha \sin \delta| = 1/2(\omega\tau + 1/\omega\tau)$.

The "transfer" observed in [298] in lithium niobate pertains to the phenomena of induced scattering on conduction electrons in semiconductors [301]. On the other hand, all types of induced scattering permit analogous "holographic" interpretation and are distinguished only by the mechanisms which cause variation of the index of refraction and shift of the phase lattice with respect to the position of the interference pattern. The reason for the shift almost always is movement of the interference pattern with respect to the medium as a result of the difference in frequencies of primary and scattered radiation (the source of the "neucleating" photons with shifted frequency for spontaneously occurring induced scattering which occurs predominately in the forward and return directions, usually is the scattering

on the random dynamic fluctuations of the index of refraction). The fact that for ITS the frequency of the scattered radiation is shifted with respect to the initial in the direction opposite to the usual shift direction for induced Mandelstam-Brillouin scattering on hypersonic waves (IMBS) and induced Raman scattering (IRS) are explained simply by the fact that the nonlinearity parameter α has different signs in these cases.

Thus, the dynamic holographic correction reduced to the well-known idea of solving the problem of divergence by constructing radiation converters based on induced scattering -- no other is given. Our corrector on the thermal hologram in the moving medium is none other than the ITS amplifier with frequency shift compensated as a result of the Doppler effect. Supplementing this amplifier by feedback -- a resonator -- obviously we can construct the analogous laser.

For ITS, the frequency shift is so small that it actually is easy to compensate, shifting the medium: according to the estimates of [297] if in the diagram in Figure 5.8, a the medium is a liquid of the type of an organic solvent, the required speed of its movement is a total of ~10 cm/sec. If the shift is compensated, it is possible to use the part of the initial beam transmitted through the shaper as the amplified. The first experiments with an amplifier of this type are described in [302]; the source of primary radiation split into two interacting beams was a single-mode ruby laser operating in the "spike" mode of free lasing. With a total lasing pulse duration of ~400 microseconds, the lattice relaxation time was ~100 microseconds, which, in turn, significantly exceeded the time interval between individual "spikes"; therefore for the extent of the greater part of the pulse the lattice was in practice quasistationary. The highest energy efficiency of "transfer" was achieved for the initial ratio of the beam intensities of 10:1; after passage of a liquid moving at a speed of 8 cm/sec, this ratio became equal to 1:3, and the amplified beam power was about 50% of the total power of the initial beams.

High inertia of the thermal processes permits observation of the phenomenon of nonsteady "transfer" predicted in [303] and consisting in the fact that for short-term interaction of the beams the energy transfer to the weaker one takes place even if the medium is stationary. This has the following explanation: when the unshifted lattice begins to be recorded and the scattered radiation appears, it, in accordance with (6), leads to additional phase incursions of the initial beams. As has already been noted, for a beam with lower intensity this incursion turns out to be larger; as a result, the interference pattern, while the processes of setting up the thermal lattice are taking place, moves through the medium which causes "transfer." The direction of the displacement is such that the weak beam is subjected to amplification. As applied to the problems of correction of the wave fronts this phenomenon was experimentally studied in references [302, 304, 305,335].

Although the papers studying the "transfer" on the thermal lattices turned out to be highly useful for understanding the possibilities of dynamic holography, it is not possible now to count on the fact that by using this process we will decrease the divergence by the radiation of real lasers. Here the mechanism of recording the lattice itself is unfavorable. The heat release required for its formation has, in addition to everything else, a negative effect on the optical quality of the medium. As a result of unavoidable nonuniformity of heating of the medium, variations of the index of refraction averaged over the lattice period appear; in the liquids, in addition, light scattering begins on the formed gas bubbles and so on.

All of this, in turn, leads to an increase in the divergence of the beam itself into which the energy is "transferred." The effects of this type begin to be manifested in practice by comparatively small energy levels of the beams [335].

Now let us proceed to other types of induced scattering. For ITS the energy "transfer" to a weaker beam with the same frequency is achieved without special difficulty even in the quasistationary mode. In the presence of IMBS and, in particular, for IRS everything looks somewhat different. The frequency shifts here are not so small, and the possibility of compensation for them using the Doppler effect is for a number of reasons for the most part speculative. It is already sufficient that in the former case the medium should be shifted at the speed of sound in it, and in the latter case, many times faster. Therefore by using the given forms of induced scattering having lower thresholds in the majority of media than ITS, it is possible to construct only lasers and amplifiers of radiation with shifted frequency. Nevertheless, the "transfer" with splitting of the initial beam into the donor and amplified beams is realizable and in this case the required frequency shift of the later amplified beam can be obtained using the same induced scattering. When using this system [306] conversion on IMBS was obtained with transfer on the order of 80% of the donor beam power to the amplified beam. As a result of the conversion, the axial luminous intensity increased by more than 3 orders.

As for the IMBS and IRS lasers, their properties are quite well-known. These lasers have, of course, many specific peculiarities distinguishing them from standard inverted medium lasers. First of all here although the primary radiation frequently is called pumping radiation as before, theoretically different requirements are imposed on its coherence -- the sources of the pumping of lasers based on induced scattering usually are other lasers with spectral radiation selection. Complex phenomena arise as a result of the fact that in the case of induced scattering the theoretical role is played only by the magnitude of the frequency different $\Delta\omega$, but not the exact absolute values. Therefore when the density of the converted radiation itself begins to exceed the induced scattering threshold, lasing is excited on a frequency $2\Delta\omega$ from the initial frequency, and so on. Finally, as already been mentioned in § 4.2, with respect to the nature of the interrelation between the excitation and the generated radiation fields the converters based on induced scattering more resemble flow lasers than standard lasers with a stationary medium.

In spite of all their peculiarities, the induced scattering lasers are, of course, the most genuine lasers. The principles of the selection of the type and parameters of the resonators remain the same as in ordinary lasers; the resonator deformations exist exactly the same, including those caused by heating of the medium. Being the basic, theoretically unavoidable source of heating, the Stokes losses in the IRS and IMBS lasers are much less than in the ordinary lasers which gives rise to the prospectiveness of this entire area. At the present time a number of experimental papers have already been published in which the conversion of the radiation with the help of IMBS and, in particular, IRS, has led to a decrease in the divergence (a broad bibliography exists, in particular, in [218, 306]). It is not appropriate to enumerate all of them; let us only mention one interesting area of research,

In 1973 when studying the properties of the IRS converters [307] and IMBS converters [308] with pumping by the radiation of multimode lasers, it was possible to

observe significant amplification of narrowly directional light beams without significant variation of their spatial structure. The nontrivialness of the situation consists in the fact that the multimode pumping field is nonuniform and actually divided into a large number of randomly distributed spots with respect to volume, the characteristic dimensions of which are defined by the parameters of coherence and the geometry of the illumination. The theoretical analysis of the conditions under which the nonuniformity of the pumping field does not imply a change in the spatial structure of the amplified beam (as a result of the statistical averaging of the effect of a large number of small nonuniformities) was performed in references [309, 310]. The first purposeful experiment checking this model was described in [311].

10,845
CSO: 1862/192

NUCLEAR PHYSICS

UDC 621.384.64

LINEAR INDUCTION ACCELERATORS

Moscow LINEYNYYE INDUKTSIONNYYE USKORITELI in Russian 1978 (signed to press 21 Apr 78) pp 2-10, 244-245

[Annotation, preface and table of contents from book "Linear Induction Accelerators", by Yuriy Petrovich Vakhrushin and Aleksandr Ivanovich Anatskiy, Atomizdat, 1730 copies, 248 pages]

[Text] The book presents elements of the theory and engineering of new powerful relativistic electron beam generators--linear induction accelerators. The working principle of linear induction accelerators is described, the theory is given as well as the results of development of the accelerating system, the beam shaping and transport systems; designs of existing accelerators and those under development are examined, and their future is evaluated. Although the book is devoted to linear induction accelerators, some of the problems that are considered have wider applications; for example pulsed magnetic reversal of ferromagnetics and accelerating voltage pulse shaping can be used in the development of pulse transformers in the nanosecond range, and systems for tailoring nanosecond current or voltage pulses

The book is intended for engineers and scientists engaged in the development and application of electrophysical facilities; it may also be of use to undergraduate and graduate students in institutions of higher education that specialize in electrical engineering.

Figures 147, tables 10, references 204.

Preface

In this book the authors have attempted to present the elements of the theory and engineering of new powerful relativistic electron beam gnerators--linear induction accelerators. Interest in this question is due to the ever increasing use of intense electron beams in science and engineering: in research on controlled nuclear fusion, new efficient methods of accelerating charged particles, low-loss long-range energy transmission, high-power electronics and so on.

Although the book is devoted to linear induction accelerators, some of the problems dealt with have wider applications. For example, the materials of chapters 2 and 3 may be used in developing pulse transformers for the nanosecond range, and systems for tailoring nanosecond current or voltage pulses.

In preparing the manuscript, the authors used mainly work done with their participation at the Scientific Research Institute of Electrophysical Apparatus imeni D. V. Yefremov [NIIEFA] in connection with developing and making linear induction accelerators for various parameters. In addition, the book uses materials published in the Soviet and non-Soviet literature, most of them dealing with description of the construction of linear induction accelerators. The book summarizes the developments in this field of accelerator technology over the past decade. The authors hope that the book will attract the attention of workers in science and technology, which in turn will further the development and use of these effective generators of intense relativistic electron beams.

Chapters 1, 4, 5 and 9 were written by Yu. P. Vakhrushin, chapters 7, 8 and the appendix were written by A. I. Anatskiy, and chapters 2, 3 and 6 were written jointly by both authors.

The authors thank the reviewers for constructive comments that were taken into consideration in preparing the manuscript for print.

Introduction

In Ref. 1, devoted to the future of science, Academician M. A. Markov noted that side by side with the development of high-energy physics is the development of physics of beams of relatively low energy, but high intensity. These powerful beams have nearly limitless possibilities for practical application in engineering, medicine and the national economy. In particular, a broad scientific vista is opened up by the use of intense relativistic electron beams. This vista covers the production of plasma with heating to thermonuclear temperatures, new collective methods of ion acceleration, amplification and generation of electromagnetic microwave radiation in the optical and x-ray bands, creating high pressures, studying solid-state phase transitions and properties of materials and so on [Ref. 2]. For these purposes, the beams must have the following parameters: electron energy 0.5-30 MeV, beam current 10^3-10^6 A, pulse duration 5-500 ns, and beam energy 10^3-10^6 J.

To produce such beams, many laboratories around the world have developed and are now operating accelerators of intense electron beams [Ref. 3]. But they have limits on pulse recurrence rate and efficiency. However, as work with intense electron beams makes the transition from the field of research into the area of industrial application (for example to produce an ion beam with high average current by using a collective-field accelerator [Ref. 4], to produce intense x-ray bursts [Ref. 5], to make a powerful industrial microwave oscillator [Ref. 6, 7] and so on), accelerators become necessary that not only produce electron beams with the required parameters, but that have high efficiency, and are capable of operating at a pulse recurrence rate of tens and thousands of hertz. It is also obvious that these relativistic electron beam generators must be simple to use and reliable in operation.

These requirements are met in large measure by linear induction accelerators. The idea of developing such an accelerator was proposed by A. Bouwers as far back as 1923 [Ref. 8]; however, forty years elapsed before practical realization became feasible as technology reached a level where the necessary accelerating fields

could be produced in acceleration of an intense beam of charged particles. The first accelerators of this type were made in the United States in the early sixties under the direction of N. Christofilos [Ref. 9] in connection with work on thermonuclear fusion, and in the Soviet Union [Ref. 10] under the direction of V. I. Veksler in connection with realization of the idea of an effective method of acceleration called "collective-ion acceleration." Fig. I.1 [photo not reproduced] shows the U. S. Astron accelerator, and Fig. I.2 [photo not reproduced] shows the Soviet LIU-3000 accelerator.

Operation of the first accelerators showed that this quite simple method of acceleration enables highly efficient production of relativistic electron beams with high recurrence rate and with good reliability and repeatability of beam parameters.

Many laboratories around the world are doing intense research on linear induction accelerators, developing theory and methods of design, improving construction. This work has given rise to a new field of accelerator technology [Ref. 11-13]. Right now, a considerable number of accelerators with various parameters are in different stages of development and construction. Some of them are shown in Table I.1 [Ref. 13].

A laboratory of linear induction accelerators was set up at NIIEFA in 1968 for producing accelerators to meet the requirements of science and industry. The research done at this laboratory has been the basis for this book.

Chapter 1 describes the working principle of the accelerator and defines the limiting ranges of parameters that accelerators of this class can have. Chapter 2 analyzes problems of design of the ferromagnetic induction system. Although in the first approximation the induction system can be represented as a series circuit of single-turn pulse transformers, the very first experiments showed that the theory that had been developed for pulse transformers of the microsecond range could not give satisfactory results when applied to the induction system. Therefore a theory of pulsed magnetic reversal is proposed for calculation. Chapter 2 presents the fundamentals of this theory as applied to calculation of the induction system, compares theoretical results with experimental data obtained by studying a large group of magnetically soft alloys and ferrites at pulse durations of 500, 250 and 150 ns typical of linear induction accelerators. These data enabled selection of ferromagnetics in relation to the requirements to be met by the accelerator.

In chapter 3 an examination is made of problems of shaping the accelerating voltage pulse with consideration of the peculiarities of the ferromagnetic induction system, which are due to the nonlinear law of behavior of the magnetic reversal current during a pulse, and the necessity of accounting for the time of commutation of the thyratrons and the dissipative inductances of the accelerating system. This chapter also describes the shaping arrangements that are most preferable for linear induction accelerators, including designs that were proposed in the process of developing the accelerators at the institute [NIIEFA].

In accelerator design, the problem arises of the spatial distribution of the accelerating field, its relation to the dimensions and construction of the induction system. This is covered in chapter 4, where expressions are derived that relate the accelerating field to the dimensions of the induction system, and experimental

TABLE I.1

Linear Induction Accelerators

Accelerator	Building site	Beam Energy, MeV*	Beam current, A	Duration of flat part, ns	Frequency of bursts, pulses/sec	Energy spread, %	Emittance π, cm/mrad
Astron injector (before reconstruction)	Livermore, U.S.A.	3.7	350	300	60 (5)	<3	50
LIU-3000**	Dubna, USSR	3(1.8)	200	250	25 (1)	--	--
LIU-30/250**	"	30	250	500	50	--	--
Astron injector (after reconstruction)	Livermore, U.S.A.	4.2	800	300	60 (5)	<2	25
ERA injector	Berkeley, U.S.A.	4.25	500	45	1	0.5	70
Silund	Dubna, USSR	3(2)	2000 (600)	20	50 (1)	2	--
Iron-free linear induction accelerator	Moscow, USSR	2	2000	70 (semi-sine)	1	--	--
Plasma betatron	Khar'kov, USSR	0.1	500 1000	--	1	Appreciable	--
LIU-0.5/50**	Moscow, USSR	0.5	100	50	10	--	--
LIU-5/5000**	"	5	5000	50	1	--	--
LIU-0.75/250**	Leningrad, USSR	0.75	250	500	50	3	--

*The value of the parameter at which the facility usually operates is shown in parentheses.
**Designed at NIIEFA.

and theoretical results are given that were found in the development of plans for making such a system worked out at NIIEFA. In particular, data on the resistive accelerating tube can be used in developing not only linear induction accelerators, but powerful low-inductance resistors as well.

The reliable operation of a high-current accelerator in general, and of linear induction accelerators in particular would be impossible without effective solution of the proelem of containment of the radial dimension of the beam, especially in frequency operation, since the energy content of the beam is so great that even relatively small losses could damage the integrity of accelerator components adjacent to the beam. In some cases, beam quality must meet severe requirements that can be satisfied only by proper selection of the focusing system. Practice has shown that an effective focusing system cannot be made apart from the design of the induction system. Therefore, chapter 5 covers containment of an intense beam within given dimensions, and gives data on the structure of powerful electron beams. In the process of research, considerable experience has been acquired in the construction and experimental investigation of linear induction accelerators. These topics are covered in chapter 6. In writing this chapter, materials were used that were obtained in developing Soviet accelerators in the laboratories of our nation, and also materials published elsewhere. Some of the proposals that have been made during work on the development of linear induction accelerators can be used in other areas of accelerator and pulse technology. Of interest in this regard is a design for a pulse transformer that can transmit very short voltage pulse fronts. And the data from experimental studies of the operation of linear induction accelerators will no doubt be of interest to engineers involved in developing and using not only linear induction accelerators, but other accelerators of intense relativistic electron beams.

Chapter 7 gives information on the system of accelerator control, which is of interest to engineers who design and use high-current accelerators.

Chapter 8 gathers together the material that has been published on the construction and experimental study of different varieties of linear induction accelerators. In particular, a design is given of a linear induction accelerator in which the magnetic reversal current is commutated by the relativistic electron beam itself. The accelerator designs described in this chapter have not yet come into extensive use, but future widespread use of some of them cannot be ruled out.

Chapter 9 examines the future of induction accelerators. On the basis of this material in combination with published data on analysis of the paths of development of science and technology, possible fields of application of linear induction accelerators in the near future are suggested.

The appendix presents the characteristics of magnetic reversal of the most widely used magnetically soft materials, and describes the conditions under which they were found.

It should be pointed out that the book does not reflect the technological experience of developments in this area, although the production of industrial facilities of the linear induction accelerator type has necessitated the mastery of new techniques for making the major components of the accelerator. In particular, a technique has been developed for winding and annealing large-size cores from tape with

thickness of 10 μm. Special facilities have been developed for winding cores with two tapes.

REFERENCES

1. Markov, M. A., "The Future of Science (Coming Generations of Elementary Particle Accelerators)", USPEKHI FIZICHESKIKH NAUK, Vol 111, No 4, 1973, p 719.

2. Bogdankevich, L. S., Rukhadze, A. A., "Problems of Intense Relativistic Electron Beams. (Report to a Scientific Session of the Department of General Physics and Astronomy and the Department of Nuclear Physics of the USSR Academy of Sciences)", USPEKHI FIZICHESKIKH NAUK, Vol 107, No 2, 1972, p 327.

3. Vallis, G., Zauer, D., Zyunder, D., Rosinskiy, S. Ye., Rukhadze, A. A., Rukhlin, V. G., "Injection of Intense Relativistic Electron Beams into Plasma and Gas", USPEKHI FIZICHESKIKH NAUK, Vol 113, No 3, 1974, p 435.

4. Chuvilo, I. V., Kapchinskiy, I. M., Koshkarev, D. T. et al., "High-Current Collective-Ion Accelerator", ATOMNAYA ENERGIYA, Vol 37, No 3, 1974, p 223.

5. Tsukerman, V., Tarasova, L., Lobov, S., "New X-Ray Sources", USPEKHI FIZICHESKIKH NAUK, Vol 103, No 2, 1971, p 319.

6. Kapitsa, P. L., "Elektronika bol'shikh moshchnostey" [High-Power Electronics, Collected Papers], Moscow, Izdatel'stvo AN SSSR, 1962.

7. Nation, J., Gardner, C. "Experimental Study of Microwave Emission of an Intense Relativistic Electron Beam", ATOMNAYA TEKHNIKA ZA RUBEZHOM, No 12, 1971, p 23.

8. Bouwers, A., "Elektrische Höchstspannungen", Berlin, 1939, p 83.

9. Christofilos, N. S., Hester, R. E., Lamb, W. A. S. et al., "High-Current Linear Induction Accelerator for Electrons", REV. SCIENT. INSTRUM., Vol 35, No 7, 1964, p 886.

10. Anatskiy, A. I., Bogdanov, O. S., Bukayev, P. V., Vakhrushin, Yu. P. et al., "Linear Induction Accelerator", ATOMNAYA ENERGIYA, Vol 21, No 6, 1966, p 439.

11. Vakhrushin, Yu. P., "State and Prospects for Development of Linear Induction Accelerators" in: "Razrabotka i prakticheskoye primeneniye elektronnykh uskoriteley. Tezisy dokladov vsesoyuznoy konferentsii (5-7 sentyabrya 1972 g., Tomsk)" [Development and Practical Application of Electron Accelerators. Abstracts of the All-Union Conference (5-7 Sep 72, Tomsk)], Tomsk, Izdatel'stvo Tomskogo universiteta, 1972, p 37.

12. Vakhrushin, Yu. P., Matora, I. M., "Linear Induction Accelerators--New Generators of Intense Relativistic Electron Beams", USPEKHI FIZICHESKIKH NAUK, Vol 110, No 1, 1973, p 115.

13. Vakhrushin, Yu. P., "Sil'notochnyye lineynyye induktsionnyye uskoriteli (LIU) s ferromagnitnoy induktsionnoy sistemoy" [High-Current Linear Induction

Accelerators (LIA) with Ferromagnetic Induction System], Preprint NIIEFA, V-0244, Leningrad, 1975.

Contents

6610
CSO: 1862/219

UDC 621.384.649+539.172.2

INTENSE STEADY-STATE ELECTRON BEAMS: EXTRACTION INTO THE ATMOSPHERE AND INVESTIGATION

Moscow IZVESTIYA AKADEMII NAUK SSSR: ENERGETIKA I TRANSPORT in Russian No 3, May-Jun 81 pp 3-13

[Article by V. M. Iyevlev and A. S. Koroteyev]

[Text] An intense concentrated steady-state electron beam in the atmosphere or in dense media can be used to solve a number of scientific and engineering problems such as creating highly efficient plasma generators for studying magnetogasdynamic processes and heat exchange at high temperatures and for simulating working processes in plasma power facilities, high-speed drilling and cutting, electron-beam welding in the atmosphere, realization of some promising plasma-chemical processes [Ref. 1, 2] and so on.

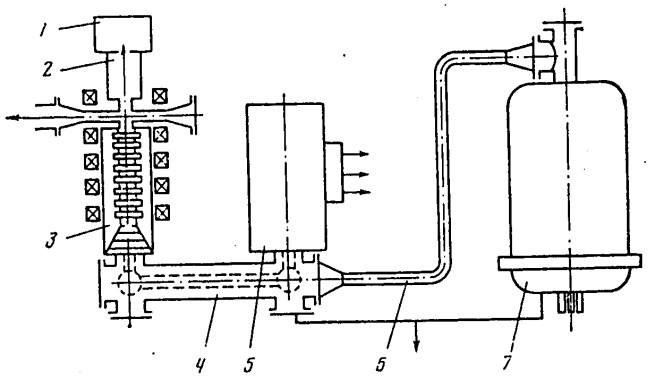

Fig. 1. Schematic diagram of the facility: 1--working part; 2--system of electron beam extraction; 3--housing of acceleration tube; 4--gas feeder; 5--electron gun control tank; 6--high-voltage cable; 7--source of high voltage

The problem of getting such beams has been reduced primarily to solution of the following major problems: development of high-intensity steady-state electron accelerators, methods of testing and handling them, transportation of the high-intensity electron beam from vacuum to a region at atmospheric pressure.

The following problems have been of fundamental importance:

1. Assurance of stability of the transported beam. During motion of a high-current electron beam there is the danger of arisal of various kinds of instabilities due to energy exchange between the beam and the plasma that arises on its path.

2. Choosing and implementing a method of electron beam focusing that ensures high accuracy and stability of the beam guide with confinement of the beam on the path and prevention of electrons from reaching elements of the structure.

3. Minimizing energy losses during beam transportation, and at the same time making compact and economic systems for bringing the beam from vacuum to a region at atmospheric pressure.

The satisfaction of these conditions in turn has required solution of the problem of the most effective gasdynamic flow part of the system of electron beam transportation through a system of lock chambers and development of high-efficiency magnet systems for controlling and stabilizing the electron beam with specially selected field configuration.

A schematic diagram of a facility for producing a concentrated electron beam in atmosphere is shown in Fig. 1. This facility includes: a high-voltage transformer made in a common module with a rectifier; an extensible electron tube; a system for beam transportation from vacuum into the atmosphere. Let us consider the major components of the facility in more detail.

High-Current Electron Accelerator. The direct-action high-current electron accelerator with extensible tube operates in the continuous state with rated power of up to 5 MW and energy of accelerated particles up to 500 keV. The high-voltage source is a transformer-rectifier module that consists of a three-phase high-voltage transformer and rectifier cells made up of semiconductor diodes shunted by a mechanical gating device. Following the transformer-rectifier, the voltage goes through a high-voltage cable to the extensible electron tube. To reduce overall dimensions, the housing of the high-voltage source, the electron-gun control tank, the housing of the acceleration tube and the feeder that connects the control tank and the tube housing are filled with sulfur hexafluoride (insulating gas) that has high electrical strength. The acceleration tube is made on the basis of an evacuated cermet envelope with spaced accelerating electrodes; an indirectly heated lanthanum hexaboride cathode is used. The accelerator is described in detail in Ref. 3, 4.

By the time our work began, the maximum power of steady-state electron accelerators had reached 20 kW.

Increasing the power level required not only the creation of a new class of steady-state electron accelerators with appreciably higher parameters, but also a method of handling them and the corresponding test equipment. The first part of the statement needs no explanation. The essence of the second part is to determine where the electron beam is to settle in developing high-power accelerators, what the target should be like to be capable on the one hand of receiving the power of the electron beam for a long time, and consequently without being destroyed, while on the other hand it does not affect the operation of the accelerator itself. Such difficulties have not come up in the operation of accelerators with power of several

kW, or even a few tens of kW because following the accelerator the beam could be distributed by scanning systems developed especially for these purposes over a surface of the separating membrane between the zone of acceleration and the atmosphere such that it could be cooled from energy release as a consequence of interaction of the electron beam with the material of the output diaphragm. Then after the beam had been coupled out into the atmosphere it could either strike a target or simply relax in the atmosphere without having any effect on the operation of the accelerator.

The density of energy release per unit of surface of the diaphargm through which the electron beam passes is

$$q \approx \Delta\varepsilon\rho dN/E \cdot s,$$

Here $\Delta\varepsilon$ are the losses of energy in the material referred to the unit mass mean free path, ρ and d are the density and thickness of the diaphragm material, N is electron beam power, and S is the cross sectional area of the electron beam.

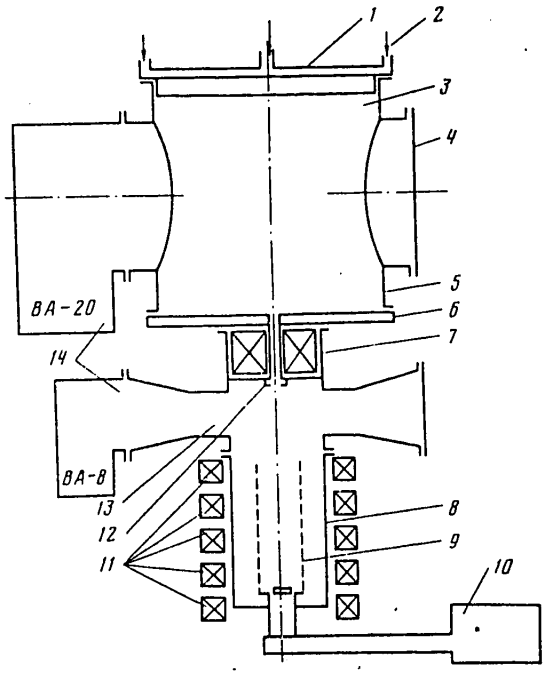

Fig. 2

This quantity must be less than q_{cool}--the heat flux density that must be removed by the coolant. Since the quantity S is limited by strength considerations, the power of the beam that can be transported through the diaphragm is limited as well. Estimates show that the process of extraction through the diaphragm becomes practically unrealistic at a beam power of more than 100 kW.

A second possible variant is to let the beam settle on a target in vacuum after distribution over a surface such that the density of the thermal action can be offset by intense cooling, i. e. over a surface that corresponds to the condition $S \geqslant N/q$ (q is the density of the heat flux from the beam to the target).

However, when a target is bombarded by an intense electron beam, considerable x-ray and ultraviolet emission arises, affecting the electric strength of the accelerating gap and structural elements in the electron accelerator, and processes near the cathode, and thus makes the operation of the accelerator during tests different from its operation in routine use, which is of course inadmissible.

Fig. 2 shows a version of a target that is free of these deficiencies. The target is a component part of a stand that consists of high-current steady-state electron accelerator 8 that is to be modified, its power supply 10, working chamber 3, magnet systems 7 and 11 and vacuum system 14. The working channel is equipped with upper cover 1 cooled by water 2, and with side walls, and has optical observation tubes and provisions for motion picture recording 4 with special protection. The dimensions of the working chamber permit accommodation of various sensors of the measurement system and will withstand reception of electron beams with power of up to 10,000 kW. The electron beam enters the channel through an aperture in bottom cover 6. Acceleration tube 9 and the entire channel for beam transport in the chamber are in a longitudinal magnetic field. The magnetic system terminates in solenoid 7, which together with the system of magnetic electrodes 5 and 6 that protect the working space from the magnetic field sets up an axial-radial magnetic field in the beam transit region at the inlet to the chamber. Interaction of the electrons with this field causes expansion of the beam, and consequently reduces the density of the heat flux incident on the reception cover of the target chamber. Magnet systems 7, 11 can change the diameter of the surface exposed to the electron beam over a wide range (from 2 cm to 1.5 cm).

The gas released from heated and electron-bombarded surfaces is evacuated from working chamber 3 by a diffusion pump. Even after an experiment of only a few seconds duration under conditions with high beam power, the pressure in the chamber rises from the initial ~10^{-4} Pa to (5-10) 10^{-3} Pa, which is much higher than the permissible pressure for normal operation of the acceleration tube. To prevent the pressure from increasing in the acceleration tube as well, it is separated from the working chamber by prechamber 13 and molecular overflow tube 12 located on the axis of rotating solenoid 7. The gas leaking into the prechamber is evacuated, which enables maintenance of a working pressure close to 10^{-4} Pa steadily in the acceleration tube. The lower pressure also acts as a shield (except for a small cavity in the molecular overflow tube) against bremsstrahlung and ultraviolet radiation. This target enabled us to develop a high-current electron accelerator for a power of up to 5 MW.

System for Coupling the Electron Beam out of Vacuum Into a High-Pressure Zone. A system of transfer chambers was used for extraction of high-intensity concentrated electron beams. W. E. Pauli was the first to develop a system of dynamic pressure stages consisting of an intermediate chamber and two stages designed for extracting a beam with size measured in fractions of a millimeter [Ref. 5]. This system was subsequently developed and improved by S. T. Sinitsyn and A. M. Trokhan, who suggested substituting a cryogenic system for the pump evacuation system for diagnostic low-current electron beams [Ref. 6]. The devices considered in all

cases were for coupling out low-current electron beams of small diameter (less than a millimeter), and as a rule into a region at lower than atmospheric pressure.

Calculation of the trajectory of motion of electrons with consideration of energy release caused by ionization losses and scattering has shown that beam transit through transfer chambers requires openings between stages of several millimeters (~6-8 mm). In the classical system of dynamic pressure stages (sequential transfer chambers with evacuation), maintaining operability of the stages with deep vacuum when the openings are of these dimensions requires a large number of vacuum units, and this leads to unreasonably large overall dimensions of the entire facility. Therefore a gasdynamic gate--a transverse supersonic steam nozzle--is incorporated to reduce the overall dimensions of the lock system and minimize the vacuum equipment used between stages with relatively high pressure (more than 100 kPa) and vacuum stages (10 Pa or less).

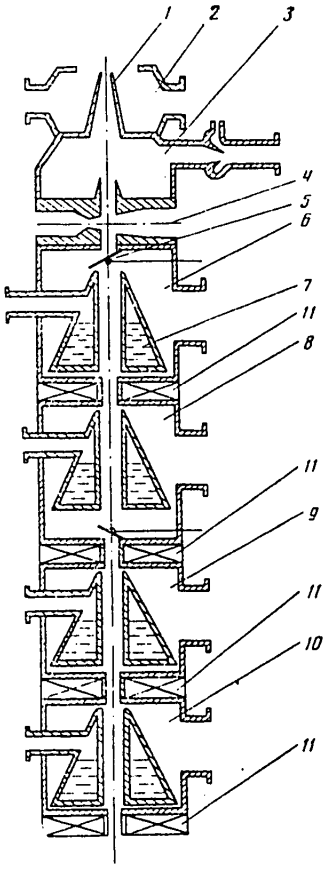

Fig. 3. Transfer chamber system: 1--intake pipe; 2, 3, 6, 8, 9, 10--transfer chambers; 4--steam nozzle; 5--vacuum valve; 7--desublimator-cooler; 11--focusing solenoid

The entire system of transfer chambers has the following appearance. The gas (see Fig. 3) from the working chamber, which may have pressure even higher than atmospheric, goes through a nozzle into the first lock and is ejected into the atmosphere under the action of excess pressure (about $5 \cdot 10^4$ Pa). The gas is evacuated from the second stage by a supersonic gas ejector that brings the pressure in the stage to about 10^4 Pa. Between the second and third stages is the gasdynamic gate--a transverse supersonic steam nozzle. The supersonic jet of superheated steam will not pass the overflowing gas from the second stage to the third, and maintains the operation of the vacuum stages constant regardless of external conditions.

The steam condenses (or more precisely it desublimes) on the walls of the chamber of the third stage, which are cooled by liquid nitrogen. The pressure in the stage is maintained at a level of 10-100 Pa. The next three stages,

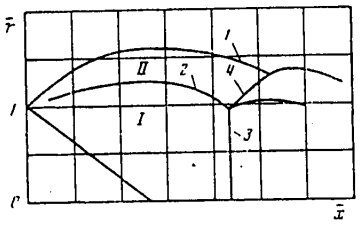

Fig. 4. Initial section of underexpanded jet: 1--free boundary of jet; 2--hanging shock; 3--central shock (Mach disk); 4--reflected shock

like the third stage, are cryogenic pumps cooled by liquid nitrogen that are connected in addition to a vacuum exhaust system with relatively low productivity for expelling only the uncondensed gas that enters the stage along with the steam.

Between the working section and the first transfer chamber is the supersonic nozzle and an adapter for intake of the gas leaking into the first lock (see Fig. 3). Proper selection of the place of installation of this intake, as well as of the intake into the second transfer chamber, considerably reduces overall dimensions and the energy inputs to the transfer chambers. The fact is that two flow regions are formed on the initial section of an underexpanded jet (Fig. 4): I--a central region where flow is independent of ambient pressure, and corresponds to discharge of the supersonic jet into vacuum from a tapered nozzle, and II--a peripheral region (compressed gas flow region). When the degree of underexpansion is increased beyond four, ten percent or less (depending on the degree of underexpansion) of the entire flowrate of the gas passing through the critical cross section of the nozzle flows through the cross section situated in front of the Mach disk in the central region (see Fig. 4). Therefore, in order to reduce the amount of gas flowing to subsequent locks, to reduce energy losses of the electron beam and to reduce the overall pressure of the gas entering the reducer pipe, the intake of this pipe is located in the central zone of the underexpanded jet. The installation of fast-acting remote-controlled vacuum valve 5 prevents atmospheric air from entering the third transfer chamber during preparation of the system for testing, or inleakage of steam as the steam nozzle is being brought up to working parameters.

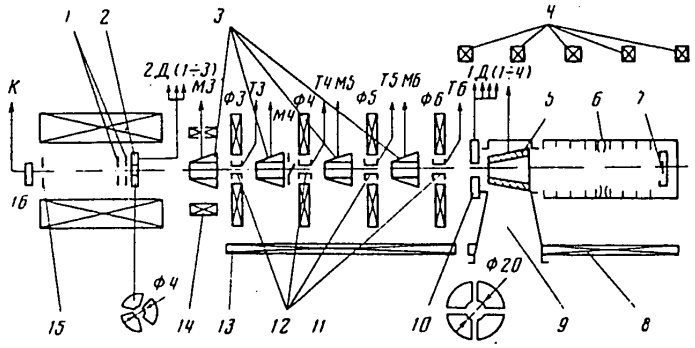

Fig. 5. Diagram of system for measurements and for controlling the beam position: 1--nozzle washers; 2--sectoral sensor; 3--desublimers; 4--solenoids of the acceleration tube; 5--microtarget for tube conditioning; 6--envelope of the acceleration tube; 7--cathode; 8, 13, 14--moving-coil solenoids for adjustment of beam position; Ф3-Ф6--precipitation sensors on the tubes of the lock solenoides; М3-М6--precipitation sensors in cooler channels; 9--funnel for tube evacuation; 10--sectoral sensor; 11--valve of isolating vacuum gate; 12--tubes of the lock solenoids; 15--control washer; 16--beam pickup sensor

A tracking magnetic field is used for focusing the electron beam, and ensuring high precision and stability of transport with beam confinement on a given path. The use of a tracking magnetic field gives high precision and reliability in transporting an electron beam over great distances, increases the electrical strength of the acceleration channel, and enables variation of the beam diameter on the

path. The latter capability results from the fact that the beam is magnetized on the path, and during its motion the condition $Br^2 = idem$ is satisfied. In particular, changing the induction B of the magnetic field enables a reduction in beam diameter d in the throats of the transfer chambers by local intensification of the field through the addition of focusing solenoids (see Fig. 3).

The magnetic field is set up by specially designed miniature solenoids that surround the electron tube and the entire transportation channel. The system for coupling out the electron beam is equipped with a system for measurements and for controlling the beam position (Fig. 5) with provisions for monitoring and correcting the position of the beam during passage along the electron channel of the facility, which is particularly important because of a relatively long channel of variable cross section and the possibility that the geometric and magnetic axes of the system may not coincide. The beam position is corrected by pairwise-connected deflecting moving-coil solenoids with continuous current control. Beam position is monitored by sectoral sensors.

A distinguishing feature of the arrangement for checking the coverage of the electron channel of the facility is the capability for simultaneous observation of the readings of measurements of current and temperatures on the screen of a cathode-ray oscilloscope for each of three sets of sensors, which considerably facilitates correction of beam position with a change in working conditions or after modifications of the working section. There is also a system for synchronous recording of major parameters of the beam transit, and accelerator operation with digital printout of the results.

As has already been pointed out, electron beam transportation involves the potential danger of arisal of instabilities due to energy exchange between beam and plasma. In this connection, consideration should be given in the first instance to the possibility of development of waves of perturbations of electron concentration in the plasma produced by the beam with phase velocity of the wave approximately equal to the velocity of the particles in the beam. (This is the resonance condition for energy takeoff.) Analysis shows that the distribution of pressure along the electron beam transportation channel must be chosen to minimize the extent of the most dangerous zones (from the standpoint of the possibility of arisal of instabilities), making them coincide with the throats of the transfer chambers. Stable transportation of the electron beam was ensured by a properly chosen law of variation in the pressure and magnetic field along the path.

Some Results of Experiments With Concentrated Steady-state Electron Beams. Increasing the range of propagation of a concentrated electron beam. It should be expected that as an intense concentrated electron beam travels through the atmosphere, its range will increase considerably over that of the electrons of low-current beams, since the energy release on the path of the beam should lead to a rise in temperature and reduction in density of the medium. Another significant factor may be the focusing influence of scattering of electrons from the denser (less heated) ambient gas.

As an example, Fig. 6 shows experimental data on the range of propagation of a concentrated electron beam in the atmosphere. The limits of the beam were determined by registration of bremsstrahlung.

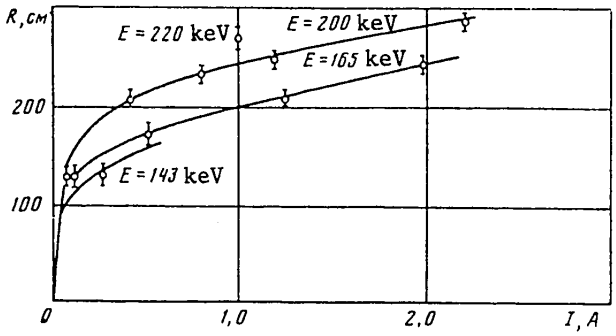

Fig. 6

The maximum mean free path of an electron in air at pressure of $9.8 \cdot 10^4$ Pa, temperature of 300 K and energy of 200 keV is approximately 30 cm. It can be seen from the data of Fig. 6 how the range of an electron beam under these same conditions increases as a consequence of heating of the gas and reduction of its density along the path. Estimates show that the beam density on the path corresponds to a temperature of the heavy gas component close to 3000 K.

Visual observations of the height of the flare produced by the electron beam agree satisfactorily with the results given by bremsstrahlung.

An increase in the range of action of a concentrated electron beam has great practical significance since this makes it realistically usable for such technological processes as welding and cutting in atmosphere, high-speed drilling and cutting of rocks.

Energy efficiency of destruction of materials under the action of an electron beam. The problems of technological utilization of electron beams are responsible for the great interest in investigation of the particulars of destruction of materials under the action of concentrated beams. In this article we cannot go into any detail in discussing the physical and mechanical aspects of this interesting and complicated phenomenon. We will only point out one interesting result by way of formulation of the problem.

A concentrated electron beam in falling on the surface of a material heats matter in the zone bounded by the beam dimensions and the depth of penetration of electrons. If the rate of heat release is lower than the rate of energy removal as a consequence of heat conduction, heating will take place with formation of a hemispherical (or nearly so) molten region. And vice versa, if the rate of energy release is much greater than the rate of energy removal (which corresponds for practical purposes to an energy flux density $q \gtrsim 10^6$-10^7 W/cm^2), the material is intensively melted and vaporized and in part is also split off because of the thermal stresses that arise. Under the action of excess vapor pressure, the products of destruction are expelled from the zone of energy release and, what is extremely important, the products of expulsion contain matter not only in gaseous form, but also in the liquid and even the solid phase.

Let us introduce into consideration the energy equivalent of action defined as $h = q/m$, where q is the energy flux density per unit of surface, and m is the mass flowrate per second of the products of destruction.

As a consequence of the concept presented above, it is to be expected that the value of this equivalent will in the case of action of an electron beam on matter, be the lower (other things being equal), the greater is the concentration of energy in the melting zone, and the higher the electron energy, since this increases the depth of penetration.

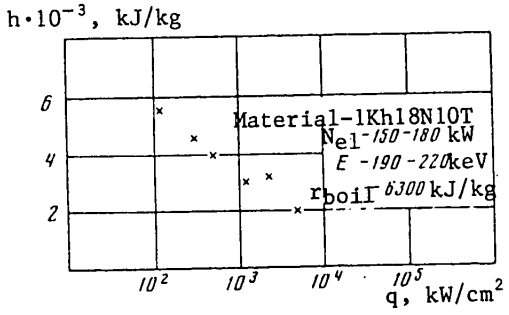

Fig. 7

Fig. 7 shows experimental values of the energy equivalent of action of an electron beam that confirm the assumption stated above. Of interest is the fact that the quantity h is much less than the heat of vaporization, which indicates an appreciable fraction of at least a liquid phase in the products of destruction. From this we get the practically important recommendation to the effect that it is more advantageous from the standpoint of energy expenditures to machine a material with highly concentrated electron fluxes (and preferably at higher energies) that penetrate to a certain depth, than for example with high-temperature plasma jets or laser radiation that act only on the surface of the material being destroyed. Of particular advantage is modulated action, since the electron beam is more effective at instants when the channel has been cleared of the vapor of the destruction products, as otherwise a certain amount of beam power is expended on additional heating of the products of destruction. Experiments have shown that the frequency of ejection of matter fluctuates from 10^2 to 10^5 Hz, depending on beam parameters, and the way that the material is being machined by this beam.

Propagation of an electron beam in a magnetic field. An experimental study has been done on the propagation of an electron beam in air in a longitudinal magnetic field. The results show as expected that a longitudinal magnetic field reduces beam scattering in the transverse direction. In studying relaxation of a comparatively low-current beam with power of about 10 kW and energy from 300 keV to 1 MeV as the magnetic field was varied from 0.7 T to 1.4 T, it was found that the behavior of beam radius as a function of magnetic induction is close to linear with $dr/dB = -0.35$ cm/T at a depth of penetration into matter of $\rho x = 0.250$ g/cm^2. It was established in the same experiments that the change in beam radius with respect to depth of the target in a constant field $B = 1/T$ is $dr/d(\rho x) = 8$ cm/g/cm^2.

Nevertheless, we may speak of so-called channeled propagation of the electron beam with a considerable degree of arbitrariness even for beams with power of more than 1000 kW, since scattering causes rather appreciable widening of the channel formed by the beam-heated atmosphere. For example, experimental data on the distribution of electron concentration in the beam (by registration of bremsstrahlung) show that the beam expands "faster" than lines of force. This result agrees satisfactorily with the theoretical picture of relaxation of an electron beam in a longitudinal magnetic field.

It is also of interest to note that experimental studies of the energy distribution of electrons over the relaxation zone in a longitudinal magnetic field show that the electron spectrum increases in hardness along the radius in the direction of the beam axis.

Experiments on electron beam welding in atmosphere. The extensive application and advantages of using electron-beam welding in vacuum are well known, particularly in welding parts of large thickness. However, the region of application of electron-beam welding is limited by the volume of vacuum chambers, and productivity is determined chiefly by the process of evacuating the chambers. It is natural that the increasing overall dimensions of welded structures and the use of materials that do not necessarily require "vacuum shielding" in welding would bring about conditions for intense development of electron-beam welding methods for use under atmospheric conditions.

The feasibility in principle of realizing this technique is known from research at the Institute of Electric Welding imeni Ye. O. Paton, the (Gereus) Company in West Germany, Westinghouse in the United States and others.

We did experiments on welding with a concentrated electron beam with power of up to 50 kW coupled out into the atmosphere with helium shielding using aluminum alloy specimens moving at a rate of 100-160 m/hr relative to the beam. The conventional arrangement of argon-jet shielding of the molten bath that is extensively used in welding is inadvisable when melting metal by an electron beam extracted into the atmosphere because of the high density of argon that leads to additional losses of electron energy upon traversing the gas gap and to an increase in beam cross section. These factors are detrimental to the formation of the molten zone, particularly at low rates of transportation of the workpieces.

Strength tests of welded seams, metallographic studies of weld structure and measurements of the microhardness for three levels of cross sections of seams have shown that the given technique can be considered quite effective, especially for welding items of large overall dimensions with great thickness of the components to be joined.

It has also been established that by proper choice of welding conditions it is possible to produce high-quality welds (at least for aluminum alloy parts) even without using special inert-gas shielding of the molten bath. This is done by changing to increased speeds of transportation of workpieces and to a high level of energy release, leading to the formation of a weld under conditions of active vaporization of metal from the surface of the melt. Radiograms of a weld made at a rate of 160 m/hr without shielding of the bath confirm absence of defects of the blister and pore type, as well as absence of inclusions in the seam.

Using electron beams to produce high-purity plasma. An investigation was made of the feasibility of using electron beams to generate plasma streams of high purity. In studying high-temperature heat exchange, magnetogasdynamics, and also for various engineering applications, use is made of high-temperature plasma flows that are produced by heating working fluids, usually in electric-arc plasmotrons. The working fluid always contains a certain amount of impurity due to destruction of the electrodes; moreover, due to specific effects inherent in an electric discharge, the flow is characterized by some pulsation of parameters. Plasma generators based on the use of electron beams are free of these deficiencies [Ref. 7]. A diagram of such a plasma generator is shown in Fig. 8. From the elec-

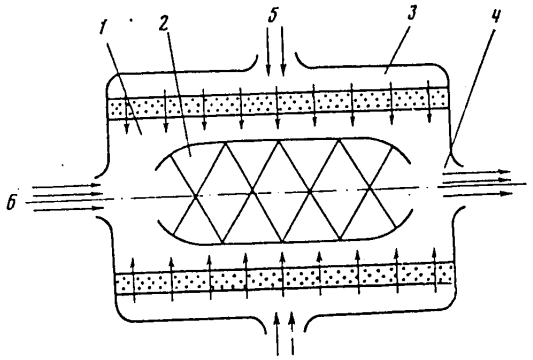

Fig. 8

tron source following the system of extraction into a high-pressure zone, the beam, accelerated to an energy of several tens or hundreds of keV (the required energy is selected as a function of the density of the medium being heated), is injected through inlet 6 into working chamber 1 and forms a zone of energy release 2, heating the gas therein to a high temperature. Gas flows through intake 5 into collector 3, and then through the porous wall into chamber 1. The gas flows radially in the greater part of the chamber. The heated gas flows out through nozzle 4. The described system has been successfully used for heating air to temperatures of several thousand degrees at pressures up to 2 MPa. The heated gas contained no impurities and showed no fluctuation of parameters. This system should be particularly effective at a power level of several tens of megawatts and at high pressures.

Conclusions. 1. The authors have demonstrated and realized the feasibility of selecting a law of change in pressure and magnetic field along a system of transfer chambers enabling extraction of an electron beam into the atmosphere with low losses without development of instabilities.

2. The use of several stages with an intake nozzle in the zone of minimum pressure, replacing air with components that condense or freeze out on cryogenic panels in combination with a magnetic control system can give small and highly economic systems for extraction of concentrated electron beam.

3. The mean free path of a concentrated electron beam is greater than that of electrons in low-current beams. This is primarily due to heating of the medium by energy released on the path.

4. Scattering of the electron beam in the transverse direction upon relaxation in the atmosphere is appreciably reduced by an external longitudinal magnetic field.

5. Destruction of materials by highly concentrated electron beams that penetrate to a certain depth in a material is energetically advantageous.

6. The use of concentrated electron beams enables the realization of new high-efficiency technological processes and devices, and in particular the implementation of electron-beam welding at atmospheric pressure, and development of high-efficiency low-temperature plasma generators.

7. The general recommendations on methods of generating concentrated electron beams and coupling them out into dense media can be used in solving specific technological problems.

REFERENCES

1. Abramyan, Ye. A., "Outlook for Using Relativistic Electron Beams in Industrial Technology", VESTNIK AKADEMII NAUK SSSR, No 11, 1979, p 57.

2. Rykalin, N. N., Zuyev, I. V., Uglov, A. A., "Osnovy elektronno-luchevoy obrabotki materialov" [Principles of Electron-Beam Machining of Materials], Moscow, Mashinostroyeniye, 1978, 237 pages.

3. Gaponov, V. A., "Vypryamitel' na napryazheniye 500 kV i tok nagruzki 10 A" [Rectifier for Voltage of 500 kV and Load Current of 10 A], Novosibirsk, Preprint, Institute of Nuclear Physics, Siberian Department, USSR Academy of Sciences, 74-11, 1974, 19 pages.

4. Iyevlev, V. M., Koroteyev, A. S., Koba, V. V., "Experimental Facility for Generating a Concentrated Beam of Relativistic Electrons in the Atmosphere", IZVESTIYA SIBIRSKOGO ODTELENIYA AKADEMII NAUK SSSR. OTDEL TEKHNICHESKIKH NAUK, No 3, 1977, p 52.

5. Pauli, W. E., PHYS. LEITSCHRIFT, Vol 21, No 1, 1920, p 11.

6. Trokhan, A. M., "Coupling Electron Beams out of Vacuum Into Gas Through a Gas-Dynamic Window", ZHURNAL PRIKLADNOY MEKHANIKI I TEKHNICHESKOY FIZIKI, No 5, 1965, p 108.

7. Koroteyev, A. S., "Elektrodugovyye plazmotrony" [Electric Arc Plasmotrons], Moscow, Mashinostroyeniye, 1980, 176 pages.

6610
CSO: 8144/1589

OPTOELECTRONICS

UDC 621.395

RADIO HOLOGRAPHY AND OPTICAL DATA PROCESSING IN MICROWAVE TECHNOLOGY

Leningrad RADIOGOLOGRAFIYA I OPTICHESKAYA OBRABOTKA INFORMATSII V MIKROVOLNOVOY TEKHNIKE in Russian 1980 (signed to press 24 Oct 80) pp 2-4, 181-183

[Annotation, preface and article abstracts from book "Radio Holography and Optical Data Processing in Microwave Technology", edited by Associate Member of the USSR Academy of Sciences L. D. Bakhrakh and Candidate of Technical Sciences A. P. Kurochkin, Izdatel'stvo "Nauka", 2150 copies, 184 pages]

[Text] This collection examines questions of the use of holography and optical data processing in microwave technology: methods and equipment for visualizing microwave fields and imaging objects; holographic method of determining the parameters of antennas in the near zone; problems of constructing acousto-optical devices for processing radio signals and the peculiarities of operation of such devices; investigation of correlational optical recognition of cosmic images.

Preface

The papers in this collection cover the following topics: holographic methods and equipment for visualizing microwave and acoustic fields, and also for producing images of objects exposed to waves in the microwave range; various aspects of the holographic method of determining the parameters of microwave antennas in the near zone; optical processing of signals of antenna arrays; problems of constructing acousto-optical devices for radio signal processing.

Articles by A. V. Avrorin et al. and by L. I. Bayda et al. deal with constructing high-speed equipment complexes designed for producing microwave and acoustic holograms and images.

The paper by A. S. Klyuchnikov and P. D. Kukharchik investigates a new type of display for holograms in the millimeter and submillimeter bands--films of various liquids.

The article by O. V. Bazarskiy and Ya. L. Khlyavich is devoted to analysis of a generalized criterion for evaluating resolution of radio holograms.

Results of experimental research on correlational optical recognition of cosmic images are given in the article by A. I. Balabanov et al.

The articles by A. G. Buday et al. and by Yu. V. Sysoyev are devoted to development of a holographic method of determining the parameters of antennas in the near zone.

The next group of articles deals with different aspects of optical processing of signals of antenna arrays and sources of radio emission. Two theoretical articles by A. Yu. Grinev et al. are devoted to signal processing algorithms and evaluation of the parameters of radio-optical antennas of systems of different configurations.

A hybrid opticodigital system for processing signals received from pulsars is proposed and studied by N. A. Yesepkina et al.

The collection concludes with articles by Ye. T. Aksenov et al. and by S. V. Kulakov devoted to acousto-optical devices for data processing based on nonlinear acoustic interaction, and to the investigation of the influence that shock waves and nonlinearity of light modulators have on the parameters of acousto-optical correlators.

The editors hope that the papers included in this collection will attract the attention of specialists and bring about further improvement and more extensive practical application of methods of holography and optical data processing in microwave technology.

UDC 778.4:534.6

REAL-TIME LONG-WAVE HOLOGRAPHY

[Abstract of article by Avrorin, A. V., Breytman, B. A., Volkov, Yu. K., Votentsev, V. N., Gruznov, V. M., Kopylev, Ye. A., Korshever, I. I., Kotlyakov, M. I., Kuznetsov, V. V. and Remel', I. G.]

[Text] An investigation is made of questions of developing rapid-action devices for recording long-wave holograms and reconstructing images in the centimeter band of radio and acoustic waves. Results that are given from experimental studies of discrete holographic systems show that the use of certain methods of processing and digital reconstruction of images gives close to the limit of spatial resolution, close to a single wavelength. An examination is also made of schemes of setting up matrix systems for registration of acoustic and microwave holograms. A description is given of a specialized computer system to control multichannel devices for collecting information and reconstructing images. Ways are pointed out for increasing the speed of the systems.

UDC 621.396.671

ELECTRONIC EQUIPMENT FOR RECORDING AMPLITUDE-PHASE DISTRIBUTIONS OF ACOUSTIC FIELDS

[Abstract of article by Bayda, L. I. (deceased), Belash, G. P., Belyayeva, A. I., Kachanov, Ye. I. and Yurkov, Yu. V.]

[Text] An investigation is made of the particulars of construction of measurement devices that operate under conditions of the near field of acoustic antennas. Diagrams are given of electronic measuring devices that process signals with a wide dynamic range, and an examination is made of the pecuiliarities of their operation

and of the sources of errors that limit measurement accuracy. Attention is given to the development of matching devices for interfacing a measurement device with a computer to enable machine processing of the measured amplitude-phase distribution of a near field. Results of experiments are given on obtaining one-dimensional holograms of different types of antennas. It is shown that the given near-field measurements have independent significance for analysis of the particulars of antenna characteristics.

UDC 621.396

INTERFERENCE-HOLOGRAPHIC METHODS OF VISUALIZING MICROWAVE FIELDS

[Abstract of article by Klyuchnikov, A. S. and Kukharchik, P. D.,]

[Text] An examination is made of a method of visualizing microwave fields in the millimeter and submillimeter bands by using displays based on thin liquid films. The proposed displays do not require thermostabilization or sensitization, enable repeated use of the recording medium, and extend the range of application of microwave holography. Based on the developed display, a technique is proposed for visualizing the spatial polarization structure of diffraction emitters of different shapes.

UDC 621.382.049.77

RESOLUTION OF RADIO HOLOGRAMS AND WAYS TO IMPROVE IT

[Abstract of article by Bazarskiy, O. V. and Khlyavich, Ya. L.]

[Text] Based on the theory of statistical solutions, a generalized Rayleigh criterion is constructed that accounts not only for the diffraction limitations of forming apertures, but also for the signal-to-noise ratio in the image, and the probability of making the correct decision on the number of resolvable sources. The conditions of resolution of extended sources are found that ensure both separate observation and exact reconstruction of dimensions. An analysis is made of the possibilities for increasing the resolution of forming apertures beyond the classical Rayleigh limit based on analytical continuation and compression of the spatial spectrum.

UDC 621.396.671

RECONSTRUCTION OF AN ANTENNA RADIATION PATTERN FROM NEAR-FIELD MEASUREMENTS ON A CYLINDRICAL SURFACE

[Abstract of article by Buday, A. G., Bulkin, V. M., Kolosov, Yu. A., Kremenetskiy, S. D., Kurochkin, A. P. and Litvinov, O. S.]

[Text] An examination is made of problems of measuring the near field of an antenna on the surface of a cylinder, and also realization of an algorithm for converting the near field to the far field. The authors discuss the results of numerical modeling of the problem of reconstructing the radiation pattern of an antenna with large electrical dimensions and low level of side lobes.

UDC 621.396.67.012.12

PROBLEMS OF REALIZING THE RADIO HOLOGRAPHIC METHOD OF DETERMINING ANTENNA RADIATION PATTERNS

[Abstract of article by Sysoyev, Yu. V.]

[Text] A method is proposed for quantitative evaluation of the required degree of orthogonalization of channels of correlational measurement systems for the radio holographic method of determining antenna radiation patterns. The author gives the results of an experimental study of random errors in measurement by this method. Capabilities are demonstrated with regard to a graphic program package in FORTRAN (GRAFOR) for constructing planar projections of antenna radiation patterns.

UDC 621.396.677.49

PLANAR RADIO-OPTICAL ANTENNA ARRAYS

[Abstract of article by Grinev, A. Yu., Voronin, Ye. N. and Kurochkin, A. P.]

[Text] An examination is made of the energy, accuracy and dispersion characteristics of linear and planar antenna arrays with coherent-optics signal processing based on various space-time light moculators. A [design] is proposed for an optical processor that has a number of advantages (in particular, it eliminates ambiguity of direction-finding for two-band signal input to the processor). Estimates are made of the diffraction efficiency of the processor, the influence of the pupil of the modulator channels, and also the effect of the mutual influence between them.

UDC 621.396.677.49

NONPLANAR ANTENNA ARRAYS WITH FORMATION OF RECEPTION BEAMS BY METHODS OF COHERENT OPTICS

[Abstract of article by Grinev, A. Yu. and Voronin, Ye. N.]

[Text] Methods are described for synthesizing coherent-optics processors of nonplanar antenna arrays that operate in the parallel scanning mode. In addition to the general approach, special cases are examined: piecewise-plane, cylindrical and annular antenna arrays. An investigation is made of effects that are detrimental to the pattern-forming properties of the processors, and methods of eliminating them are pointed out.

UDC 523.84:534.535

HYBRID OPTICODIGITAL SYSTEM FOR PROCESSING PULSAR SIGNALS

[Abstract of article by Yesepkina, N. A., Bukharin, N. A., Kotov, B. A., Kotov, Yu. A. and Mikhaylov, A. V.]

[Text] The paper gives the results of an experimental study of a pilot model of an acousto-optical correlator with time integration. It is shown that use of such

a device for processing pulsar signals eliminates the influence of dispersion of the interstellar medium, and could improve parameters of existing radiometers. Used as multielement photosensors with storage in the investigated processor were bit lines of charge-coupled devices and the auxiliary buffer memory of the Elektronika-100 computer.

UDC 523.84

MEASUREMENT OF THE COORDINATES OF REFERENCE POINTS OF A TERRAIN, AND DETERMINATION OF SHIFTS IN CLOUD FORMATIONS BY USING AN OPTICAL HETERODYNE CORRELATOR

[Abstract of article by Balabanov, A. I., Korbukov, G. Ye., Feoktistov, A. A. and Tsvetov, Ye. R.]

[Text] The paper gives the results of experimental studies on the feasibility of using an optical heterodyne correlator to measure the coordinates of reference points of a terrain and shifts of cloud formations in satellite photographs of the earth's surface. It is shown that under condition of preliminary approximate correlation of geometric distortions, fragments of images of the terrain can be tied in by correlational recognition with an error much less than the size of an element of resolution. Shifting of cloud formations is well defined by correlational comparison of images obtained by geostationary satellites with an interval of 30 minutes.

UDC 534/535.241:621.371

ACOUSTO-OPTICAL DATA PROCESSING DEVICE BASED ON NONLINEAR ACOUSTIC INTERACTION

[Abstract of article by Aksenov, Ye. T., Yesepkina, N. A. and Shcherbakov, A. S.]

[Text] An examination is made of the feasibility of developing a new class of acousto-optical devices that use nonlinear interaction of elastic waves. Results are given from an experimental study of pilot models of such devices based on lead molybdate and gallium phosphide crystals that realize displacement, convolution, correlation and controllable delay of signals. The studies were done on frequencies of 80-500 MHz, using cw and pulsed signals. With electric power input up to 0.5 W, the relative efficiency of the device reached several percent.

UDC 621.317.757

INFLUENCE THAT ATTENUATION OF ELASTIC WAVES HAS ON THE OUTPUT SIGNAL OF AN ACOUSTO-OPTICAL DEVICE FOR CORRELATION ANALYSIS

[Abstract of article by Kulakov, S. V.]

[Text] An investigation is made of the influence that attenuation has on signal shape in an acoustic light modulator, and on the output signal of an acousto-optical device for correlation analysis. Relations are given for selecting the medium of acousto-optical interaction with respect to admissible error energy.

UDC 621.317.757

INFLUENCE THAT NONLINEARITY OF ACOUSTIC LIGHT MODULATORS HAS ON CORRELATIONAL PROCESSING OF NARROW-BAND SIGNALS

[Abstract of article by Kulakov, S. V. and Bragina, L. P.]

[Text] An investigation is made of nonlinear deterministic models of an acousto-optical device for correlational processing of narrow-band input signals and Raman-[Nat] and Bragg diffraction modes.

6610
CSO: 1862/203

THREE CHANNEL ELECTRO-OPTICAL WAVEGUIDE COMMUTATOR

Leningrad PIS'MA V ZHURNAL TEKHNICHESKOY FIZIKI in Russian Vol 7, No 7, 12 Apr 81 (signed to press 18 Mar 81) pp 418-421

[Article by I. G. Voytenko and V. P. Red'ko, Mogilev Department, Institute of Physics, Academy of Sciences BSSR]

[Text] Devices for commutation of a light beam over individual channels are an inseparable part of a fiber-optics communication line. Switches based on the electro-optical effect that have maximum speed and simplicity of design are the most promising for this purpose. Devices based on striplines are most attractive at the present time [Ref. 1].

This paper gives the results of an experimental study of an electro-optical commutator that switches light in a waveguide over three independent channels. The waveguide was made by thermal diffusion of tungsten oxide into a lithium niobate Y-cut. The diffusant was sputtered by the rf-method in an atmosphere of argon and oxygen directly from a tungsten oxide target. The thickness of the sputtered layer was ~200 Å. The waveguide was formed for an hour at a temperature of 940°C. The waveguide could support only the TE mode with effective index of refraction of $n_e = 2.2031$ on a wavelength of 0.6328 μm. Commutation of light in the waveguide was accomplished by a system of aluminum electrodes separated by a 5 μm gap. Each pair of electrodes was 0.8 mm long. The electrodes were applied to a planar waveguide passing into a stripline 5 μm wide that was interrupted on a 0.8 mm section. This section was covered by the electrodes. Effective excitation of the stripline was accomplished by using a horn transition going from 50 to 0.5 μm over a length of 2.5 mm. To reduce losses due to the influence of the metallic electrodes, a buffer film of SiO_2 2000 Å thick was sputtered on the waveguide surface [Ref. 2]. A diagram of the commutator is shown in Fig. 1.

In the absence of a controlling voltage, the light passed freely beneath the electrodes and was introduced into the stripline section. Electrodes 1 and 2 were at an angle of $\theta = 2.2°$ to the direction of propagation of the light beam. With application of potential difference V to electrodes 1, the index of refraction of the crystal in the interelectrode gap decreased due to the linear electro-optical effect, and the light beam was reflected in the plane of the waveguide in the direction of channel A. Thanks to the symmetry of the device, an analogous effect is produced for the beam that is deflected by electrodes 2 in the direction of channel C. The change in the index of refraction under the effect of the electric field for the TE mode can be calculated from the formula [Ref. 3]

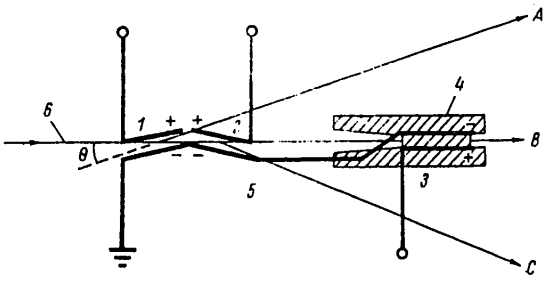

Fig. 1. Diagram of a three-channel waveguide commutator: 1, 2, 3--electro-optical cells; 4--non-waveguide region; 5--planar optical waveguide; 6--light beam

$$\Delta n = \pm \frac{1}{2} n_e^3 r_{33} \frac{V}{d} \quad ,$$

where n_e is the effective index of refraction of the waveguide mode, r_{33} is the electro-optical coefficient, d is the width of the gap between electrodes. An electric field of opposite polarity was applied to electrodes 3. In this case a region was induced in the interelectrode gap with elevated index of refraction and waveguide properties, and the light propagating in the stripline appeared at the output of channel B.

The effectiveness of light reflection in a device of this kind depends appreciably on the angle of incidence of the optical beam on the electro-optical cell. Assuming that the distribution of the electric field in the interelectrode gap can be considered uniform, the critical angle of incidence on the reflecting cell is found from the relation [Ref. 4]

$$\theta = \frac{\pi}{2} - \arcsin\left(1 - \frac{1}{2} n_e^2 r_{33} \frac{V}{d}\right) .$$

For a lithium niobate Y-cut the quantity $n_e = 2.2031$, $r_{33} = 30.8 \cdot 10^{-10}$ cm/V. A voltage of 46 V is required for total internal reflection through an angle of 2.2° and $d = 5$ μm. In our experiments, 100% reflection occurred at a voltage of 50 V. The discrepancy of the results to all appearances can be attributed to disorientation of the electric field in the interelectrode gap with the z-axis of the crystal. To lower the control voltage, it is necessary to reduce the angle of incidence of the light beam or the width of the gap between electrodes.

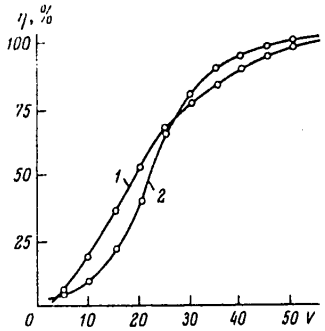

Fig. 2. Switching efficiency as a function of the amplitude of the controlling voltage (in volts): 1--channels A, C; 2--channel B

In devices of this kind the controlling voltage amplitude must be the same to switch the channels with assurance of equal intensity at the output of each of the channels. Fig. 2 shows the switching efficiency as a function of the controlling voltage for channels A and B. It can be seen from the figure that the curves behave approximately the same in the interval from 23 to 35 V. At a voltage of 27 V the curves intersect, and the switching efficiency for channels A, B and also for B, C, becomes equal at 65%. Such a mode of commutator operation is the optimum.

One of the main parameters of switches in optical communication lines is the modulation interference at the output of the device. It can be seen from the design of the device that such interference can arise only in channel B when the efficiency of deflection to the other channels is less than 100%. In this case the magnitude of the interference is determined by the mode of the substrate and by the depth of penetration of the modulating field into the substrate. When a prism device is used for coupling out the radiation, the mode of the substrate is weakly coupled and has practically no effect on operation of the commutator. Under the conditions of our experiment the interference was calculated by the formula $10 \lg I/I_0$, and was -16 dB, where I is the intensity of the light in relative units at the output of channel B when cell 1 or 2 is switched on, and cell 3 is switched off, and I_0 is the intensity of the light at the output of channel B when cell 3 is switched on and cells 1 and 2 are switched off. Decoupling between channels was determined with the commutators working in the optimum mode.

REFERENCES

1. Mitsunaga Kazumaso, Masuda Masamitsu, Koyama Jiro, OPT. COMMUN., Vol 27, No 3, 1978, p 361

2. Masuda, M. and Koyama, J., APPL. OPT., Vol 16, 1977, p 2994.

3. Schmidt, R. V., Kaminow, I. P., APPL. PHYS. LETT., Vol 25, No 8, 1974, p 458.

4. Tsai Chen, S., Kim Bumman, IEEE J. QUANT. ELECTRON, Vol 14, No 7, 1978, p 513.

6610
CSO: 1862/196

- END -